Global Production Networks and Asset Prices*

Teodor Dyakov† Hao Jiang‡

This Draft: March 2026

Abstract

We identify choke points in global production networks as strategic industries bridging flows across global value chains. Validating their structural importance, we find that these industries exhibit low substitutability: US firms exposed to Chinese choke points during the 2022 Covid-19 lockdowns experienced large and persistent sales declines. Further, the Red Sea crisis demonstrates how negative shocks to a single choke point—the water transport industry—propagate throughout the global network. This structural fragility is priced in global stock markets: firms in choke point industries earn annualized benchmark-adjusted returns exceeding 6%. We show that this premium compensates for aggregate consumption risk, as downturns in choke point industries strongly predict lower future US and global consumption growth.

Keywords: Global Supply Chain, Choke Points, Production Networks, Asset Prices

JEL Classifications: F10, F30, G10, G12, G15

*We thank Kenneth Ahern, Andy Naranjo, Jun Pan, Jincheng Tong, Raman Uppal and the participants in the 2025 EFA, NFA, and SAIF Annual Research Conference and seminars held at the National University of Singapore, University of Florida, and University of Nebraska–Lincoln for helpful comments.

†EDHEC Business School. Address: 393 Promenade des Anglais BP 3116, 06202 Nice Cedex 3, France. Phone: +33 4 93 18 69 55. E-mail: teodor.dyakov@edhec.edu.

‡Broad College of Business, Michigan State University. Address: Eppley Center, 667 N. Shaw Lane Rm 332, East Lansing, MI 48824, USA. Phone: +1 517 3554109. Email: jiangh@broad.msu.edu.

1 Introduction

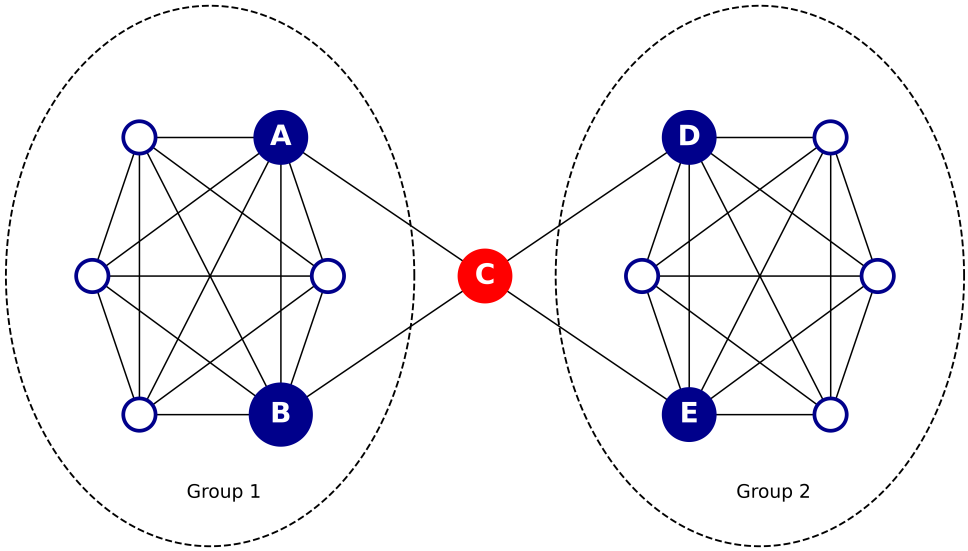
A central question in economics and finance is whether the structure of production networks, not merely the size of individual sectors, can be a source of aggregate fragility and systematic risk. Standard results suggest that in a sufficiently diversified economy, sector-level shocks wash out (Lucas, 1977); more recent work shows this breaks down when production linkages are granular or asymmetric (See, e.g., Acemoglu et al., 2012; Gabaix, 2011). We advance this line of inquiry to the global economy by identifying a specific topological feature—"choke points" industries that bridge otherwise disconnected production blocs—as the structural driver of fragility in global value chains.

What makes a node a choke point? Motivated by recent theories of network fragility (See, e.g., Acemoglu and Tahbaz-Salehi, 2024; Elliott et al., 2022; Elliott and Jackson, 2024), we formalize this concept using the topology of global value chains. Figure 1 illustrates the intuition with a stylized network featuring two regionally integrated production blocs. Node C serves as a strategic bridge, interconnecting these disparate modules and transforming the topology into a small-world network. This architecture drives global productivity by facilitating efficient, short-path trade flows; however, it simultaneously engenders a structural fragility. By channeling aggregate flows through a single, non-substitutable gateway, Node C becomes the network's Achilles' heel, transforming local shocks into systemic risks.

We show that this structural fragility has real consequences and is priced in financial markets. Using the 2022 Covid-19 lockdowns in China as a natural experiment, we find that US firms with greater exposure to Chinese choke point industries experienced significantly larger and more persistent sales declines, consistent with the low substitutability these industries imply. The Red Sea crisis offers a complementary test, demonstrating how a shock to a single choke point — water transport — propagates throughout the global network, disproportionately affecting industries with high choke point exposure. Turning to asset prices, we find that firms in choke point industries earn annualized benchmark-adjusted returns exceeding 6%, a premium we show compensates for aggregate consumption risk: downturns in choke point industries strongly predict lower future US and global consumption growth.

Central to our analysis is a new topological measure—Choke Point Value (CPV)—that quantifies how critical an industry is to the flow of value across the global economy. We construct this measure from OECD World Input-Output Tables (1995–2020), covering 45 industries across

Figure 1: Choke Points in a Stylized Global Production Network with Two Regionally Integrated Production Blocs

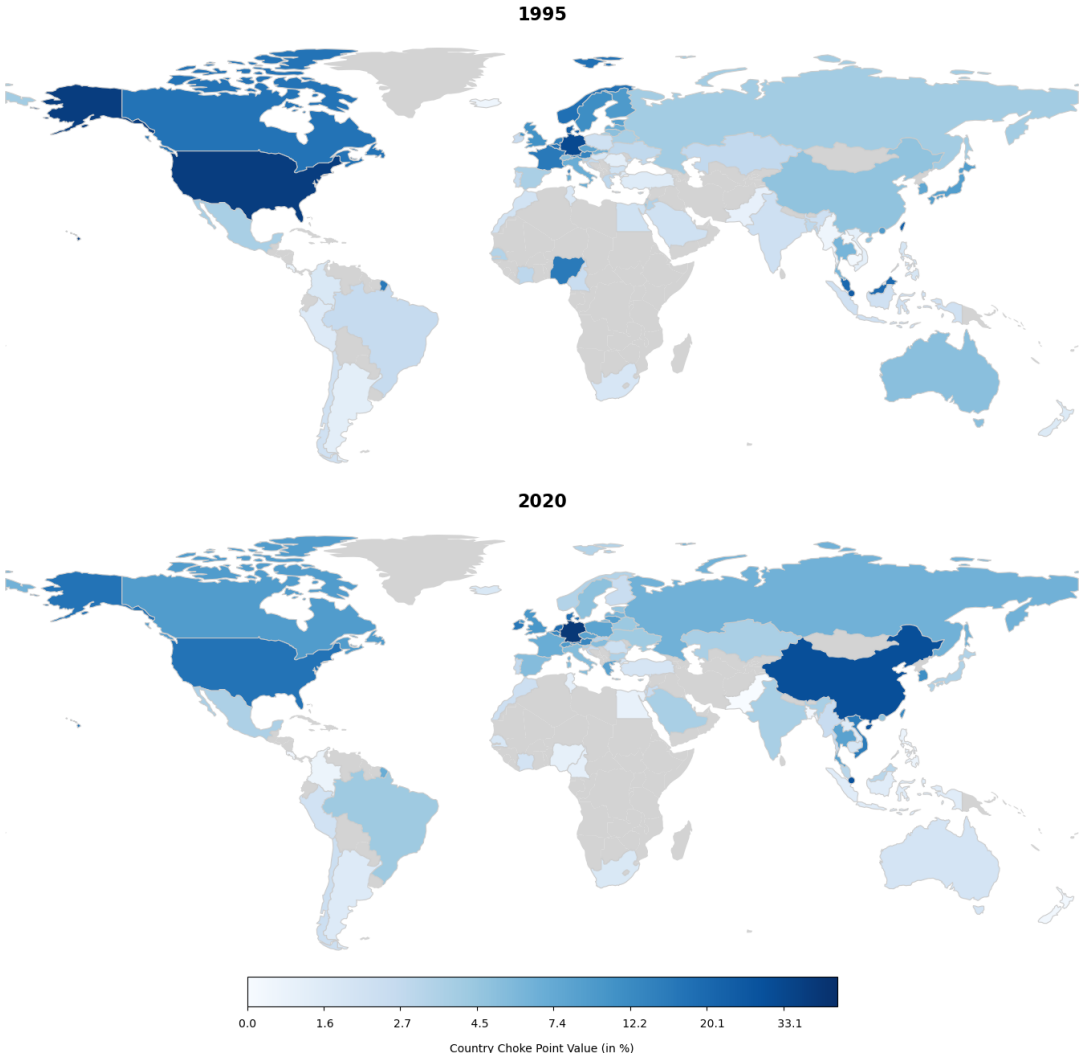


77 economies. We model the global economy as a directed, weighted graph where edges represent the value-added flows embedded in international trade. This topology allows us to map the "weighted shortest paths" of global commerce—the economic backbone along which value flows most efficiently. CPV isolates strategic nodes that bridge flows between otherwise disconnected production blocs; while a choke point may not be the largest industry by size, it dictates the aggregate flow between regions.

Applying this measure to our sample from 1995 to 2020 reveals a global production network with a shifting topology. While the industrial hierarchy remains relatively stable—with Water Transport, Wholesale and Retail, Basic Metals, and ICT/Electronics consistently ranking as top choke points—the geographic distribution of these nodes has undergone a tectonic shift, as shown in Figure 2. In 1995, the United States was the world's dominant choke point economy, dwarfing Germany and Singapore. By 2020, however, the US had fallen out of the top five, ranking 6^{th}. Conversely, China leapfrogged from the 35^{th} rank in 1995 to become the 2^{nd} most critical choke point economy in 2020, eclipsed only by Germany. Our analysis shows that this secular decline of the US and the simultaneous rise of China were significantly accelerated by China's entry into the World Trade Organization (WTO) in 2001.

Figure 2: Geographic Distribution of Choke Point Values Over Time

This figure depicts economy Choke Point Values for years 1995 and 2020, computed as the ratio of the number of shortest paths passing through an economy to all the shortest paths. Higher intensity of blue represents higher economy Choke Point Value. Economies with no data are depicted in light gray.



A defining characteristic of choke point industries is their low substitutability, a concept echoing the strong complementarities found in the O-ring theory of Kremer (1993). In modern production functions, a single weak link caps aggregate output because substituting a critical, high-precision input with a lower-quality alternative causes performance to collapse. The Taiwan Semiconductor Manufacturing Company (TSMC) exemplifies this rigidity. As Miller (2022) documents, customers cut off from TSMC often face a complete lack of near substitutes. The 2021 chip shortage, for instance, forced major US automakers to halt production lines and stockpile unfinished vehicles, demonstrating that the loss of a single choke point input can paralyze downstream manufacturing.

The 2022 Covid-19 lockdowns in China provide a natural experiment to test this low

substitutability. The lockdowns sharply curtailed access to key inputs from Chinese choke point industries, creating plausibly exogenous disruptions to these segments of global supply. If these industries are indeed hard to replace, US firms with greater exposure to them should experience persistent, adverse real effects. Empirically, the evidence is consistent with this hypothesis: US firms with higher global value chain exposure to Chinese choke point industries exhibit significantly larger post-lockdown sales declines. Quantitatively, a 10% increase in exposure to the top five Chinese choke point industries is associated with a 16% reduction in sales over the subsequent four quarters. This persistence indicates that the CPV measure successfully identifies industries characterized by high switching costs and low input substitutability.

The empirical confirmation of low substitutability in choke point industries has important macroeconomic implications using the framework of Baqaee and Farhi (2019). While Hulten's Theorem suggests that a sector's aggregate influence is limited to its sales share, this linearity breaks down when the elasticity of substitution drops below unity. In the regime of complementarity, the network's response to shocks becomes non-linear and convex: a negative shock to a critical node causes its expenditure share, its "influence weight", to rise endogenously, effectively amplifying the distress. This leads us to study the second defining feature of choke points: their ability to propagate and amplify local shocks.

A large network literature shows that production linkages can transform idiosyncratic firm-level disturbances into aggregate fluctuations, both in theory (Acemoglu et al., 2012) and in historical episodes such as the Great East Japan Earthquake (Carvalho et al., 2021). Yet the role of network topology remains relatively underdeveloped in this work. Our analysis advances this literature by focusing on the distinctive network position of choke points. Situated at the intersection of many efficient supply chains (shortest paths), disruptions at these nodes sever a disproportionate number of productive customer–supplier relationships. This motivates the view of choke points as accelerators: shocks at these strategic nodes do not remain local but cascade through the network, disproportionately affecting industries with high exposure to them.

We test our hypothesis using the recent Red Sea crisis as another experiment. The Red Sea is a vital maritime artery connecting Asia and Europe via the Bab el-Mandeb strait. From late 2023, Houthi forces began attacking merchant vessels, which promoted most shipping companies to divert their fleets for the much longer and more costly alternative around Africa's Cape of

Good Hope. This disruption to the water transport industry—itself a key choke point in global production networks—provides a clean setting to test our hypothesis. We examine whether industries with higher exposures to this specific choke point disruption were, in fact, hit harder. Our estimates show that industries with higher exposures tend to perform worse after the Red Sea crisis, supporting our hypothesis. For instance, we find that industries with a 10% increase in the exposures to the Red Crisis deliver a lower abnormal return of 1.68% per week during the first four weeks in 2024.

Given their structural importance, low substitutability, and capacity to amplify shocks, choke point industries embody heightened, non-diversifiable risk. This raises the question of whether this disruption risk is priced in global equity markets. To address this question, we first test for the presence of choke point premiums in stock returns. We then examine the underlying sources of these premiums by relating choke point returns to aggregate consumption dynamics and by evaluating alternative risk-based and non-risk-based explanations.

Our asset pricing tests begin by constructing annual portfolios that rank economy-industry pairs into quintiles based on their CPV. These portfolio sorts reveal a statistically significant and economically substantial risk premium. Specifically, stocks in the top CPV quintile outperform those in the bottom quintile by more than 6% annually. Critically, this performance differential cannot be explained by conventional risk factors. The annualized alpha of the long-short CPV strategy reaches 5.8% relative to the World CAPM and rises to 7.2% when controlling for the international Fama-French five-factor model augmented with momentum. These findings indicate that the choke point premium constitutes a distinct source of return variation not captured by established global asset pricing benchmarks.

We further corroborate these results through Fama-MacBeth cross-sectional regressions, which enable us to control for an extensive set of covariates. Our most comprehensive specification accounts for standard industry characteristics—including market beta, size, book-to-market, profitability, investment, dividends, and momentum—as well as economy-level factors such as population, GDP growth, inflation, and currency returns. Even after absorbing this rich variation, the relationship between CPV and future stock returns remains both economically meaningful and statistically significant. This persistence suggests that the choke point premium is not merely a proxy for known risk factors or local economic conditions.

To understand the nature of the choke point premium, we begin with the fundamental

principle that risk premiums arise when assets underperform in states where the stochastic discount factor is high. In deep structural models such as consumption-based capital asset pricing models (e.g., Rubinstein, 1976; Breeden, 1979), these "bad states" correspond to periods of low aggregate consumption growth. Within a production network context, choke point industries are structurally capable of amplifying idiosyncratic shocks into aggregate fluctuations, precipitating broader economic downturns that elevate investors' marginal utility. Consequently, investors demand higher expected returns to hold choke point stocks as compensation for bearing this systematic consumption risk.

Two additional theoretical channels reinforce this logic. First, under the long-run risk framework of Bansal and Yaron (2004), assets that contain information about persistent shifts in expected consumption growth command a premium even when contemporaneous consumption responses are modest. If choke point disruptions alter not just the level but the trajectory of aggregate consumption–as our preceding evidence on persistent, multi-quarter effects suggests—then choke point risk maps naturally onto the long-run risk channel (Hansen et al., 2008). Second, the rare disaster literature (Barro, 2006; Gabaix, 2012) highlights that assets exposed to low-probability, high-impact economic contractions carry substantial premia. While choke point disruptions such as the Covid-19 lockdowns and the Red Sea crisis are not themselves consumption disasters on the scale of world wars or the Great Depression, they reveal a structural vulnerability: when disaster-level shocks do occur, choke points are the channels through which cascading failures propagate, amplifying the severity of aggregate contractions. The non-substitutability and network position of these industries make them critical transmission mechanisms that can transform large shocks into catastrophic outcomes. Both channels predict that choke point exposure commands a risk premium, and both are consistent with the patterns we document.

To empirically test the link between choke point risk and aggregate consumption, we adopt the ultimate consumption risk framework of Parker and Julliard (2005). Their seminal work highlights a critical intertemporal dynamic: asset prices incorporate news instantaneously, whereas reported aggregate consumption adjusts gradually due to measurement errors and consumption smoothing frictions. Leveraging this insight, we employ predictive regressions to test whether the return spread between high and low choke point industries forecasts future aggregate consumption growth. If choke points embody genuine macroeconomic risk, their returns

should contain forward-looking information about the trajectory of aggregate consumption.

Our predictive regression tests show that the return spread between the highest (Q5) and lowest (Q1) CPV quintiles serves as a robust leading indicator for the real economy. Specifically, a decline in the returns of high-CPV industries relative to peripheral ones strongly predicts a contraction in consumption growth across the US, developed markets, and the global economy over the subsequent four quarters. This predictive power remains significant even after controlling for lagged market returns, Fama-French factors, momentum, and business cycle variables. These findings confirm that choke points function as informative signals of aggregate consumption risk, providing the economic foundation for our central result: stocks in these structurally critical industries command a distinct risk premium.

We consider several alternative interpretations, starting with the possibility that the CPV premium reflects market power rather than risk compensation. One might argue that firms in choke point industries leverage their strategic positions to extract superior profits, which subsequently drive higher stock returns. To address this, we perform double sorts on CPV and profitability. We find that the choke point premium persists regardless of the industry's profitability level. This result indicates that the higher returns associated with choke points are not merely a function of superior operating performance or rent extraction, but rather compensation for structural network risk.

Finally, we distinguish the choke point premium from other network-based asset pricing factors. Herskovic (2018) identifies network concentration and sparsity as priced systematic risks . However, our double-sort analysis confirms that CPV predicts returns independently of these topological features. Similarly, we show that our results are not subsumed by eigenvector centrality (Acemoglu et al., 2012; Ahern, 2013), which captures general connectedness rather than the specific bridging role of choke points. Our findings also withstand controls for a battery of related risks, including globalization risk (Barrot et al., 2019), supply chain disruptions (Lieberman et al., 2025), geopolitical risk (Caldara and Iacoviello, 2022) and industry size (Acemoglu et al., 2012).

The remainder of the paper is organized as follows. Section 2 reviews related literature. Section 3 details the construction of the global production network using OECD World Input-Output Tables and formally defines our CPV measure. Section 4 validates the economic characteristics of these choke points—specifically their low substitutability and propensity to prop-

agate shocks—through two natural experiments: the 2022 Covid-19 lockdowns in China and the Houthi blockade of the Red Sea. Section 5 presents our central asset pricing results, documenting the risk premium associated with choke point industries and establishing its link to aggregate consumption risk. Section 6 explores alternative interpretations, robustness checks, and comparisons with other network centrality measures. Section 7 concludes.

2 Related Literature

This paper sits at the intersection of three literatures: the macroeconomics of production networks, the empirics of supply-chain disruption, and the asset pricing of network-based risk. We discuss each in turn, emphasizing what our contribution adds and where the boundaries of the existing work leave room for our analysis.

Production networks and macroeconomic fragility. A foundational question in macroeconomics is whether sector-level shocks can generate aggregate fluctuations or whether diversification renders them irrelevant (Lucas, 1977). Acemoglu et al. (2012) showed that the answer depends on network structure: when the distribution of input-output linkages is sufficiently fat-tailed, idiosyncratic shocks to individual sectors do not average out but instead propagate through the network to produce aggregate volatility. Their result provides the key theoretical premise for our paper: if CPV is fat-tailed—as we document in Section 3.2.2, with a tail index $\zeta \approx 2$ implying diverging variance—then shocks to high-CPV industries are precisely the kind that survive aggregation and generate systematic risk.

Baqaee and Farhi (2019) extend this insight beyond first-order (Hulten's theorem) effects, showing that with complementarities in production, microeconomic shocks have *second-order* macroeconomic consequences that are disproportionately concentrated at bottleneck nodes. Choke points, as we define them, are the empirical counterpart of these bottlenecks: they sit on the efficiency-maximizing shortest paths of the global network, and the strong complementarities documented in our China-lockdown experiment (Section 4.1) confirm that alternative sourcing is not readily available. The combination of fat tails and complementarity means that choke-point disruptions generate aggregate effects that are both larger and more persistent than a symmetric network would predict.

On the theoretical side, recent work has formalized why production networks endoge-

nously develop fragile architectures. Acemoglu and Tahbaz-Salehi (2024) show that relationship-specific investments lead to networks in which small shocks trigger discontinuous output collapses. Elliott et al. (2022) demonstrate that as production grows more complex and reliant on essential inputs, supply chains become increasingly prone to precipitous contractions. Elliott and Jackson (2024) extend this logic to show how globalization amplifies these vulnerabilities. Our contribution is to take these theoretical insights to data: we construct the global production network, identify the specific nodes where fragility concentrates, and trace the consequences through to real output (Section 4) and financial markets (Section 5).

An important conceptual antecedent is the O-ring theory of Kremer (1993), in which production consists of a sequence of complementary tasks and the failure of any single input sharply reduces the value of final output. We view choke point industries as the global-network analogue of O-ring inputs: they are the binding constraints along efficiency-maximizing trade paths, and their disruption causes cascading failures disproportionate to their size.

Empirical identification of supply-chain propagation. A growing empirical literature exploits natural experiments to trace how shocks propagate through production networks. Carvalho et al. (2021) use the 2011 Great East Japan Earthquake to show that disruptions to upstream suppliers reduce the output of downstream firms, even those with no direct exposure to the affected region. Barrot and Sauvagnat (2016) provide perhaps the most direct precedent for our identification strategy: using US natural disasters, they show that firms dependent on inputs with few substitutes experience large output declines, and that this input specificity is a key determinant of propagation. Our analysis shares their emphasis on low substitutability as the mechanism through which network position translates into real-economy fragility, but differs in scope: we operate at the level of the *global* production network, using international input-output data to identify choke points that bridge flows across economies rather than across domestic industries.

Our two identification exercises—the 2022 Covid-19 lockdowns in China and the 2023–2024 Red Sea crisis—complement these earlier studies by exploiting shocks that are global in origin and that differentially stress industries our CPV measure identifies as structurally critical. The China-lockdown experiment tests the low-substitutability channel: if high-CPV Chinese industries can be easily replaced, exposed US firms should be unaffected. The Red Sea

experiment tests the propagation channel: a shock to a single choke point (water transport) should cascade to industries with high topological exposure. Both experiments confirm the predictions, providing causal evidence that CPV captures economically meaningful structural fragility.

Asset pricing implications of production networks. The link between production-network structure and asset prices has been explored primarily in the domestic US context. Herskovic (2018) identifies time-varying network concentration and sparsity as priced risk factors, showing that innovations in these topological features carry a risk premium. Gofman et al. (2020) document that vertical creative destruction within supply chains is reflected in stock returns. Ramírez (2024) shows that firm-level network connections predict returns in the cross section. Ahern (2013) finds that industries with high eigenvector centrality in the domestic US input-output network earn higher returns, a finding consistent with the general-connectedness channel of Acemoglu et al. (2012).

Our paper departs from this literature in two respects. First, we move from domestic to *global* production networks. The distinction is not merely one of scope: as we show in Section 3.4, domestic centrality measures are *negatively* correlated with our global CPV, because industries that are large domestic hubs tend to be peripheral in the cross-border bridging sense. Rather than substituting for domestic-network measures, our global approach complements them by isolating the unique vulnerabilities of nodes that bridge distinct international production blocs—risks that inherently depend on cross-border topology. Second, we focus on a specific topological feature (betweenness centrality, which captures bridging power) rather than on general connectedness (eigenvector centrality, which captures recursive importance). Our double-sort analysis in Section 5 confirms that CPV predicts returns over and above eigenvector centrality, network concentration, sparsity, and all other centrality measures we consider.

Two papers in international finance are closely related. Richmond (2019) shows that trade-network centrality predicts currency risk premia, establishing that network position in global trade carries asset-pricing implications. Our measure differs from Richmond's in that it captures *bridging* vulnerability rather than overall integration, and operates at the industry level rather than the country level. Barrot et al. (2019) document a globalization risk premium among US industries exposed to foreign competition; our results show that the CPV premium is distinct

from and survives controls for this globalization channel. More broadly, our findings connect to the literature on international asset pricing and factor models (Bekaert et al., 2009; Karolyi and Stulz, 2003; Hou et al., 2011), by providing a structural, network-based explanation for cross-sectional return variation in global equity markets.

At the level of individual supply-chain links, Cohen and Frazzini (2008) and Menzly and Ozbas (2010) document return predictability arising from customer-supplier relationships, while Lieberman et al. (2025) show that payment timeliness within supply chains predicts returns. These studies focus on bilateral links; our contribution is to show that the *geometry* of the global network—specifically, the concentration of shortest paths at choke point nodes—contains information about systematic risk beyond what any bilateral relationship can capture.

From network fragility to risk premia: the theoretical bridge. While pioneering work has established a link between network features and asset prices, the specific asset pricing implications of cross-border bridging vulnerabilities have not yet been fully integrated with the broader macroeconomic literature on global network fragility. The production-network papers cited above establish that choke points amplify shocks and reduce aggregate output, but they do not speak to expected returns. The asset pricing papers document return predictability from network features, but typically lack a structural explanation rooted in the topology of global production. Bridging these two bodies of work requires an argument for why choke-point fragility generates *non-diversifiable* risk that investors price.

We build this bridge in three steps. First, the fat-tailed distribution of CPV ($\zeta \approx 2$) implies, following Acemoglu et al. (2012), that shocks to high-CPV industries do not wash out in aggregation—they are inherently systematic. Second, the strong complementarities at choke points, formalized by Baqaee and Farhi (2019) and confirmed empirically in our China-lockdown experiment, mean that the aggregate consumption impact of a choke-point disruption is disproportionate to the size of the disrupted node. Third, standard consumption-based asset pricing theory (Rubinstein, 1976; Breeden, 1979) predicts that assets whose returns covary negatively with aggregate consumption growth in bad states must earn a risk premium. Because choke-point disruptions reduce aggregate consumption—as our predictive regressions in Section5.2 demonstrate—exposure to choke-point risk satisfies this condition.

Two additional theoretical channels reinforce this logic. Under the long-run risk frame-

work of Bansal and Yaron (2004), assets that contain information about persistent shifts in expected consumption growth command a premium even when contemporaneous consumption responses are modest. The multi-quarter persistence of our consumption-predictability results (Figure 16) is consistent with this channel: choke-point returns forecast consumption growth over horizons of two to four quarters, suggesting that CPV captures information about the *trajectory* of aggregate consumption, not merely its level. Under the rare-disaster framework of Barro (2006) and Gabaix (2012), assets exposed to low-probability, high-impact economic contractions carry substantial premia. Choke points are the structural channels through which large shocks propagate and amplify, making them natural conduits for disaster risk even if the disruptions we observe in sample (Covid-19 lockdowns, Red Sea blockade) are not themselves disasters on the scale of world wars.

3 Identifying Choke Points in Global Production Networks

3.1 Sample Construction and Summary Statistics

We construct the global production network using annual World Input-Output Tables (WIOT) from the OECD, spanning 45 industries across 77 economies from 1995 to 2020. This data set allows us to decompose gross exports into their distinct value-added origins, a method referred to as Trade in Value Added (TiVA). See Appendix A for decomposition methodology and Appendix C.1 for key TiVA variables.

We model the global economy as a directed, weighted graph $G(V, E)$ where:

- **Nodes (V):** Represent the $3,465$ distinct economy-industry pairs (77 economies $\times$ 45 industries). A node is denoted as $n(s, j)$, representing industry s in economy j.
- **Edges (E):** Represent the directional value-added flows between nodes. An edge $e_{i,j}^{r,s}$ captures the dollar value added of intermediate inputs from industry r in economy i used by industry s in economy j, scaled by the gross exports of the destination node. Since we focus on global production networks, we set all edges where $i = j$ to zero. By construction, the sum of all inward edges equals to the node's import content in exports, also referred

to as *vertical specialization* (Hummels et al., 2001) and *global value chain participation* (e.g., Johnson, 2018) in the international trade literature.[1]

Table 1 provides summary statistics for the network topology. The average edge weight is 0.006%, reflecting the granular nature of global trade. Consistent with prior literature (e.g., Johnson and Noguera, 2017), we find that foreign inputs account for approximately 21% of the average industry's value-added in exports, though this reliance varies significantly by sector. For instance, the *Mining and Quarrying* sector serves as the most dominant source of foreign value-added, while *Manufacturing* exhibits the highest dependence on foreign sourcing. Appendix B provides an overview of our sources of firm-level and economy-level data, used in the empirical tests.

3.2 Methodology: Defining Choke Point Value

We define Choke Points as strategic nodes that bridge flows between disparate parts of the global economy. To identify these nodes, we exploit the geometry of the production network, focusing on the paths that carry the most significant economic flows.

3.2.1 Flow-Weighted Shortest Paths

In a weighted, directed network, the "shortest path" between two nodes is not necessarily the one with the fewest links (geodesic path), but the one with the strongest economic connection. To operationalize this, we assign a "cost" to each edge inversely proportional to its trade volume:

$$c(e) = \frac{1}{e} \tag{1}$$

Thus, a high-volume trade link represents a "low-cost" path. We identify the **Weighted Shortest Path** between any source node $n(r,i)$ and sink node $n(s,j)$ by minimizing the total cost:

$$\text{Shortest Path}_{n(r,i)\to n(s,j)} = \arg\min_{P} \sum_{e\in P} c(e) \tag{2}$$

Using the algorithm of Dijkstra (1959), we compute these paths for all node pairs. This approach reveals the economic backbone of the network. For example, as shown in Figure 3, the direct

[1] See Antràs and Chor (2022) for an overview of the literature on global value chains in international trade.

link between the Swedish and US *Motor Vehicle* industries is negligible ($< 0.001\%$). However, the *flow-weighted shortest path* reveals a critical route: Swedish inputs flow to the Polish *Motor Vehicle* industry, then to Germany, and finally to the US. This multi-step path carries flows orders of magnitude larger than the direct link, highlighting the hidden structural dependencies in the network.[2] See Appendix C.2 for definition of network variables.

3.2.2 Computing Choke Point Values

A node's structural importance is determined by how often it lies on these critical paths. We define the **Choke Point Value (CPV)** of a node v as its flow-based betweenness centrality (Freeman et al., 1991):

$$CPV_{v,t} = \sum_{j \neq k \neq v} \frac{\sigma_{jk,t}(v)}{\delta_t} \tag{3}$$

where $\sigma_{jk,t}(v)$ is the number of shortest paths from node j to node k that pass through node v, and δ_t is the total number of shortest paths in the network at time t.

This measure captures a node's capacity to act as a bottleneck. Unlike degree-based centrality (which measures local size), CPV measures global bridging power. A high-CPV industry, like the German *Motor Vehicles* sector in our example, acts as a critical conduit; its disruption severs the optimal flow of goods between numerous upstream and downstream partners.

Panel A of Table 2 reports descriptive statistics, showing that while the average CPV is low (0.007), the distribution is highly skewed; the choke point status is concentrated among a few key players. Panel B shows descriptive statistics for a subsample of economy-industry pairs for which we have sufficient financial data to construct our stock portfolios.

Figure 4 visualizes choke points using the global production network in 2020. Each node in the graph represents an economy-industry pair. The size of each node indicates the node's CPV and the thickness of the lines between nodes $n(r, i)$ and $n(s, j)$ indicate the number of shortest paths going via $n(r, i)$ and then $n(s, j)$. We group the economy-industry pairs geographically and in terms of economic development following the classification in Table 1. In addition, economy-industry pairs within each region are grouped in three concentric circles, with the

[2]Further illustrations in Figure 3 include the shortest path connecting Machinery industry in Turkey with Fabricated Metals industry in Japan, and that connecting the Rubber and Plastics industry in Israel with Machinery industry in Italy.

outer one covering manufacturing, the middle one business services, and the inner one covering all other sectors. The topology of the global production network in 2020 looks very similar to the one in 2019 (See Appendix D.1) and hence doesn't reflect changes induced by the global pandemic.

3.3 Distribution of Choke Point Values: Heavy Fat Tails

The distribution of CPV has a heavy right tail. Although the average CPV across economy-industry pairs is just 0.007, the distribution exhibits extreme right-skew: a handful of nodes account for a disproportionate share of the global network's bridging capacity. This concentration is far more pronounced than what standard centrality measures suggest. Compared with *Eigenvector* centrality, a widely used alternative in production-network studies, the tail of the CPV distribution is dramatically fatter, and the top-ranked nodes under the two measures do not overlap at all. The distributional analysis in this subsection formalizes these claims.

To characterize the tail, we fit a power-law specification to the counter-cumulative distribution of CPV. The probability of observing an economy-industry pair with CPV at least as large as x is modeled as

$$P(x) = c\,x^{-\zeta}, \quad \text{for } \zeta > 1 \text{ and } x \geq x_{\min}, \tag{4}$$

where c is a positive constant and ζ is the tail index. Using the maximum likelihood estimator of Clauset et al. (2009) as implemented by Alstott et al. (2014), we estimate $\zeta = 2.01$ with a lower cutoff $x_{\min} = 0.0187$. A tail index near 2 implies that, in the absence of an upper bound, the second moment of the distribution would diverge—a hallmark of extreme concentration in which a small number of nodes can shift aggregate statistics.

We assess goodness of fit following the protocol of Clauset et al. (2009). The Kolmogorov–Smirnov distance between the empirical tail and the fitted power law is 0.0575; a Monte Carlo test based on 2,500 synthetic datasets rejects the pure power-law null ($p = 0.006$). Such rejections are common even in distributions that are strongly heavy-tailed, as finite-sample deviations from a strict power law are the norm rather than the exception (Alstott et al., 2014). Crucially, the power law strongly outperforms the exponential distribution (log-likelihood ratio $R = 46.91$, $p = 0.005$), confirming that the tail of CPV is not exponentially bounded and is therefore gen-

uinely heavy-tailed. Comparison with the lognormal distribution—which is heavy-tailed but not power-law—yields a marginally better fit for the lognormal ($R = 3.61$, $p = 0.096$), consistent with the well-known difficulty of distinguishing between heavy-tailed functional forms over finite samples.

The best-fitting specification is the truncated power law ($R = 4.06$, $p = 0.004$ vs. the pure power law), which captures power-law behavior over a wide range while allowing faster decay at the extreme upper end. This is a natural consequence of the fact that CPV is bounded above by one: the distribution can exhibit approximate power-law scaling over most of the tail, but the bounded maximum necessarily compresses the probability of the largest realizations. The superior fit of the truncated specification therefore reflects an intrinsic property of the variable rather than a failure of the power-law approximation.

To highlight what is distinctive about the CPV distribution, we compare it with *Eigenvector* centrality computed on the same 2020 global production network.[3] The contrast is stark. The estimated tail index for *Eigenvector* centrality is $\zeta = 5.42$—nearly three times larger than that of CPV—indicating a far more symmetric distribution in which extreme realizations are orders of magnitude less likely. Unlike CPV, the power-law specification for *Eigenvector* centrality does not outperform the exponential ($R = 6.43$, $p = 0.026$), and the lognormal provides a significantly better fit ($R = 6.42$, $p = 0.034$). These results indicate that *Eigenvector* centrality lacks the heavy-tail structure that defines CPV.

Figure 5 visualizes the difference. Plotting the counter-cumulative distributions on log–log axes (with values normalized by their respective $x_{\min}$ cutoffs to align the tails), the CPV distribution declines gradually, consistent with $\zeta_{CPV} = 2.01$, while *Eigenvector* centrality collapses rapidly, consistent with $\zeta_{EIGEN} = 5.42$. The figure also reports the top 10 economy-industry pairs under each measure: there is no overlap whatsoever, underscoring that the two centrality concepts capture fundamentally different dimensions of network structure.

3.4 Domestic vs. Global Networks

Several studies of domestic US networks are closely related to our work, including Acemoglu et al. (2012), Ahern (2013), and Herskovic (2018), all of which rely on Input-Output Accounts

[3]See Appendix C.3 for definition of *Eigenvector* centrality and other centrality measures used later in the paper.

from the US Bureau of Economic Analysis. There are two key differences that distinguish our global production network from domestic ones. First, our production network decomposes the ultimate sources of value-added in global trade, while studies constructing domestic US networks typically rely on the bi-lateral links reflecting contributions to total domestic output. Second, due to the global nature of our study, we set all domestic edges to zero, while by construction, US domestic networks have non-zero domestic edges and no connection with nodes outside of the US. Including domestic edges would conflate within-country production structure with cross-border bridging, which is precisely the distinction our measure aims to capture.

To show the difference in information content between our CPV and domestic centrality measure, we construct yearly domestic US production networks spanning our sample 1995-2020. Similarly to the global networks, the domestic networks have directional edges based on TiVA. Domestic edges from node $n(r)$ to node $n(s)$ in the US economy equal the domestic inputs from industry r scaled by the gross exports of industry s.

In Acemoglu et al. (2012), the importance of a node in the domestic production network corresponds to the node's equilibrium share of total sales, which is captured by a centrality measure equivalent to *Eigenvector* centrality. A key implication is that industries with high general connectedness in the domestic network tend to be large in size. We compute *Eigenvector* centrality and CPV for US industries based on the domestic network, and compare their correlations with our global CPV. Results are reported in Table 3. Both domestic centrality measures have a negative correlation with our CPV, supporting our intuition that the information content of CPV is not reflected in domestic centrality measures. The negative sign arises because industries that are central domestically—large industries serving the internal US market—tend to be peripheral in the global bridging sense; their importance derives from domestic scale rather than from connecting international value chains.

Our domestic network is consistent with Acemoglu et al. (2012): the correlation matrix in Table 3 shows that the *Eigenvector* centrality and CPV from a domestic network are closely related to size, which we proxy with the industry's total output. However, CPV from the global production network has a correlation of only 0.06 with its size. This result reflects our choice of setting domestic links (edges) to zero in the global production network, allowing us to capture the effect of different nodes as bridges of flows across countries rather than their contribution to domestic GDP as in Acemoglu et al. (2012).

3.5 Intertemporal and Spatial Variations

The topology of the global production network has undergone a tectonic shift over the past three decades. While the industrial hierarchy remains relatively stable, with Water Transport, Wholesale and Retail, Basic Metals, and ICT/Electronics consistently ranking as top choke points, the geographic distribution of these strategic nodes has transformed dramatically. In what follows, we describe the most salient variations over this period.

The Rise of China and the Decline of the US. Figures 6 and 7 visualize the migration of these choke points from the West to the East. In 1995, the United States was the world's dominant choke point economy, dwarfing competitors like Germany and Singapore. By 2020, however, the US had fallen out of the top five, ranking 6^{th}. Conversely, China leapfrogged from a peripheral 35th rank in 1995 to become the 2^{nd} most critical choke point economy in 2020, eclipsed only by Germany. This realignment is not merely aggregate; it reflects specific industrial specializations. For instance, Singapore's high centrality stems from its role in moving commodities, while Taiwan's centrality is anchored in the ICT and Electronics sector. Notably, Ireland also surged from 48^{th} to 7^{th} place, driven by its growing importance as a global offshore hub.

The Impact of WTO Accession. We trace the acceleration of these trends specifically to China's entry into the World Trade Organization (WTO) in 2001. As illustrated in Figures 8 and 9, this event is associate with a massive rerouting of global shortest paths. Prior to accession in 1999, only 9.3% of global shortest paths passed through China. By 2004, this figure had surged to 21.6%. Crucially, supply chains connecting Asia to the US, which previously bypassed the mainland, were structurally rerouted to flow through China. Figure 9 confirms that China's rise came at the direct expense of US centrality: in 1996, 36.3% of shortest paths originating in Europe passed through the US, but by 2004, this share had collapsed to 19.7%. This evolution confirms that choke points are not static; they migrate in response to trade liberalization and industrial policy, creating new loci of structural fragility in the global economy.

4 Stylized Features of Choke Point Industries: Causal Identification

Having defined Choke Point Value as a topological measure of bridging or brokerage in the global production network, we next examine its economic content. We posit that CPV captures structural fragility: high-CPV industries are difficult to substitute in the short run and act as amplifiers of local shocks.

Our theoretical prior is grounded in the O-ring theory of economic development (Kremer, 1993), in which production consists of a sequence of complementary tasks, and the failure of a single input ("the O-ring") sharply reduces the value of final output. By analogy, we view choke point industries—located along efficiency-maximizing shortest paths in the global input-output network—as binding constraints in world production. In the short run, the edges connecting these nodes are subject to substantial adjustment frictions: firms face significant search, contracting, and logistical costs when attempting to reroute trade flows through longer paths. As noted in the introduction, in industries such as semiconductors, economically viable substitutes for TSMC's advanced chips are effectively unavailable at scale.

We evaluate these implications using two natural experiments that differentially stress substitutability and propagation. The 2022 Covid-19 lockdowns in China generated plausibly exogenous disruptions to the availability of intermediate inputs, providing a setting to test whether high-CPV industries are harder to replace. By contrast, the 2023–2024 Red Sea crisis primarily altered shipping routes and input costs, offering a laboratory to study how shocks originating near choke points propagate through the network and affect connected industries.

4.1 Low Substitutability: Evidence from the 2022 China Lockdowns

To test the hypothesis of low substitutability, we exploit the widespread Covid-19 lockdowns in China in 2022 as an exogenous supply shock. Unlike the initial 2020 outbreak, which conflated supply and demand shocks globally, the 2022 lockdowns were driven by domestic "Zero-Covid" policy mandates and were largely orthogonal to US economic fundamentals. Specifically, the lockdowns in Shanghai (the world's busiest port) and Shenzhen (a primary ICT hub) created

severe bottlenecks in industries we identify as high-CPV nodes, such as the ICT & Electronics and Chemicals industries. This setting offers a clean identification of substitutability. If US firms can easily substitute Chinese inputs, the suspension of these specific nodes should have minimal impact on US sales. Conversely, if these nodes are structural choke points, exposure should predict significant performance declines.

4.1.1 Average Effects

For each US industry j, we construct a measure of its network *Exposure* to the Chinese choke point industries. Specifically, we define exposure of industry j in US as the fraction of its global shortest paths that traverse the top five Chinese choke point industries:

$$\text{Exposure}_j = \frac{\sum_{p \in \mathcal{P}_j} \mathbb{1}(v_{China} \in p)}{|\mathcal{P}_j|} \tag{5}$$

where $\mathcal{P}_j$ is the set of all shortest paths originating or terminating in industry j. This measure captures direct and *indirect topological exposure*, e.g., risks inherited from upstream tier-N suppliers, which traditional direct trade volume data miss.

We estimate the impact of this exposure on the sales of US firms using a difference-in-differences (DiD) specification:

$$log(\text{Sales}_{j,t}) = \lambda \cdot log(\text{Exposure}_j) \times \text{Post}_t + \alpha_j + \gamma_t + \varepsilon_{j,t}, \tag{6}$$

where the dependent variable $\text{Sales}_{j,t}$ is the aggregate sales of industry j in quarter t in \$trillion, and Post_t is an indicator variable for the onset of the 2022 lockdowns. The regressions include industry fixed effects α_j and quarter fixed effects γ_t. The sample period spans the four quarters in 2021 and the four quarters in 2022, at the end of which China lifted its zero-Covid policy.

Our results, reported in Table 4, provide strong support for the low substitutability hypothesis. Column 1 shows that a 10% higher exposure to the top 5 choke point industries in China is associated with a 4% decline in quarterly sales in 2022 during the Covid-19 lockdowns. The effect is statistically significant and economically large. In Column 6, we discretize the exposure variable to be equal to one if a US industry is in the top quintile of exposure to Chinese choke point industries and zero otherwise. The resulting estimate of the sales decline is 14% per quarter, which is also statistically significant.

As a comparison, we construct two placebo exposure variables based on the a) top 5 Chinese industries in terms of gross exports to the US, and b) *Eigenvector* centrality. For both placebo exposure variable, we add the constraint that they are not part of the top 5 choke point industries used to compute our main exposure variable. Specifically, for each US industry i, we calculate the proportion of shortest paths—either originating from or terminating in i—that pass through the top five Chinese exporters to the US (top five Chinese industries in terms of *Eigenvector* centrality). We label this ratio $Exposure^{GX\ Placebo}$ ($Exposure^{EIG\ Placebo}$). Columns 2, 3, 6 and 7 in Table 4 show that the two placebo exposure variable have no meaningful impact on the sales of US firms during the 2022 lockdowns. In Columns 4, 5, 9 and 10 where we include our main exposure variable with either of the placebo variables, the strong impact of the exposure to choke point industries remains intact. The sharp contrast highlights the unique, low substitutability of choke point industries, different from industries with merely high export volume.

A potential confounding explanation is that the decrease in sales among US industries with high exposure to Chinese chock point reflects decreased imports by Chinese industries. To test for this demand-based explanation, we collect data on gross sales by US industries to China from the US Census Bureau. Columns 11 and 12 in Table 4 rule out the demand-based explanation, as exposure to Chinese choke points remains a statistically significant explanatory variable. Because granular export data is available only for industries in the Agriculture, Mining, and Manufacturing sectors, the number of observations for the demand-based test drops more than a half.

4.1.2 Dynamic Effects

The persistence of these effects is of critical interest. If nodes were easily substitutable (allowing firms to reroute flows through alternative edges), we would expect a transient, "V-shaped" recovery. Figure 10 visualizes the impact of the 2022 Chinese lockdowns on US industry sales. We partitioned the 43 US industries into two groups based on their exposure to China's top five choke points: the Top 22 (high exposure) and the Bottom 21 (low exposure). To facilitate comparison, we standardized the aggregate sales for both groups to 1 at the end of 2021. Prior to the lockdowns, the two series follow parallel trajectories, satisfying the parallel-trends assumption required for our difference-in-differences estimation. Post-disruption, however, a significant gap emerges: sales in highly exposed industries drop relative to the control group.

This divergence is not temporary; the shortfall persists through at least the end of 2023.

To formally examine the persistence of the impact on sales we use a Dynamic Difference-in-Differences specification:

$$\log(\text{Sales}_{j,t}) = \left(\sum_{i=1}^{4} \theta_i \cdot \mathbb{1}[t = 2021\text{Q}i] + \sum_{k=1}^{4} \beta_k \cdot \mathbb{1}[t = 2022\text{Q}k] \right) \times \log(\text{Exposure}_j) + \alpha_j + \gamma_t + \epsilon_{j,t}. \tag{7}$$

We expect the pre-event coefficients, θ_i, to be statistically indistinguishable from zero, thereby satisfying the parallel-trends assumption. Conversely, if the hypothesis of low substitutability for choke-point industries holds, the post-event coefficients, β_k, should be negative and statistically significant. Panel A of Figure 11 plots these point estimates alongside 95% confidence intervals. To avoid perfect multicollinearity in the presence of industry fixed effects, we omit the coefficient θ_1 to serve as the reference period. The results indicate no significant relationship between exposure to Chinese choke points and US firm sales prior to the shock. However, during the 2022 lockdowns, industries with higher exposure experienced persistent and significant declines in sales across all four quarters. While the estimate for β_4 is slightly attenuated, consistent with the official relaxation of lockdown measures in December 2022, the overall impact remains robust in the quarter. We perform an F-test of joint restrictions to assess whether the four estimated interaction coefficients during the 2022 lockdowns (β_1–β_4) differ across quarters. With a p-value of 0.405, we fail to reject the null hypothesis that these coefficients are equal. Hence, the marginal effect of log(Exposure) is statistically indistinguishable across the four quarters of 2022. Finally, a placebo regression using export volume-based exposure variables yields no significant effects in Panel B, further supporting the causal interpretation of our main results.

4.2 Shock Propagation: The Red Sea Crisis

Our second hypothesis posits that choke points act as accelerators, propagating idiosyncratic shocks globally. We test this using the 2023–2024 disruption of the Water Transport industry—a high-CPV node—caused by Houthi attacks in the Red Sea. This event serves as a natural experiment for a "link removal" shock in network theory, allowing us to identify how disturbances at a strategic node cascade through the global production network.

4.2.1 Identification Strategy

The Red Sea is a critical maritime artery, historically accommodating approximately 30% of global container traffic. Commencing in late 2023, attacks by Houthi militants forced a massive rerouting of merchant vessels around the Cape of Good Hope (Figure 12).[4] This diversion increased transit times by approximately 10 days and drove container spot rates up by 220% (Figure 13), constituting a severe supply-side shock to the global shipping network.[5]

To causally identify the propagation of this shock, we exploit the geometric specificity of the disruption. We construct a measure of Red Sea Exposure that isolates shortest paths strictly dependent on this maritime route. Specifically, we define a "Treated Path" as a shortest path that: (1) connects a node in Developed Europe to a node in Developed or Emerging Asia-Pacific (or vice versa); (2) traverses the Water Transport industry as an intermediate node; and (3) does not pass through any economy in North or South America. This third restriction ensures that our measure excludes trade flows naturally routed via the Pacific or the Panama Canal, thereby satisfying the exclusion restriction.[6]

We quantify this exposure for each economy-industry pair (s, j) as the fraction of all its shortest paths that are Treated Paths:

$$\text{Exposure}_{s,j} = \frac{\sum_{p \in \mathcal{P}_{s,j}} \mathbb{1}(p \in \text{Treated Paths})}{|\mathcal{P}_{s,j}|} \tag{8}$$

where $\mathcal{P}_{s,j}$ is the set of all shortest paths originating or terminating in industry j of economy s.

Figure 14 visualizes the propagation of this shock. The disruption radiates outward from the Bab el-Mandeb Strait, disproportionately affecting economies in Southeast Asia and Nordic economies such as Finland and Sweden, whose integration into global value chains relies heavily on European intermediaries. This heterogeneous exposure across economy-industry pairs provides the cross-sectional variation required for our difference-in-differences design.

[4]See `https://www.reuters.com/world/middle-east/maersk-diverts-vessels-away-red-sea-for-foreseeable-future-2024-01-05/`

[5]A typical container ship going from Singapore to Rotterdam would normally take 26 days via the Red Sea (8,500 nautical miles), but after the rerouting via the Cape of Good Hope it would take 36 days (11,800 nautical miles).

[6]Table D.1 in Appendix D.2 provides descriptive statistics for the top five Water Transport industries affected by the Houthi attacks.

4.2.2 Empirical Results

We estimate the impact of Red Sea exposure on equity returns using a difference-in-differences specification around the onset of the crisis. We define the event date as January 1, 2024, corresponding to the sharp spike in freight rates (Figure 13). Our baseline model is:

$$R_{s,j,t} = \lambda \cdot \left(\log(\text{Exposure}_{s,j}) \times \text{Post}_t\right) + \delta \cdot X_{s,j,t-1} + \alpha_{s,j} + \gamma_t + \epsilon_{s,j,t}, \tag{9}$$

where $R_{s,j,t}$ is the weekly abnormal return (CAPM alpha) on the portfolio of stocks in industry j of economy s, and Post_t is an indicator equal to one for the first four weeks of 2024. $\mathbf{X}_{s,j}$ is a vector of control variables, computed at the end of November 2023. The sample periods includes the last 4 weeks in 2023 and the first 4 weeks in 2024.

Table 5 presents the results. We find a statistically significant and economically large negative effect of exposure on stock returns. In Column 2, the interaction coefficient λ is negative and statistically significant, indicating that industries with higher reliance on the Red Sea route experienced a marked decline in valuations relative to less exposed peers. In terms of economic magnitude, a 10% increase in Red Sea exposure is associated with a 1.68% lower abnormal return per week during the initial month of the crisis. In Column 3 we include economy-industry level controls as well as the geographical distance between the country's capital and the Bab el-Mandeb strait (in logs of thousand kilometers).

These results are robust to the inclusion of economy $\times$ sector fixed effects (Column 4), which absorb all time-invariant shocks common to specific sectors within a country. This rules out the concern that our results are driven by general regional headwinds or sector-specific trends unrelated to the shipping disruption.

Next, to confirm that network propagation is the primary mechanism, we conduct a placebo test using *Direct Links*. We construct an alternative exposure measure based solely on the direct input-output reliance of an industry on the Water Transport sector, ignoring the higher-order network structure. As reported in Column 5, this direct measure fails to predict abnormal returns. This null result for direct exposure, contrasted with the strong predictive power of our network-based measure, provides compelling evidence that the economic damage of the Red Sea crisis was transmitted primarily through the complex, multi-step linkages identified by our CPV framework, rather than through simple bilateral trade dependencies.

Finally, we examine whether the parallel pre-trends condition holds. We split the global sample of economy-industry pairs into two groups based on their exposure to the Red Sea Crisis: the Top 214 (high exposure) and the Bottom 213 (low exposure). For each of those groups, we compute an aggregate alpha as the value-weighted weekly alpha of the individual economy-industry pairs. Figure 15 plots the evolution of the sum of weekly aggregate alphas, starting 8 weeks before the event. It shows that the two time-series follow roughly parallel trajectories prior to the event, without a clear pre-trend. Following the chosen start of the event, we observe a large and persistent gap in the alphas of the treated group relative to the control group.

5 Choke Points and Asset Prices

We now turn to the core empirical question: is the risk associated with these choke points priced? We employ two standard methodologies: univariate portfolio sorts to establish the existence of the premium, and Fama-MacBeth cross-sectional regressions to control for covariates. Then we study the economic mechanism through the channel of aggregate consumption risk.

5.1 Choke Points and Stock Returns

5.1.1 Portfolio Analysis

To investigate the pricing of structural fragility, we construct value-weighted portfolios of publicly traded stocks within each economy-industry pair, and study their returns in relation to CPV. At the end of each year, we sort economy-industry pairs into quintile portfolios, based on their CPV. We next track their returns during the next year, after which we rebalance. Note that we value-weight stocks within each economy-industry as well as within each portfolio. Hence, the total portfolios are also value-weighted. In Panels A and B of Table 6, we present the portfolios' excess returns and risk-adjusted returns, using an asset pricing model consisting the global Fama-French 5 factors plus Momentum.

We find that the returns of top CPV portfolio (Q5) exceed those of the bottom CPV portfolio (Q1) by more than 6% per year. The risk-adjusted performance shows similar magnitudes, and we find a monotonically-increasing pattern of risk-adjusted returns. The top portfolio delivers an alpha of 0.21% per month ($t = 2.51$), while the bottom portfolio acts as a hedge with an alpha of -0.40% per month ($t = -2.97$). The spread of 0.60% per month is highly statisti-

cally significant ($t = 3.87$). Thus, choke points command both a statistically significant and an economically large premium. We further find a pattern of increasing market beta with CPV. This finding is consistent with our prediction that choke point disruptions propagate to the aggregate economy, creating systematic rather than idiosyncratic risk; the rising beta reflects the growing contribution of high-CPV industries to aggregate market fluctuations.

In Panel C, we examine the robustness of our findings and report alphas for the spread portfolio using alternative risk-adjustment models. Two potential concerns motivate these tests: first, that the premium may reflect time-varying exposures to global and local risk rather than a distinct source of compensation; second, that the choice of factor model may drive the result. To address the first concern, we compute alphas from two global CAPM models that allow for time-varying exposures. Following Bekaert et al. (2009), we compute alphas from two global CAPM models taking into account time-varying exposures to a global and a local portfolio. During our sample period, emerging economies have largely increased their share in global trade, pointing to potential time-variation in their exposures to global risk. To take this into account, each month we compute betas using the previous 36 months of economy-industry returns and a value-weighted index of all non micro-cap stocks in Compustat. Next, we use the estimated loadings and this month's realization of the world market portfolio to compute alphas. We again value-weight all alphas, after which we re-estimate betas and proceed with next month's alphas. The result from this World CAPM ($WCAPM$) model show a similar spread in performance between the top and bottom portfolios. We augment the model using a value-weighted local portfolio, covering all stocks within the region of the economy-industry pair. We follow the same classification used to allocate countries to regions based on geographical location and economy development as in Table 1. Following Bekaert et al. (2009), we orthogonalize the local factor to the global market portfolio and estimate time-varying exposures as in the $WCAPM$ model. The alphas from this World-Local CAPM ($WLCAPM$) are economically smaller, but still statistically different from zero.

To address the second concern—factor model choice—we present alphas for the spread portfolio using different subsets of the six factor model used in Panel A and find consistent results. Finally, we also compute using local Fama-French models, where we assign each economy-industry pair to its closest set of local Fama-French factors, available on Ken French's website. Similarly to the $WCAPM$ and $WLCAPM$ modes, each month we estimate time-varying betas

using the previous 36 months and then use the estimated betas and this month's factor realizations to estimate this month's economy-industry alpha. We value-weight alphas within each portfolio and the compute average alphas per portfolio. Again, we find that the spread portfolio exhibits positive alphas that are statistically different from zero.

5.1.2 Fama-MacBeth Regressions

To examine the robustness of the portfolio sorts, we perform Fama-MacBeth regressions of monthly excess returns on lagged CPV, controlling for economy-industry and economy characteristics. Results are reported in Table 7. To ease the interpretation of the estimated coefficients, we use the percentile of CPV, ranging from 0 to 100. In specification (1), we include the economy-industry beta β, log of book equity $log(BookEquity)$, and log of market equity $log(MarketEquity)$.[7] The estimated coefficient of the CPV percentile is 0.004 ($t = 2.79$), implying that a move from the 50^{th} to the 60^{th} percentile of CPV translates into an additional 0.5% per year ($10 \times 0.004\% \times 12$). This is an economically large effect.

In specifications (2) and (3), we include several other financial characteristics, known to predict returns: $Profitability$, $Dividends$, Ret^{m1} and $Ret^{m2:m12}$. In specification (4) we additionally include economy variables: $log(POPULATION)$, $\Delta GDPHEAD$, ΔCPI, and $FX\ RET$. They may reflect unobservables of economic development or macroeconomic risk otherwise correlated with both CPV and expected returns. The results are consistent. We also control for the scale of economic activity, using $log(Gross\ Output)$. Larger economy-industry pairs may earn different expected returns due to size-related risk exposures, market power, or because they participate more heavily in global trade flows. We also include $Value\ Added\ Share$ since economy-industry pairs with higher value-added intensity may differ systematically in technology, capital intensity, and other unobservable characteristics. The inclusion of the two control variables from the World Input-Output Tables (WIOT) in specification (5) does not change the impact of CPV on subsequent returns. In specification (6), we also include an economy-level beta $\beta^{Country}$, computed analogously to the economy-industry beta β. Again, the effect of CPV on subsequent stock returns remains statistically significant. Thus, the excess returns associated with choke points is unlikely to be attributed to economy-industry and economy characteristics.

[7] We estimated an economy-industry beta using a CAPM model and 60 months of past monthly data. We require at least 24 available monthly returns to compute the betas. We estimate economy betas and betas with respect to transportation costs in a similar way.

5.2 Choke Points and Consumption Risk

Our analysis of the Red Sea crisis in the preceding section illustrates that exogenous, idiosyncratic shocks to choke points tend to propagate throughout the global production network, thereby generating a non-negligible aggregate impact. For such a disruption risk to be priced in the stock market, the negative aggregate impact arising from choke point industries should be correlated with the consumption risk of aggregate households, the central idea in consumption-based asset pricing models (e.g., Rubinstein, 1976; Breeden, 1979). That is, if negative shocks to choke point industries coincide with an increase in the marginal utility of representative households/investors, i.e., a decline in their consumption growth, they require higher expected returns to hold the stocks of choke point industries as compensation for the additional exposures to consumption risk.

A natural approach to testing this link would be to compute contemporaneous consumption betas for each portfolio. However, as Parker and Julliard (2005) recognize in their seminal work, asset prices tend to react instantaneously to negative shocks, whereas reported aggregate consumption responds only gradually, due to measurement error and frictions leading to slow adjustments. This mismatch renders contemporaneous consumption betas unreliable. Exploiting their insight, we instead perform predictive regressions, using the return spread between high and low choke point industries to predict future aggregate consumption growth.

The dependent variables in these regressions involve aggregate consumption of US, developed economies excluding US, all developed economies, and the world. The US stands out, thanks to two features: its high US consumption share of the world, and its high dependence on global production networks for consumption needs. We collect quarterly economy-level data on seasonally-adjusted real consumption in constant prices from the IMF, supplemented with hand-collected observations for economies the IMF does not cover, including China, Hong-Kong, Taiwan, Russia, and Malaysia. Some of our specifications include data on industrial production that we collect from the World Bank. When we aggregate the data, we weigh economy-level observations with the lagged value of their GDP in PPP.

We regress four quarter (continuously compounded) growth in consumption on lagged yearly return of the spread portfolio from Table 6 that is long in high CPV economy-industry pairs and short in low CPV economy-industry pairs. Depending on the specification, we control for the lagged yearly return of the market, common asset pricing factors (SMB, HML, MOM,

CMA, RMW), a business cycle proxy – industrial production, lagged values of the dependent variable, the term premium in the USA and the change in the market yield on US treasury securities at 2-year constant maturity during the previous 12 months. Results are reported in Table 8, where Panel A presents results for the USA. Across all specifications, we find a positive and statistically significant coefficient of return of the CPV spread portfolio. Hence, drops in the returns of high CPV economy-industry pairs relative to their peripheral counterparts is associated with a decrease in subsequent consumption. In Panel B, we aggregate the data across all developed countries, excluding the USA. Results are similar. Hence, the relationship between the performance of choke points and subsequent consumption is not limited to the USA, but extends to other developed markets. In Panel C, we show similar results for all developed markets. Finally, in Panel D, we aggregate the consumption data across all countries, including emerging ones. Again, we find a positive relationship between the performance of choke point industries and subsequent consumption, albeit the coefficient is not statistically significant in all specifications.

Next, we examine the predictive power of the spread portfolio over horizons ranging from one to eight quarters. Specifically, we perform regressions where the dependent variable is cumulative growth in real (constant prices, seasonally-adjusted) consumption between quarters t and $t+i$, where i ranges from 1 to 8. We include the full set of controls from Table 8 and visualize the estimated coefficients on the spread portfolio in Figure 16. Depending on the set of countries included in the analysis, it takes 2 to 3 quarters for the return of the spread portfolio to have a statistically significant impact on the consumption growth. The impact of the spread portfolio on subsequent consumption growth appears to be persistent, as we observe no long-term impact of CPV on consumption growth beyond quarter 4. In Appendix D.3 we present additional evidence on the persistent impact of CPV on consumption growth and in Appendix D.4 we show that the relationship between CPV and consumption growth reflects broader macroeconomic fluctuations, as measured by GDP growth.

The persistent, multi-quarter impact of the CPV spread on consumption growth is consistent with the long-run risk interpretation outlined in the introduction. Under the framework of Bansal and Yaron (2004), assets that contain information about persistent shifts in expected consumption growth command a premium even when contemporaneous consumption responses are modest. Our evidence that choke point returns predict consumption growth over horizons of

two to four quarters—well beyond the initial shock—suggests that CPV captures information about the trajectory of aggregate consumption, not merely its level. This maps naturally onto the long-run risk channel (Hansen et al., 2008), though a full structural estimation is beyond the scope of the current paper.

6 Alternative Interpretations and Further Analyses

6.1 Alternative Interpretations: Double Sorts

The preceding analysis establishes that choke points earn a significant risk premium linked to aggregate consumption risk. A natural concern is that this premium may be driven by confounding factors rather than structural network fragility. We address this concern through a comprehensive series of double-sort analyses, organized around three categories of alternative explanations: (i) firm fundamentals—profitability and size; (ii) other network characteristics—concentration, sparsity, and eigenvector centrality; and (iii) exposure to related macroeconomic risks—globalization, supply chain stress, and geopolitical risk.

6.1.1 Rent Extraction Hypothesis: Profitability

One potential alternative explanation is that the CPV premium reflects differences in profitability rather than compensation for risk. If firms in choke points are systematically more profitable or have stronger operating margins, then the CPV premium might arise because they have different cash-flow fundamentals rather than because they drive the fragility of global production networks. To rule out this explanation, we conduct a double sort that first sorts economy-industry pairs by $Profitability$ and then sorts within those groups by CPV. Alphas of the double sorted portfolios are reported in Panel A of Table 9. $Profitability$ appears to generate a spread in alphas only for economy-industry pairs with low CPV. We further observe that the spread portfolio long in high CPV and short in low CPV generates significantly positive alphas for economy-industry pairs with low and medium degree of $Profitability$. Thus, the difference in $Profitability$ cannot account for the CPV premium that we document.

6.1.2 The Time-Varying Network Structure Hypothesis: Network Concentration and Sparsity

Herskovic (2018) studies changes in the topology of the production network over time and finds there are two network characteristics with asset pricing implications: network sparsity and network concentration. Sparsity quantifies the distribution of the size of the edges, while concentration characterizes the distribution of the sizes of the nodes. He shows that innovations in concentration and sparsity factors are priced risk factors in the domestic US production network. The main difference with us is that his focus is on the time-variation in the network topology within the USA while ours is on the cross-sectional differences in the ability of nodes to bridge flows across value chains. Differences in the location of choke points may nevertheless reflect changes in the network sparsity and concentration. To investigate this possibility, we track the returns of economy-industry portfolios double sorted on network concentration betas $\beta^{Concentration}$ (or network sparsity betas $\beta^{Sparsity}$) and CPV. We report alphas in Panels B and C of Table 9. We find that CPV has an explanatory power over and above the economy-industry pairs' betas with network concentration (Panel A) and network sparsity (Panel B). Thus, the abnormal returns associated with choke points cannot be attributed to the changes in the network topology studied by Herskovic (2018).

6.1.3 The Connectedness Hypothesis and Size Effect

Acemoglu et al. (2012) show that the importance of individual nodes in a production network can be summarized with a centrality measure closely resembling *Eigenvector* centrality. In addition, Ahern (2013) finds that industries characterized with high *Eigenvector* centrality earn higher returns in the domestic US production network. Thus, another potential alternative explanation is that CPV reflects the general connectedness of nodes reflected by *Eigenvector* centrality. To assess this possibility, we double sort economy-industry pairs on their *Eigenvector* centrality in the global production network and then CPV. We present alphas of the double-sorted portfolios in Panel D of Table 9. Consistent with Acemoglu et al. (2012) and Ahern (2013), economy-industry pairs with high *Eigenvector* centrality have higher alphas. However, economy-industry pairs with high CPV have alphas higher than their peripheral counterparts, even after accounting for *Eigenvector* centrality. Thus, choke points' ability to bridge flows across the global production network contains information about future return beyond the

general connectedness of nodes, associated with *Eigenvector* centrality.

As we explain in Section 3.4 and following Acemoglu et al. (2012), industries central to the domestic network are likely to be large in size. To disentangle the impact of size and choke points, we double sort economy-industry pairs in portfolios based on $MarketEquity$ and then CPV. The alphas of the double-sorted portfolios are presented in Panel E of Table 9. We find that the abnormal return premium associated with choke points is particularly strong among economy-industry pairs that are large in size. We also consider the total output of the economy-industry pair as an alternative measure of size as it captures total global sales. Results, reported in Appendix D.6, indicate that CPV explains alphas also over and above this alternative measure of economy-industry size. Thus, the CPV premium cannot be attributed to the size of the economy-industry pairs.

6.1.4 Globalization and Supply Chain Pressures

Barrot et al. (2019) show that firms operating in industries with low shipping costs face a greater risk of displacement by foreign competitors, and that this displacement risk is priced among US industries. This raises another potential alternative explanation for our CPV premium: choke point industries may be characterized with low shipping costs and therefore command the globalization risk premium in Barrot et al. (2019). To test this, we first sort economy-industry pairs based on their beta with respect to the transportation cost factor of Barrot et al. (2019) ($\beta^{TransporatationCosts}$). We estimate these betas in regressions of monthly returns on monthly changes in the transpiration cost factor of Barrot et al. (2019) during the last five years, requiring at least 24 valid monthly observations. Next, we additionally sort portfolios based on CPV. Alphas of the double-sorted portfolios are reported in Panel F of Table 9. Consistent with Barrot et al. (2019), we find strong evidence of a globalization risk premium – economy-industry pairs with high $\beta^{TransporatationCosts}$ have lower alphas than their counterparts characterized with low sensitivity to shipping costs. However, CPV explains alphas over and above $\beta^{TransporatationCosts}$. Thus, the abnormal returns associated with choke points are not driven by the displacement risk documented in Barrot et al. (2019).

We also examine if the CPV premium reflects compensation for exposure to global supply-chain stress rather than structural fragility. Industries that occupy central positions in global production networks are also likely to be more sensitive to fluctuations in the tightness of

global supply chains. Lieberman et al. (2025) show that industries with high exposure to supply-chain stress, measured by the Global Supply Chain Pressure Index (GSCPI) of Benigno et al. (2022), earn higher expected returns. This raises the possibility that our CPV measure captures systematic supply chain risk exposure. To address this, we estimate industry-level GSCPI betas β^{GSCPI} and conduct a double sort on those GSCPI betas and CPV. We estimate β^{GSCPI} in regressions of monthly returns on monthly changes in GSCPI during the last five years, requiring at least 24 valid monthly observations. The results of the double sorts are presented in Panel F of Table 9. We find that high CPV economy-industry pairs have higher alphas than low CPV ones among both low and high GSCPI beta portfolios. Thus, exposure to global supply-chain stress cannot explain the CPV return premium.

6.1.5 Geopolitical Risk

Last, we consider whether choke point industries earn higher returns because they are more exposed to geopolitical risk. Choke points may coincide with industries located in politically sensitive economies or along physically vulnerable trade routes, making them candidates for carrying high geopolitical-risk betas. To rule out the possibility that the premia for choke point is capturing geopolitical risk, we estimate geopolitical-risk betas using the news-based geopolitical risk index of Caldara and Iacoviello (2022) and conduct double sorts on these betas and CPV. First, for each economy-industry pair, we estimate a geopolitical risk beta $\beta^{GeopoliticalRisk}$ by regressing weekly returns on weekly changes in the geopolitical risk index during the portfolio formation year. We sort our economy-industry pairs in portfolios, based on their geopolitical risk beta. Next, we double-sort on CPV. We report alphas in Panel G of Table 9. Among low and medium geopolitical risk portfolios, economy-industry pairs with high CPV have statistically higher alphas than economy-industry pairs with low CPV. Hence, the information content of CPV is not subsumed by geopolitical risk betas. Our performance results are therefore unlikely to be attributed to sensitivities to geopolitical risk.

6.2 Alternative Measures of Centrality

Our Choke Point Value (CPV) captures how frequently an economy-industry pair lies on the shortest paths that connect other nodes within the global production network. Thus, CPV identifies economy-industry pairs whose position makes them critical conduits for the flow of

intermediate goods and services. While CPV emphasizes the connectivity of the network, other network features, such as the scale of flows an industry receives from abroad or provides to the rest of the world, may also be relevant for explaining differences in expected returns. To assess whether CPV contains information beyond these alternative forms of centrality, we construct measures of foreign dependence and foreign influence and study whether they subsume the CPV's predictability of subsequent returns. Appendix C provides a definition of all centrality measures with a correlation matrix in Table C.1.

There are several measures of foreign dependence, used in the literature. The impact of first-degree connections is captured by *Weighted Indegree*, which sums all edges leading to a node. In our setup, that translates to the total reliance on foreign sourcing of an economy-industry pair. To capture the broader, recursive reliance of an economy-industry pair beyond its immediate suppliers, we use *Eigenvector* centrality, which assigns higher scores to nodes that are connected to other highly central nodes.[8] In this way, the importance of an economy-industry pair reflects not only its direct foreign sourcing, but also the systemic importance of the nodes on which it relies. Closely related to *Eigenvector* centrality is *Katz-Bonacich* centrality, which has an additional parameter that can adjust the influence of distant nodes (Katz, 1953; Bonacich, 1987). Economy-industry pairs with high values on these centrality measures typically come from the manufacturing sectors of countries that are resource-dependent on foreign countries.

The *Weighted Indegree*, *Eigenvector* centrality and *Katz-Bonacich* centrality essentially capture the same information, with correlations among them higher than 0.96. We assess the information content of CPV relative to *Eigenvector* centrality by including both measures in predictive Fama-MacBeth regressions. The results, reported in specification (1) of Table 10, show that CPV explains future returns over and above the *Eigenvector* centrality. The results are consistent with the double-sorts presented in Panel D of Table 9. Using *Katz-Bonacich* centrality and *Weighted Indegree*, we find similar results (specifications (2) and (3)). In addition, we define *In-Closeness* centrality as the reciprocal of the average cost of weights of the shortest paths *ending* in a node. Recall that the cost of an edge within a shortest path is the reciprocal of the directed link between two nodes. Nodes with high *In-Closeness* centrality are therefore lying at the end of production paths with heavy global flows. We find that *In-Closeness* centrality does not subsume the effect of CPV on future stock returns (specification (4)).

[8]This is the same centrality measure we use in the double sorts in Panel D of Table 9.

We extend the set of centrality measures with measures of foreign influence. First, we consider *Weighted Outdegree*, which sums all edges outgoing from a node. The measure is analogous to *Weighted Indegree* and captures the direct impact of an economy-industry pair on its customers. We also define *Out-Closeness* centrality as the reciprocal of the average sum of costs of the shortest paths *originating* from a node. Thus, nodes with high *Out-Closeness* centrality are economy-industry pairs important as suppliers for downstream consuming industries. Similarly to CPV, some of the top economy-industry pairs with high out-closeness centrality include the Wholesale and Retail industries (e.g. USA and China). This reflects the importance of commodity suppliers in the global production network. The measure also captures the importance of crude-oil producing countries, such as Russia and Saudi Arabia. The two measures of foreign influence are naturally closely related, with a correlation of 0.92. The results in the last two specifications of Table 10 show that CPV is a stronger predictor of future performance than the two measures of foreign influence. Overall, our results indicate that CPV predicts subsequent returns better than any of the other centrality measures.

6.3 Additional Results

6.3.1 Persistence of Return Predictability

One potential caveat with our pricing tests is that we use the most recent production network to construct centrality. Naturally, there would be a delay before the data on global trade becomes public or before market participants are able to infer the choke points using alternative data. We therefore replicate the univariate portfolio sorts using a lagged CPV instead of the most-recently available one. Results are summarized in Table 11. We report the excess returns and abnormal returns from various asset pricing models for the low and high portfolio, as well as for the spread portfolio. We find results consistent with those in Table 6. The abnormal return of the spread portfolio remains statistically different from zero across all asset pricing models.

7 Conclusion

This paper investigates the structural fragility of global production networks and its implications for asset prices. By constructing a dynamic network from World Input-Output Tables spanning 1995 to 2020, we propose a novel measure, Choke Point Value (CPV), to identify strategic

industries that serve as critical bridges in global value chains. Unlike traditional centrality measures that focus on local importance or size, CPV captures the geometric "bottlenecks" of the global economy—nodes through which a disproportionate volume of the network's shortest paths traverse.

Our analysis documents significant shifts in the topology of global production over the past decades. We observe a secular migration of choke points from the United States to Asia, particularly following China's entry into the WTO. Through the lens of two quasi-natural experiments—the 2022 Covid-19 lockdowns in China and the Houthi blockade of the Red Sea—we validate the economic materiality of these choke points. The evidence confirms that these industries are characterized by low substitutability and a high propensity to propagate idiosyncratic shocks, generating cascading disruptions to treated firms and economies.

Crucially, we show that this structural importance translates into a distinct risk premium in global stock markets. A portfolio strategy long in high CPV industries and short in peripheral industries generates an annualized alpha exceeding 6%, a spread that cannot be explained by standard international factor models, industry concentration, or profitability. We establish that this premium represents compensation for aggregate consumption risk; downturns in choke point industries are a strong predictor of subsequent declines in U.S. and global consumption growth.

These findings offer a new perspective on the "fragility" of the global economy. While the integration of global value chains has enhanced efficiency, it has created exposure to specific strategic nodes where risks accumulate. For investors, identifying these choke points provides a metric for assessing non-diversifiable, priced risk. For policymakers, our results highlight that supply chain resilience is not merely a matter of domestic capacity, but of understanding the complex geometry of global flows. As geopolitical tensions and economic nationalism reshape global trade, future research should examine the endogenous formation of these choke points and how corporate efforts to diversify supply chains might alter the risk premia associated with these structural vulnerabilities.

References

Acemoglu, D., Carvalho, V. M., Ozdaglar, A., and Tahbaz-Salehi, A. (2012). The network origins of aggregate fluctuations. *Econometrica*, 80(5):1977 – 2016.

Acemoglu, D. and Tahbaz-Salehi, A. (2024). The macroeconomics of supply chain disruptions. *The Review of Economic Studies*, pages 1–40.

Ahern, K. (2013). Network centrality and the cross section of stock returns. *Working Paper*.

Alstott, J., Bullmore, E., and Plenz, D. (2014). powerlaw: A Python Package for Analysis of Heavy-Tailed Distributions. *PLoS ONE*, 9(1):e85777.

Antràs, P. and Chor, D. (2022). Global value chains. In Gopinath, G., Helpman, E., and Rogoff, K., editors, *Handbook of International Economics: International Trade*, volume 5, pages 297–376. Elsevier.

Antràs, P., Chor, D., Fally, T., and Hillberry, R. (2012). Measuring the upstreamness of production and trade flows. *American Economic Review*, 102(3):412–16.

Bansal, R. and Yaron, A. (2004). Risks for the long run: A potential resolution of asset pricing puzzles. *The Journal of Finance*, 59(4):1481–1509.

Baqaee, D. R. and Farhi, E. (2019). The macroeconomic impact of microeconomic shocks: Beyond hulten's theorem. *Econometrica*, 87(4):1155–1203.

Barro, R. J. (2006). Rare disasters and asset markets in the twentieth century. *The Quarterly Journal of Economics*, 121(3):823–866.

Barrot, J.-N., Loualiche, E., and Sauvagnat, J. (2019). The globalization risk premium. *The Journal of Finance*, 74(5):2391–2439.

Barrot, J.-N. and Sauvagnat, J. (2016). Input specificity and the propagation of idiosyncratic shocks in production networks *. *The Quarterly Journal of Economics*, 131(3):1543–1592.

Bekaert, G., Hodrick, R. J., and Zhang, X. (2009). International stock return comovements. *The Journal of Finance*, 64(6):2591–2626.

Benigno, G., Giovanni, J. D., Groen, J. J. J., and Noble, A. I. (2022). The gscpi: A new barometer of global supply chain pressures. Staff Reports 1017, New York, NY.

Bonacich, P. (1987). Power and centrality: A family of measures. *American Journal of Sociology*, 92(5):1170–1182.

Breeden, D. T. (1979). An intertemporal asset pricing model with stochastic consumption and investment opportunities. *Journal of Financial Economics*, 7(3):265–296.

Caldara, D. and Iacoviello, M. (2022). Measuring geopolitical risk. *American Economic Review*, 112(4):1194–1225.

Carvalho, V. M., Nirei, M., Saito, Y. U., and Tahbaz-Salehi, A. (2021). Supply chain disruptions: Evidence from the great east japan earthquake*. *The Quarterly Journal of Economics*, 136(2):1255–1321.

Clauset, A., Shalizi, C. R., and Newman, M. E. J. (2009). Power-Law Distributions in Empirical Data. *SIAM Review*, 51(4):661–703.

Cohen, L. and Frazzini, A. (2008). Economic links and predictable returns. *The Journal of Finance*, 63(4):1977–2011.

Dijkstra, E. (1959). A note on two problems in connexion with graphs. *Numerische Mathematik*, 1:269–271.

Elliott, M., Golub, B., and Leduc, M. V. (2022). Supply network formation and fragility. *American Economic Review*, 112(8):2701–47.

Elliott, M. and Jackson, M. O. (2024). Supply Chain Disruptions, the Structure of Production Networks, and the Impact of Globalization. Working Paper, available at: `https://ssrn.com/abstract=4580819`.

Feenstra, R. C., Inklaar, R., and Timmer, M. P. (2015). The next generation of the Penn World Table. *American Economic Review*, 105(10):3150–82.

Freeman, L. C., Borgatti, S. P., and White, D. R. (1991). Centrality in valued graphs: A measure of betweenness based on network flow. *Social Networks*, 13(2):141–154.

Gabaix, X. (2011). The granular origins of aggregate fluctuations. *Econometrica*, 79(3):733–772.

Gabaix, X. (2012). Variable rare disasters: An exactly solved framework for ten puzzles in macro-finance. *The Quarterly Journal of Economics*, 127(2):645–700.

Gofman, M., Segal, G., and Wu, Y. (2020). Production Networks and Stock Returns: The Role of Vertical Creative Destruction. *The Review of Financial Studies*, 33(12):5856–5905.

Hansen, L. P., Heaton, J. C., and Li, N. (2008). Consumption strikes back? measuring long-run risk. *Journal of Political Economy*, 116(2):260–302.

Herskovic, B. (2018). Networks in production: Asset pricing implications. *The Journal of Finance*, 73(4):1785–1818.

Hou, K., Karolyi, G. A., and Kho, B.-C. (2011). What factors drive global stock returns? *The Review of Financial Studies*, 24(8):2527–2574.

Hummels, D., Ishii, J., and Yi, K.-M. (2001). The nature and growth of vertical specialization in world trade. *Journal of International Economics*, 54(1):75–96.

Jensen, T. I., Kelly, B., and Pedersen, L. H. (2023). Is there a replication crisis in finance? *The Journal of Finance*, 78(5):2465–2518.

Johnson, R. C. (2018). Measuring global value chains. *Annual Review of Economics*, 10(Volume 10, 2018):207–236.

Johnson, R. C. and Noguera, G. (2017). A portrait of trade in value-added over four decades. *Review of Economics & Statistics*, 99(5):896 – 911.

Karolyi, G. A. and Stulz, R. M. (2003). Are financial assets priced locally or globally? In Constantinides, G. M., Harris, M., and Stulz, R. M., editors, *Handbook of the Economics of Finance*, volume 1B, pages 975–1020. Elsevier.

Katz, L. (1953). A new status index derived from sociometric analysis. *Psychometrika*, page 39–43.

Kremer, M. (1993). The o-ring theory of economic development. *The Quarterly Journal of Economics*, 108(3):551–575.

Leontief, W. (1986). *Input-Output Economics*. Oxford University Press.

Lieberman, P., Mihov, A., Naranjo, A., and Velikov, M. (2025). Show me the receipts: B2b payment timeliness and expected returns. *Journal of Financial Economics*, 172:104108.

Lucas, Jr., R. E. (1977). Understanding business cycles. *Carnegie-Rochester Conference Series on Public Policy*, 5(1):7–29.

Menzly, L. and Ozbas, O. (2010). Market segmentation and cross-predictability of returns. *The Journal of Finance*, 65(4):1555–1580.

Miller, C. (2022). *Chip War: The Fight for the World's Most Critical Technology*. Scribner, New York.

Opsahl, T., Agneessens, F., and Skvoretz, J. (2010). Node centrality in weighted networks: Generalizing degree and shortest paths. *Social Networks*, 32(3):245–251.

Parker, J. A. and Julliard, C. (2005). Consumption risk and the cross section of expected returns. *Journal of Political Economy*, 113(1):185–222.

Ramírez, C. A. (2024). Firm networks and asset returns. *The Review of Financial Studies*, 37(10):3050–3091.

Richmond, R. J. (2019). Trade network centrality and currency risk premia. *The Journal of Finance*, 74(3):1315–1361.

Rubinstein, M. (1976). The valuation of uncertain income streams and the pricing of options. *The Bell Journal of Economics*, 7(2):407–425.

Figure 3: Shortest Paths Examples

This figure presents several shortest paths and direct paths in the global production network for 2020. The thickness of the line between two nodes represents the edge, labeled as percentage.

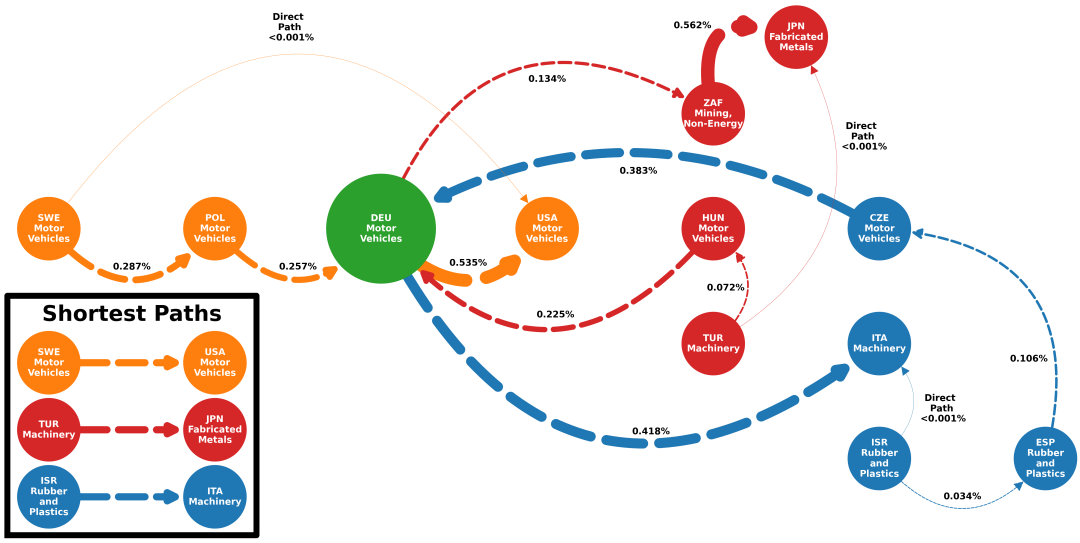


Figure 4: The Economy-Industry Global Production Network in 2020

This figure presents a visual representation of the global production network in 2020, where each node is an economy-industry pair. The thickness of the arrow from node A to node B represents the total number of shortest paths passing from node A to node B. The size of the node represents the total number of shortest paths passing via the node, i.e. the node's Choke Points Value. We group nodes into seven groups, based on the geography and economic development, following the classification in Table 1. Within each group of nodes, we place all manufacturing industries in the outer circle, all business services industries in the middle circle, and all other industries in the inner circle.

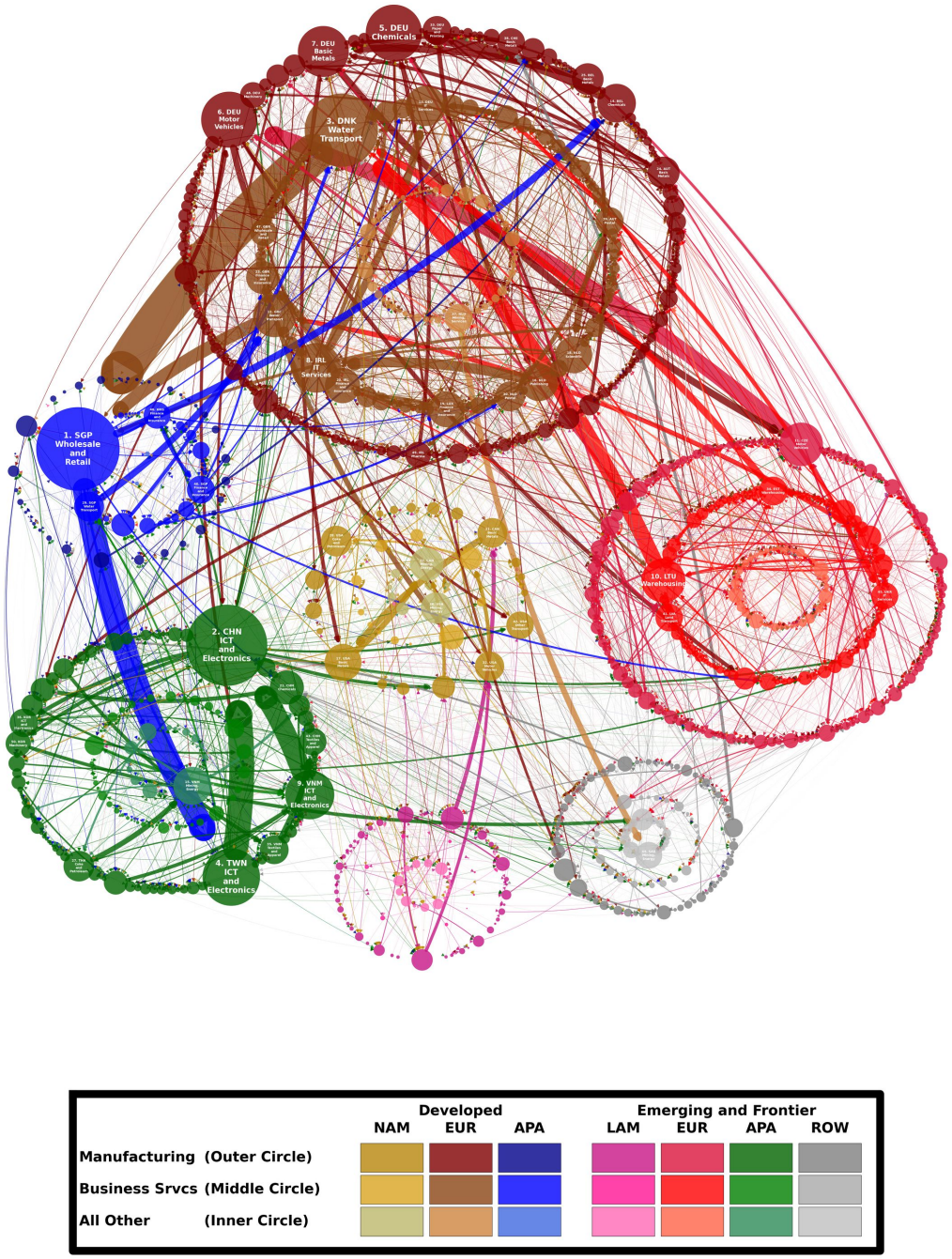
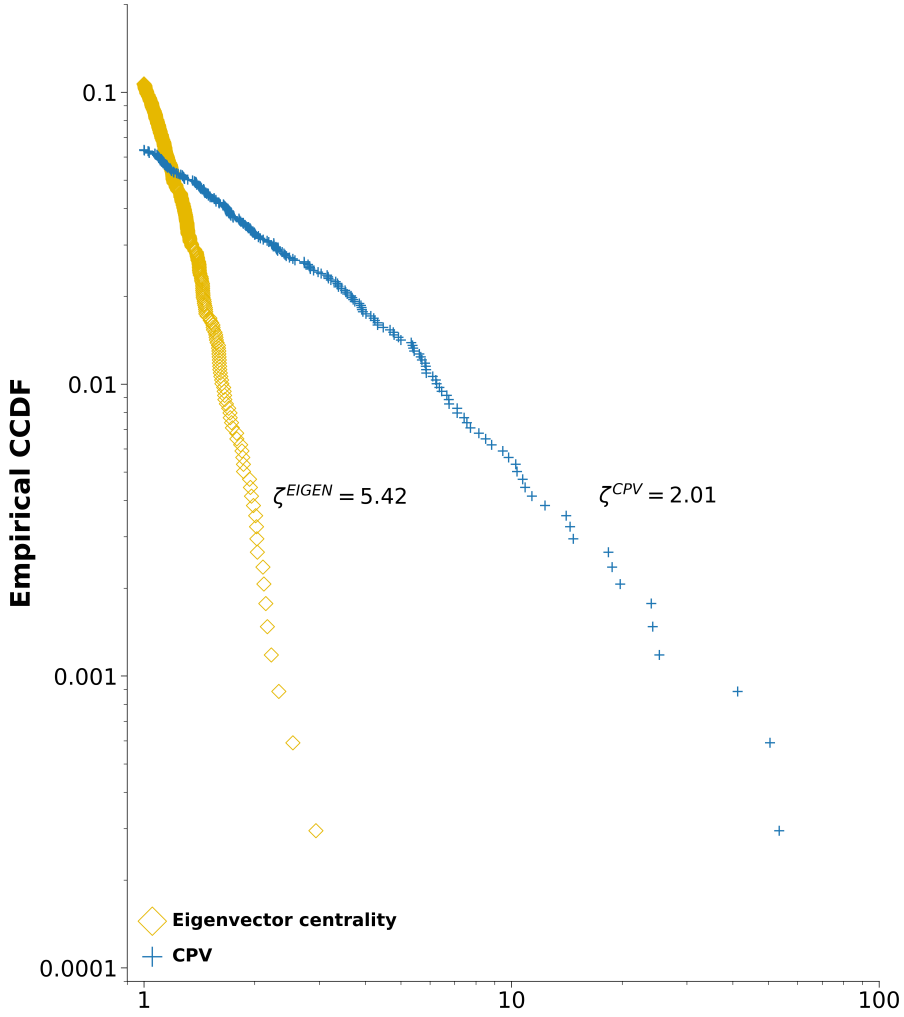


Figure 5: Tail Distributions of Choke Point Value and Eigenvector Centrality for year 2020

This figure presents the 2020 tail distributions of Choke Point Value (CPV, blue +) and Eigenvector Centrality (orange ◇). For each measure, the sample is restricted to observations above the estimated lower cutoff $x_{\min}$ of the power-law fit. The x-axis reports values rescaled by their respective $x_{\min}$ so that both tails start at one, presented on a log scale. The y-axis shows the empirical counter-cumulative distribution: the probability of finding an economy-industry pair with a CPV (*Eigenvector* centrality) larger than or equal to x, presented on a log scale. We label the estimated tail exponents ζ for both distributions. We provide a table with the ten economy-industry pairs with the largest values of CPV and *Eigenvector* centrality.

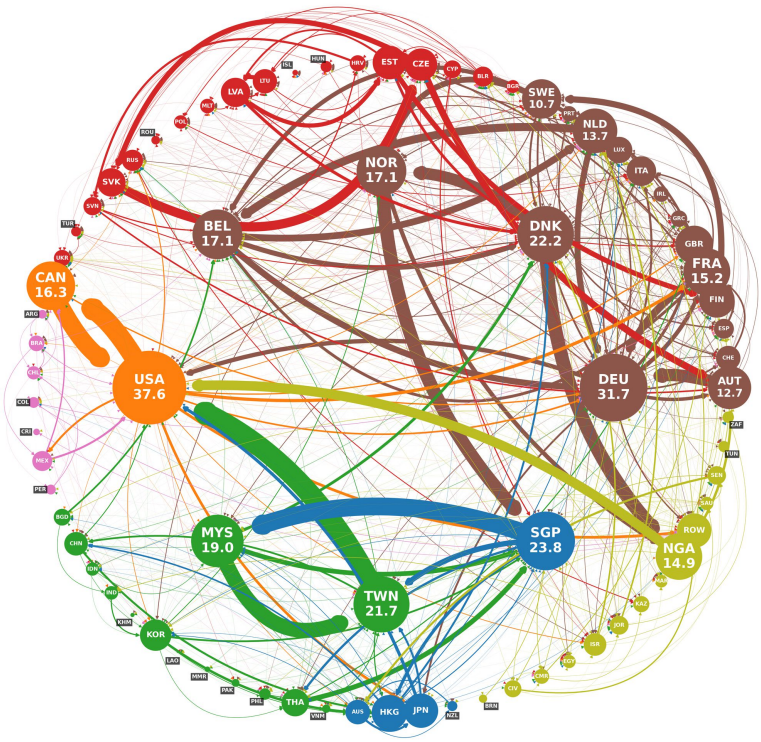


Top 10 Economy-Industry Pairs in 2020			
CPV		Eigenvector Centrality	
1	SGP, Wholesale and Retail	1	SVK, Motor Vehicles
2	CHN, ICT and Electronics	2	HUN, Motor Vehicles
3	DNK, Water Transport	3	SVK, ICT and Electronics
4	TWN, ICT and Electronics	4	SVN, Motor Vehicles
5	DEU, Chemicals	5	HUN, ICT and Electronics
6	DEU, Motor Vehicles	6	BEL, Motor Vehicles
7	DEU, Basic Metals	7	PRT, Motor Vehicles
8	IRL, IT Services	8	EST, ICT and Electronics
9	VNM, ICT and Electronics	9	KHM, ICT and Electronics
10	LTU, Warehousing	10	AUT, Motor Vehicles

Figure 6: The Economy-Level Global Choke Point Values in 1995 and 2020

This figure presents a visual representation of the global choke points in 1995 (top) and 2020 (bottom) in global production networks, where each node is an economy. The thickness of the arrow from node A to node B represents the total number of shortest paths passing from node A to node B. The size of the node represents the total number of shortest paths passing via the node as a fraction of all shortest paths in the network, i.e., the economy's Choke Points Value (CPV). We label the CPV for all countries with CPV above 10%. We group countries into seven groups, based on the geography and economic development, following the classification in Table 1.

1995



2020

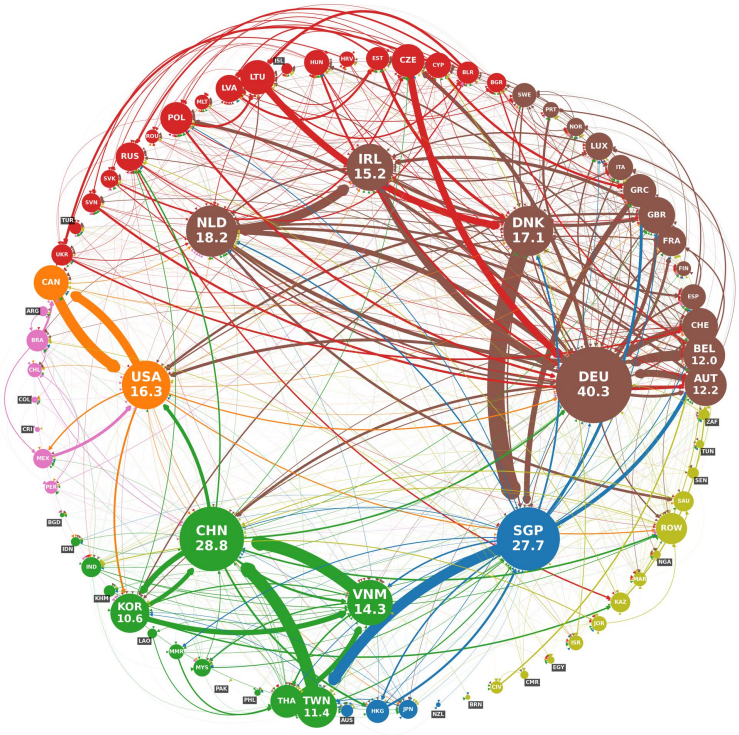


Figure 7: Top Economies and Industries with Highest Choke Point Values

This figure presents the top ten economies (Panel A) and top 10 industries (Panel B) with highest Choke Point Values in 1995 and 2020. The gray lines track changes in the rank of countries and industries over time. The size of each bar represents the Choke Point Value, expressed in percentages.

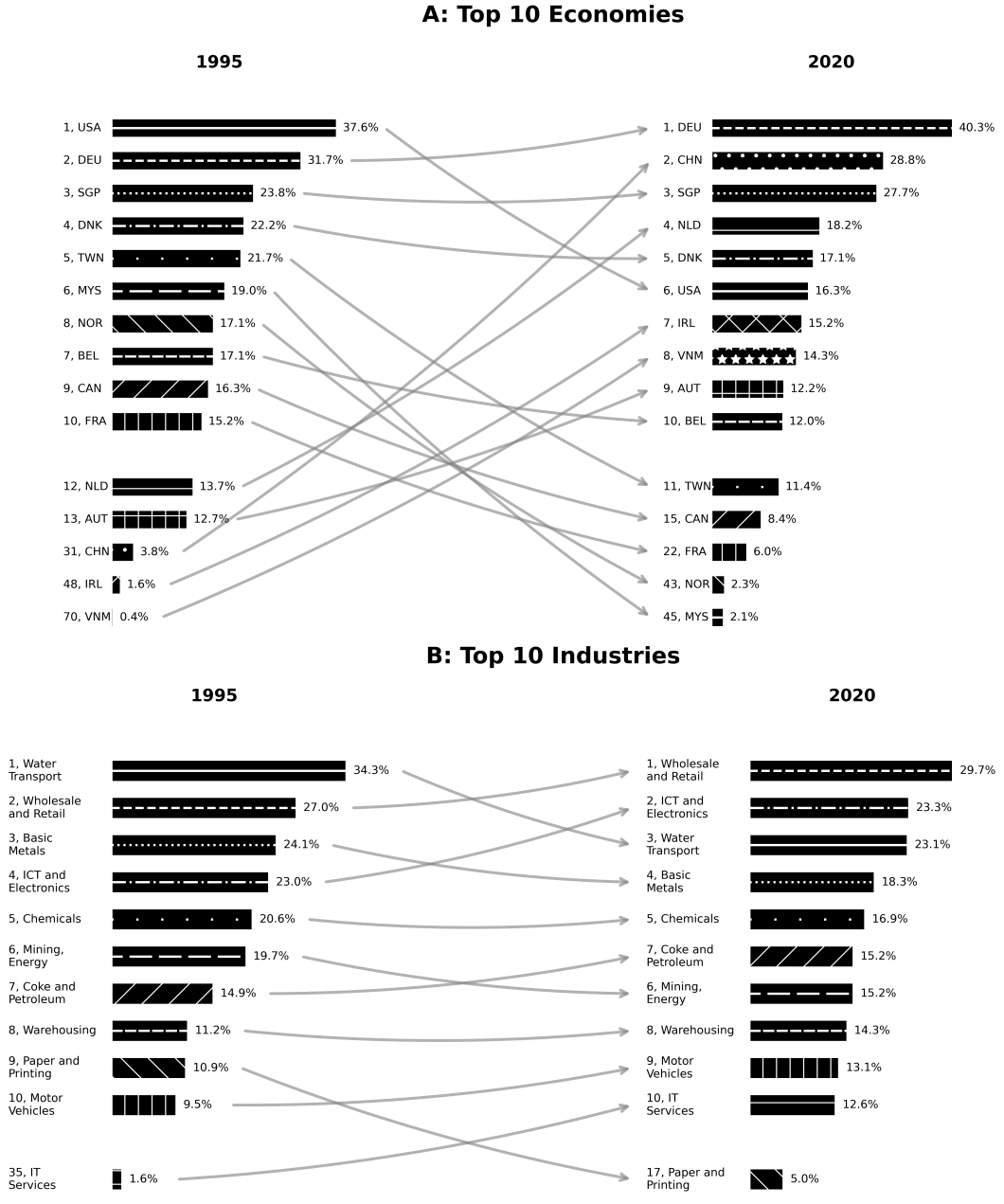


Figure 8: The Impact of China's WTO Accession on the Choke Point Value of China

This figure presents a visual representation of the global network of shortest paths passing via China before and after its WTO accession in December 2001. The size of node China (in cyan, in the middle) represents the percentage of all shortest paths in the network passing via China, i.e., the economy's Choke Point Value. The thickness of the arrow from any of the other nodes represents the number of shortest paths originating from the source node that pass through China (label=out, expressed as a percentage of all shortest paths originating from the node). The thickness of the arrow from China to any target node represents the number of shortest paths from a source node that pass through China and end in the target node. The colors illustrate the flow of the shortest paths. For instance, color blue tracks shortest paths originating from Asia-Pacific Developed, passing via China, and ending in any node. We present the global network separately for the three years prior to the WTO accession (top row) and the three years subsequent to the WTO accession.

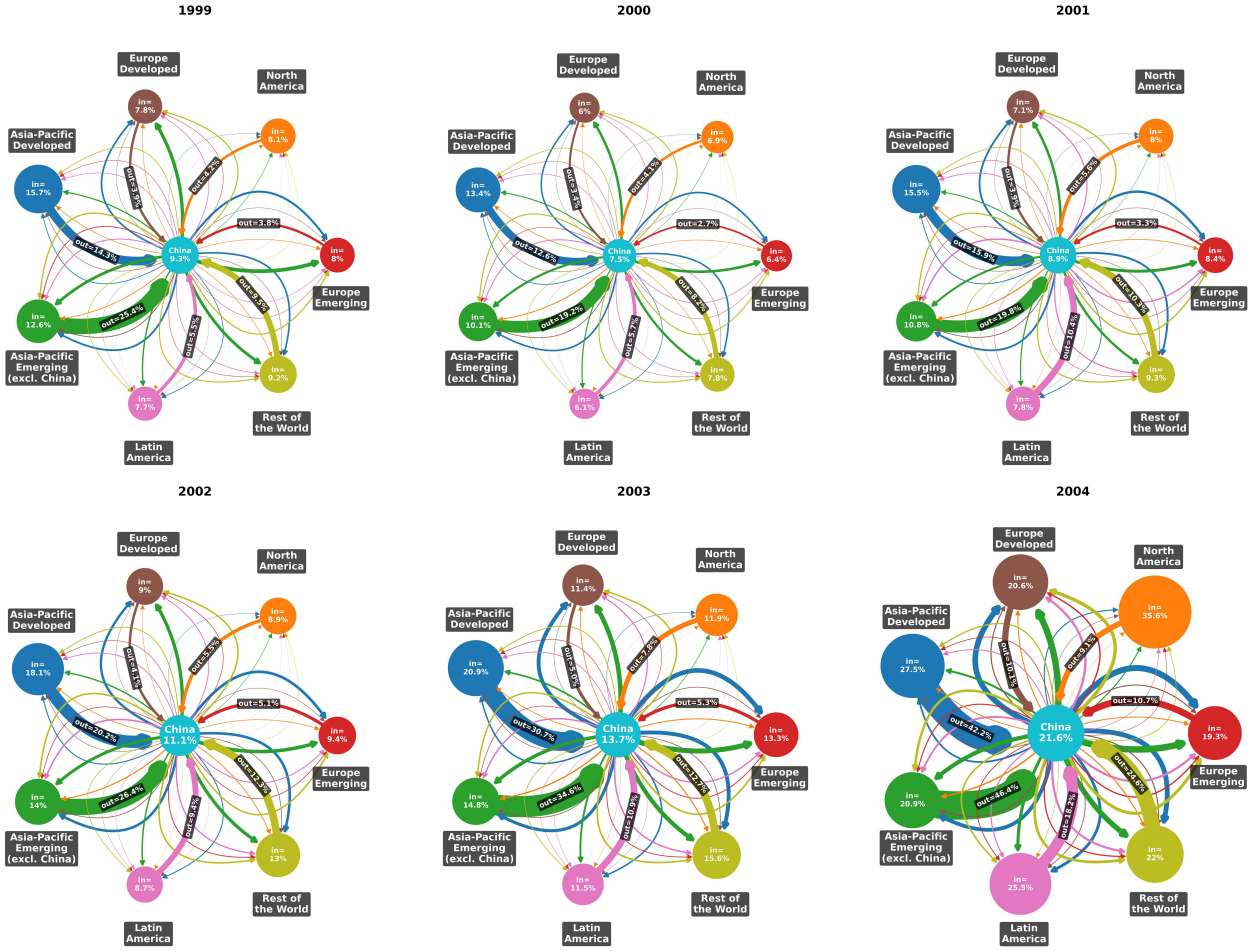


Figure 9: The Impact of China's WTO Accession on the Choke Point Value of the USA

This figure presents a visual representation of the global network of shortest paths passing via the USA before and after China's WTO accession in December 2001. The size of node USA (in cyan, in the middle) represents the percentage of all shortest paths in the network passing via USA, i.e. the economy's Choke Point Value. The thickness of the arrow from any of the other nodes represents the number of shortest paths originating from the source node that pass through USA (label=out, expressed as a percentage of all shortest paths originating from the node). The thickness of the arrow from USA to any target node represents the number of shortest paths from a source node that pass through USA and end in the target node. The colors illustrate the flow of the shortest paths. For instance, color blue tracks shortest paths originating from Asia-Pacific Developed, passing via USA, and ending in any node. We present the global network separately for the three years prior to the WTO accession (top row) and the three years subsequent to the WTO accession.

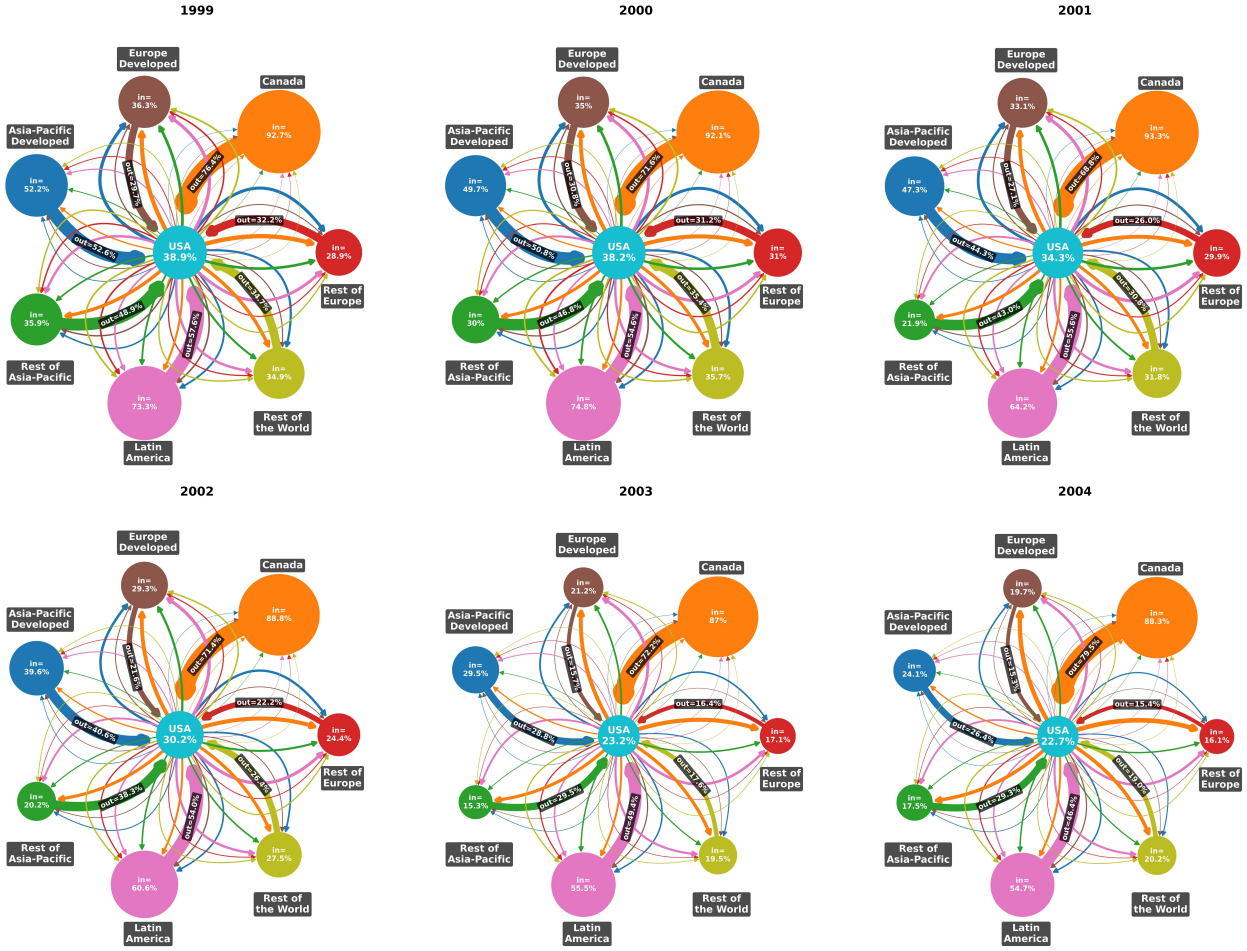


Figure 10: Time Series of Sales for the Top and Bottom US Industries with Exposure to the 2022 Covid Lockdowns in China

This figure presents time series of the aggregate sales for the top half and bottom half of US industries with exposure to the 2022 Covid lockdowns in China. We define exposure of US industries to the 2022 Covid lockdowns in equation 5. We compute time series of the aggregate level of sales for the top 22 economy-industry pairs in the United States (Top US Industries) and the bottom 21 economy-industry pairs in the United States (Bottom US Industries). We standardize the two time series using their December 2021 values. The dashed line separates the before and after periods used for the regression analysis in Table 4.

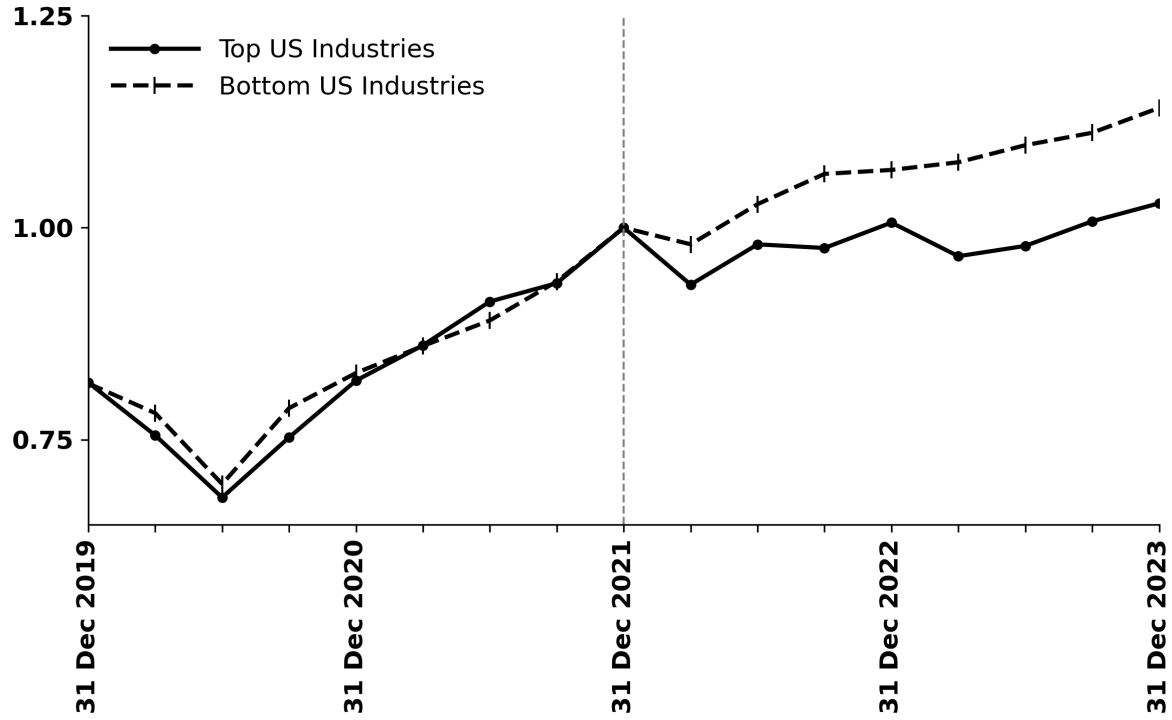


Figure 11: Dynamic Effects of Exposure to the 2022 Covid Lockdowns in China on the Sales of US Industries.

This figure presents the results of the estimated dynamic difference-in-differences model, according to equation 7. In Panel A, we present the estimated coefficients on the quarterly pre-event and post-event dummy interactions with log(Exposure), together with 95% confidence intervals. The dashed line separates the periods before and after the 2022 Covid Lockdowns in China. In Panel B (C), we present placebo results, where we estimate equation 7 using log(Placebo GX Exposure) (log(Placebo EIG Exposure)) instead of log(Exposure).

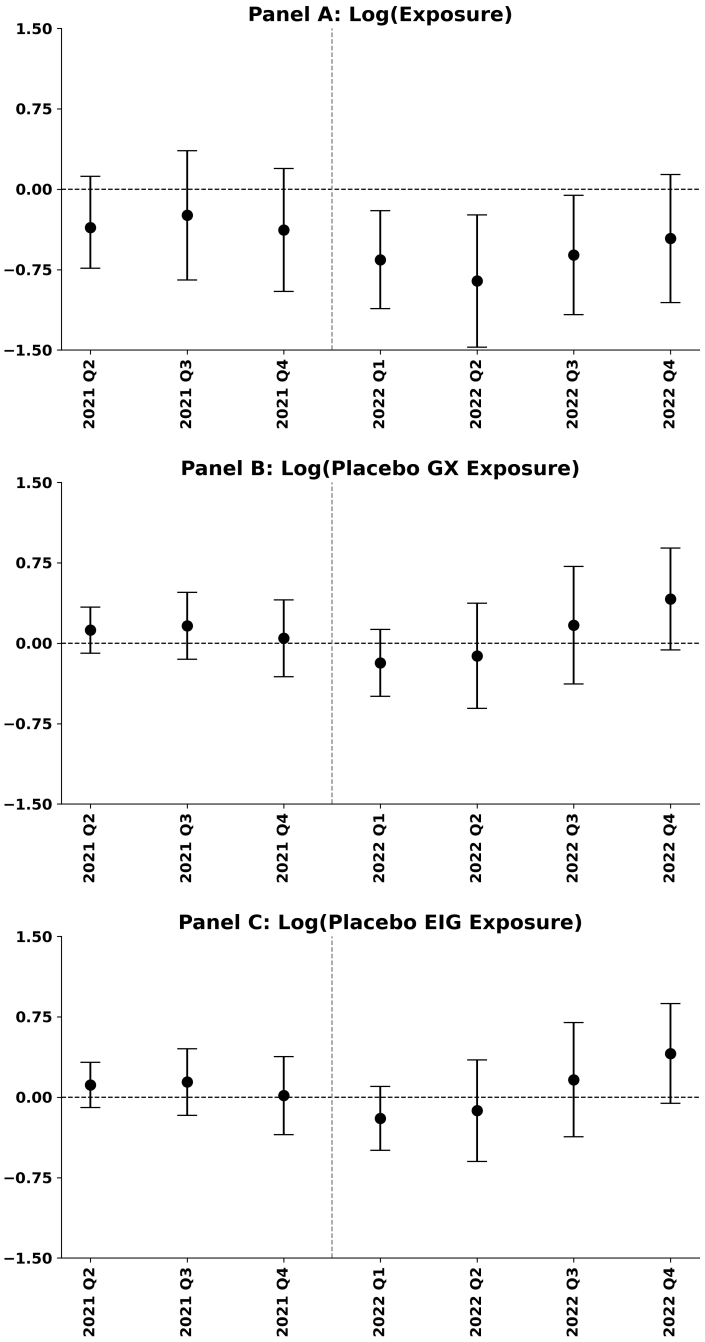


Figure 12: Daily Number of Container Ships Passing through the Red Sea Around the Houthi Attacks

This figure presents the daily number of container ships in the Red Sea. The data comes from the Kiel Institute for the World Economy. The dashed line separates the before and after periods used for the regression analysis in Table 5.

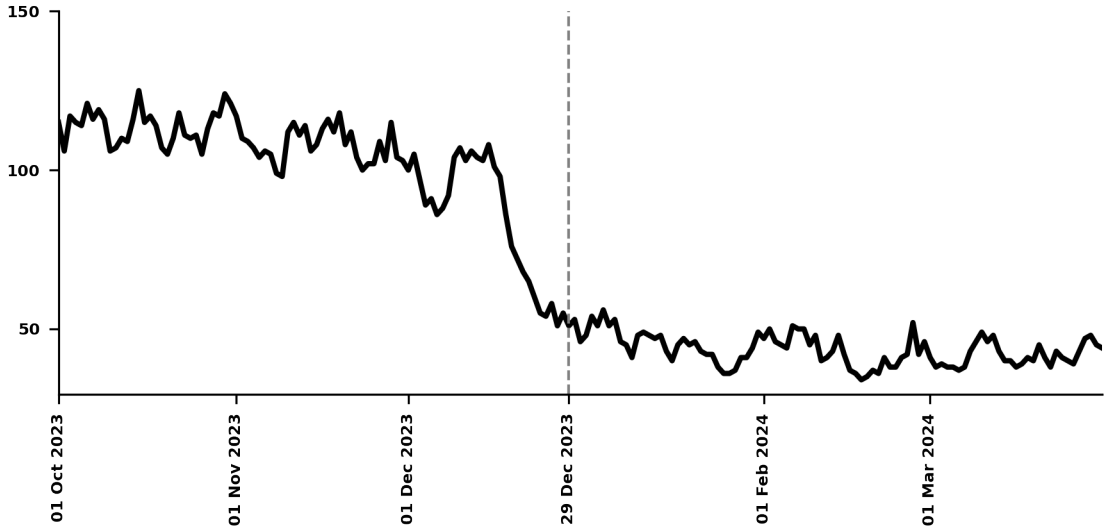


Figure 13: Container Price Index on the Far East to North Europe Trade Lane Around the Houthi Attacks

This figure presents an index on freight rates for less than 32 days for a standard 40' container on the trade lane between Far East and North Europe. The index is computed by Xeneta, using committed quotes reported by their customers. Xeneta computes dollar median rates for each Customer - Service Provider pair. The Index level is then computed as the weighted average of the median rates. (Refinitiv Code: *.XSICFENE*). The dashed line separates the before and after periods used for the regression analysis in Table 5.

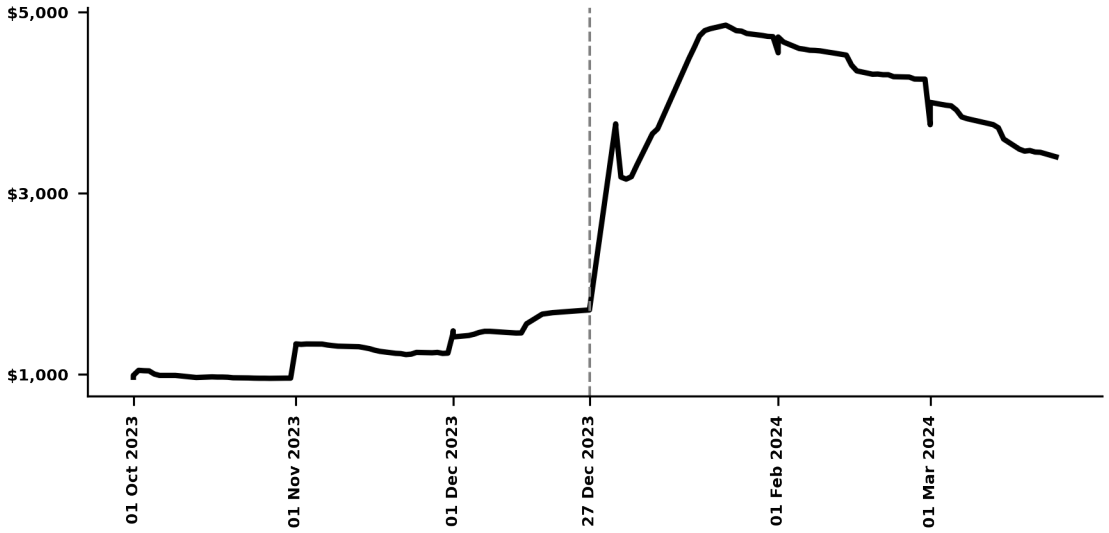


Figure 14: Propagation of the Shock to Water Transport in the Red Sea Across the World

This figure depicts the propagation of the shock to Water Transport industries using connecting shortest paths between Developed Europe and Developed and Emerging Asia-Pacific propagated. For each economy in Developed Europe and Developed and Emerging Asia, we compute the total number of treated paths as the the total number of shortest paths with either a source or a sink in that economy that pass through any Water Transport industry, additionally requiring that the shortest paths do not pass through any economy in North and South America. We express these as a fraction of all shortest paths with either a source or a sink in that economy ("Fraction of All Economy to Economy Shortest Paths, Affected by the Houthi Attacks"). Higher intensity of blue represents higher Fraction of All Economy to Economy Shortest Paths, Affected by the Houthi Attacks. All other countries are depicted in light gray. We label the 15 countries with highest values. The red dot represents the Bab el-Mandeb strait. The thickness of the solid arrows from the Bab el-Mandeb strait to any other economy represent the number of shortest paths connecting the strait with that economy. The thickness of the dashed arrows represent the directional number of shortest paths passing in that direction. For example, the thickness of the arrow labeled "Singapore → Taiwan" represents the number of shortest paths passing via Singapore in the direction of Taiwan that eventually sink in another economy.

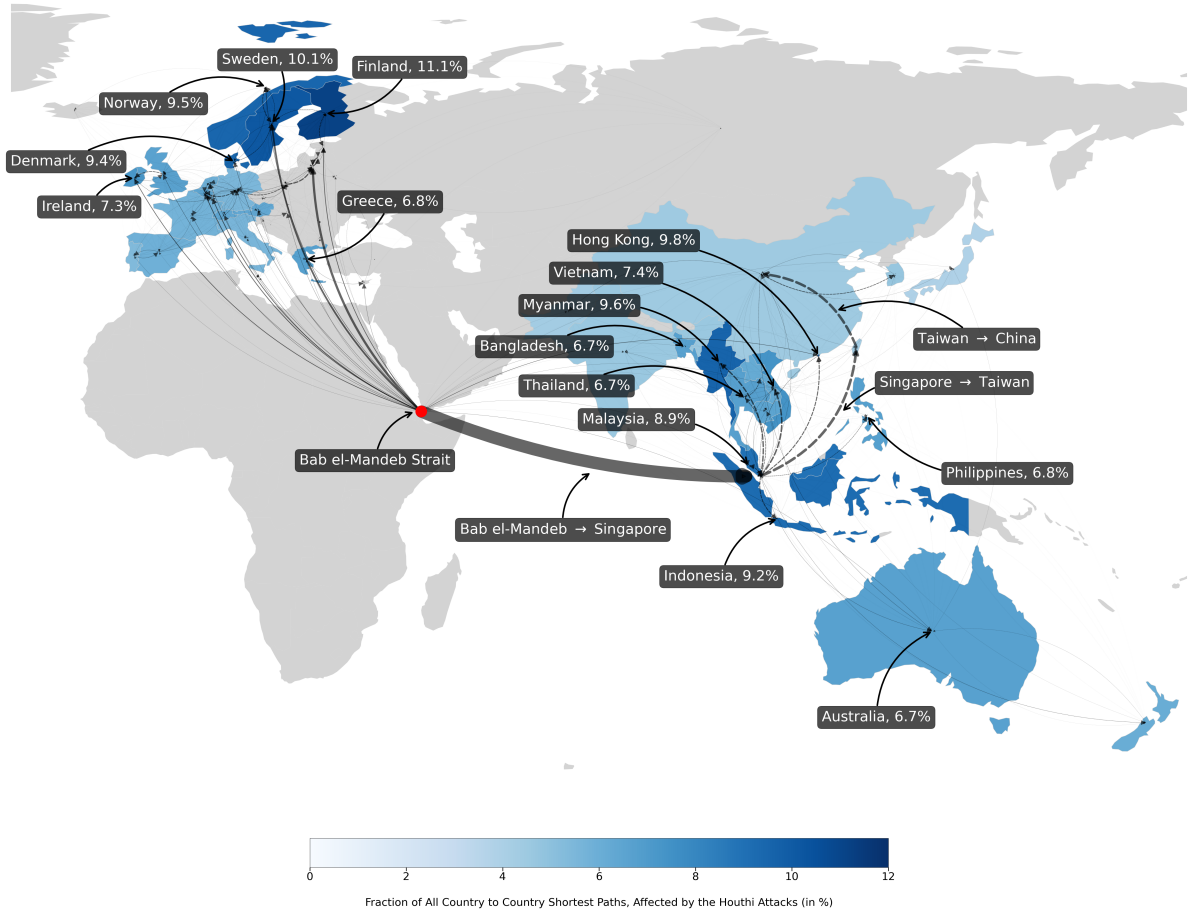


Figure 15: Time Series of Alphas for the Top and Bottom Industries with Exposure to the Red Sea Shocks

This figure presents time series of the aggregate alphas for the top half and bottom half of industries with exposure to the Red Sea Shocks. We define exposure of global economy-industry pairs to the Red Sea Shocks in equation 8. We compute time series of the aggregate weekly alpha for the top 214 global economy-industry pairs (Top Global Industries) and the bottom 213 global economy-industry pairs (Bottom Global Industries), where we weigh alphas using the lagged economy-industry market capitalization. The dashed line separates the before and after periods used for the regression analysis in Table 5.

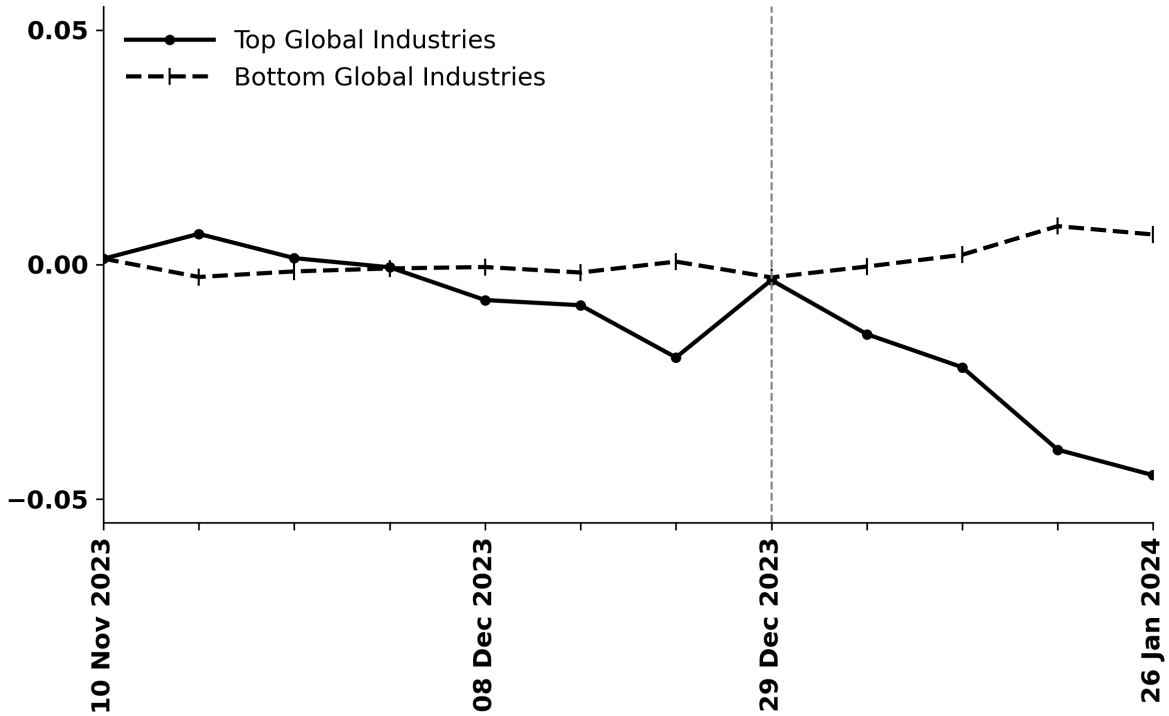


Figure 16: Predictability of Consumption Growth Over 8 Quarters

We run quarterly regressions of aggregate consumption growth on the return of a spread portfolio long in high Choke Point Value (CPV) economy-industry pairs and short in low CPV economy-industry pairs. The dependent variable is cumulative growth in real (constant prices, seasonally-adjusted) consumption between quarters t and $t+i$, where i ranges from 1 to 8. CPV H-L stands for the lagged cumulative 12 month return of the the spread portfolio long in high CPV economy-industry pairs and short in low CPV economy-industry pairs constructed in Panel A of Table 6. Control variables include the lagged cumulative 12 month return of the market portfolio (Mrkt-rf), the lagged cumulative 12 month return of the factors used in Panel A of Table 6 (SMB, HML, MOM, CMA, RMW), the cumulative four quarter growth in industrial production, lagged cumulative 12 month consumption growth, the term permium in the USA, and the change in the market yield on US treasury securities at 2-year constant maturity during the previous 12 months. We plot the estimated coefficients on CPV H-L for the United States in Panel A, the sample of developed countries (excluding the USA) in Panel B, the sample of all developed countries in Panel C, and the whole sample in Panel D. In Panels B, C, and D we aggregate country-level variables using lagged GDP in PPP before running the regressions. We additionally plot 95% confidence intervals using the light blue area, based on Newey-West standard errors with 4 lags.

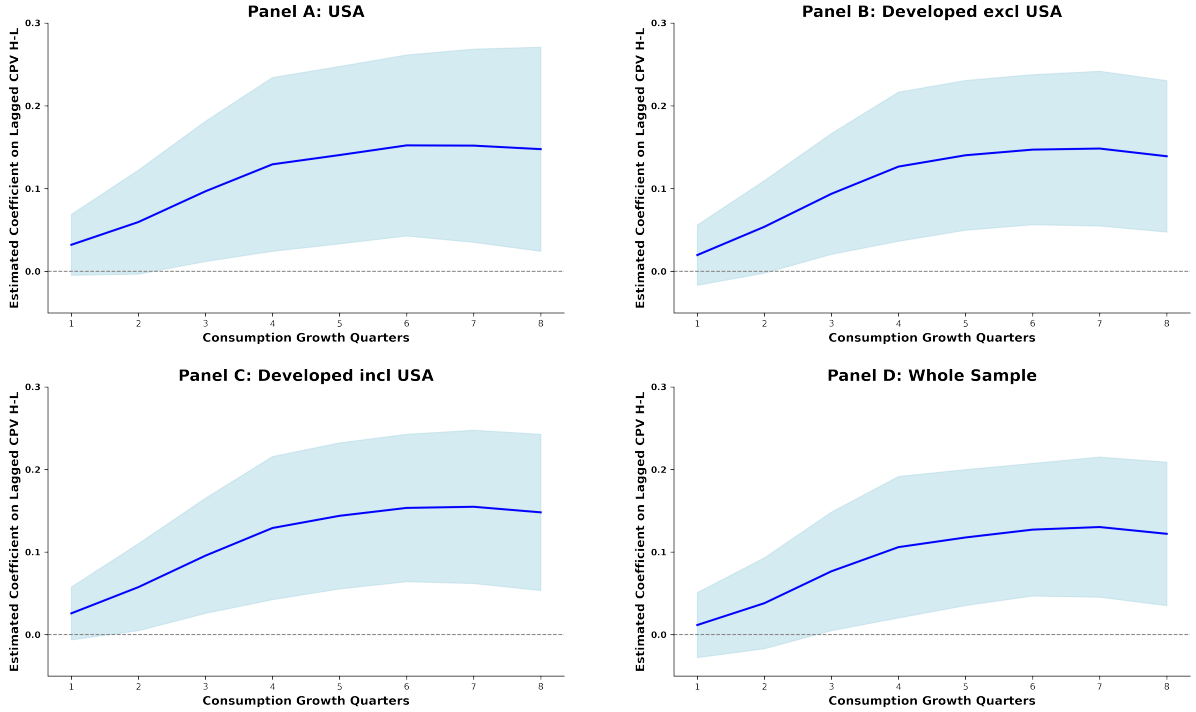


Table 1: Descriptive Statistics of the Global Production Network

This table presents summary statistics for the Global Production Network, based on OECD's Trade in Value Added (TiVA) between 1995 and 2020. A directed edge connects two nodes $n(r,i)$ and $n(s,j)$ and is equal to the value added by industry r in economy i to industry s in economy j, i.e. $FVA_{i,j}^{r,s}$ (in percentages). Note that since $FVA_{i,j}^{r,s} = 0$ if $i = j$, all edges linking industries from the same economy are set to 0. Each year we compute a mean and a standard deviation for all incoming and outgoing edges. We present the averages of the mean and standard deviations across all years, as well as global minimum and maximum values. We present the summary statistics for all nodes and for nodes belonging to geographical regions and sectors. Developed Asia-Pacific (APA) includes AUS, HKG, JPN, NZL, and SGP; Developed Europe (EUR) includes AUT, BEL, CHE, DEU, DNK, ESP, FIN, FRA, GBR, GRC, IRL, ITA, LUX, NLD, NOR, PRT, and SWE; Developed North-America (NAM) includes CAN and USA; Emerging and Frontier Asia-Pacific (APA) includes BGD, CHN, IDN, IND, KHM, KOR, LAO, MMR, MYS, PAK, PHL, THA, TWN, and VNM; Emerging and Frontier Europe (EUR) includes BGR, BLR, CYP, CZE, EST, HRV, HUN, ISL, LTU, LVA, MLT, POL, ROU, RUS, SVK, SVN, TUR, and UKR; Emerging and Frontier Latin America (LAM) includes ARG, BRA, CHL, COL, CRI, MEX, and PER; the Rest of the World (ROW) includes BRN, CIV, CMR, EGY, ISR, JOR, KAZ, MAR, NGA, ROW, SAU, SEN, TUN, and ZAF. The sectors breakdown includes Agriculture, Forestry and Fishing (AGR), Mining and Quarrying (MIN), Manufacturing (MAN), Electricity, Gas, Water Supply, Sewerage, Waste and Remediation Services (UTL), Construction (CON), Total Business Sector Services (BUS), and all other (OTH) including Public Admin, Education and Health, and Social and Personal Services.

	ALL	Region							Sector						
		Developed			Emerging and Frontier										
		APA	EUR	NAM	APA	EUR	LAM	ROW	AGR	MIN	MAN	UTL	CON	BUS	OTH
Economies	77	5	17	2	14	18	7	14	77	77	77	77	77	77	77
Industries	45	45	45	45	45	45	45	45	2	3	17	2	1	14	6
Nodes:															
Econ-Ind Pairs	3465	225	765	90	630	810	315	630	154	231	1309	154	77	1078	462
Edges IN:															
Mean	0.006	0.006	0.006	0.004	0.006	0.007	0.004	0.005	0.005	0.005	0.009	0.004	0.005	0.005	0.003
StDev	0.071	0.069	0.070	0.056	0.071	0.083	0.055	0.063	0.039	0.051	0.100	0.087	0.032	0.044	0.021
Min	0	0	0	0	0	0	0	0	0	0	0	0	0	0	0
Max	72.15	31.33	41.21	12.80	37.79	49.72	24.75	72.15	11.11	20.00	72.15	37.41	6.99	20.40	12.25
Edges OUT:															
Mean	0.006	0.007	0.010	0.028	0.005	0.003	0.002	0.004	0.003	0.013	0.005	0.004	0.002	0.009	0.001
StDev	0.071	0.051	0.059	0.132	0.039	0.074	0.023	0.104	0.030	0.222	0.043	0.021	0.008	0.055	0.004
Min	0	0	0	0	0	0	0	0	0	0	0	0	0	0	0
Max	72.15	9.79	41.21	24.39	18.27	49.72	22.09	72.15	11.11	72.15	23.84	6.37	0.72	20.40	3.55

Table 2: Descriptive Statistics of Choke Point Values

This table presents summary statistics of the main variables used in the study. In Panel A, we provide descriptive statistics for Choke Point Values, between 1995 and 2020 (see Section **??**) We present averages of the mean and standard deviations across all years, as well as global minimum and maximum values. We present summary statistics for all nodes and for nodes belonging to geographical regions and sectors as defined in Table 1. In Panel A, we present summary statistics for the whole sample, and in Panel B we present summary statistics for the economy-industry pairs with sufficient financial data to be included in our asset-pricing tests.

Panel A: Descriptive Statistics of Choke Point Value

	ALL	Region							Sector						
		Developed			Emerging and Frontier										
		APA	EUR	NAM	APA	EUR	LAM	ROW	AGR	MIN	MAN	UTL	CON	BUS	OTH
	All 3465 Economy-Industry Pairs														
Choke Point Value:															
Mean	0.007	0.010	0.012	0.027	0.006	0.005	0.002	0.003	0.002	0.006	0.010	0.001	0.001	0.007	0.000
StDev	0.040	0.059	0.055	0.066	0.043	0.018	0.008	0.021	0.007	0.037	0.045	0.004	0.005	0.047	0.002
Min	0	0	0	0	0	0	0	0	0	0	0	0	0	0	0
Max	1	1	1	1	1	0.52	0.20	0.85	0.08	0.85	1	0.12	0.14	1	0.06
	All Economy-Industry Pairs with Financial Data														
#Economies	41	4	12	2	11	3	3	6	3	8	23	9	20	41	5
#Industries	41	35	27	39	34	7	3	8	1	3	17	2	1	13	4
#Econ-Ind Pairs	358	73	78	55	122	10	5	15	3	15	145	11	20	154	10
Choke Point Value:															
Mean	0.030	0.028	0.023	0.042	0.033	0.001	0.000	0.004	0.005	0.027	0.047	0.005	0.000	0.021	0.001
StDev	0.101	0.107	0.051	0.086	0.125	0.001	0.001	0.009	0.002	0.048	0.126	0.008	0.001	0.086	0.002
Min	0	0	0	0	0	0	0	0	0	0	0	0	0	0	0
Max	1	1	1	1	1	0.02	0.01	0.18	0.02	0.35	1	0.12	0.01	1	0.02

–continued from previous page

Panel B: Descriptive Statistics of Other Variables

	US				Non-US				Whole Sample			
	mean	stdev	p25	p75	mean	stdev	p25	p75	mean	stdev	p25	p75
Covid-19 Experiment												
$log(Sales)$	10.57	1.53	9.62	11.69								
$log(Exposure)$	0.286	0.102	0.224	0.351								
$log(Placebo\ GX\ Exposure)$	0.022	0.064	0.002	0.008								
$log(Placebo\ EIG\ Exposure)$	0.020	0.064	0.002	0.006								
$log(GX^{China})$	5.576	0.649	5.219	6.060								
Houthi Experiment												
α $(weekly,\ in\ \%)$	-0.048	1.958	-1.109	1.086	-0.018	2.561	-1.507	1.443	-0.020	2.522	-1.482	1.404
$log(Exposure)$	0.000	0.000	0.000	0.000	0.046	0.034	0.022	0.066	0.043	0.035	0.012	0.065
$log(Sum\ DirectLink)$	0.011	0.014	0.002	0.014	0.012	0.015	0.001	0.016	0.012	0.015	0.001	0.016
$log(Geo\ Distance)$	2.453				1.842	0.409	1.644	2.110	1.886	0.425	1.700	2.153
Financial Variables												
$Ret–rf$ $(monthly,\ in\ \%)$	0.763	6.635	-2.623	4.448	0.544	8.339	-3.727	4.822	0.579	8.091	-3.543	4.751
β	0.957	0.363	0.699	1.186	1.008	0.459	0.705	1.277	1.000	0.445	0.704	1.262
$log(BookEquity)$	8.774	1.312	7.835	9.732	7.767	1.461	6.693	8.765	7.928	1.485	6.887	8.933
$log(MarketEquity)$	12.26	1.38	11.33	13.21	10.75	1.23	9.89	11.59	10.99	1.37	10.03	11.89
$Profitability$	0.605	3.508	0.265	0.462	0.214	1.281	0.136	0.279	0.277	1.835	0.148	0.317
$Investment$	0.314	0.775	0.071	0.254	0.293	0.765	0.049	0.272	0.296	0.767	0.054	0.269
$Dividends$	0.121	1.120	0.027	0.084	0.094	0.725	0.030	0.087	0.098	0.802	0.030	0.087
Ret^{m1}	0.008	0.066	-0.026	0.044	0.006	0.084	-0.037	0.048	0.006	0.081	-0.035	0.048
$Ret^{m2:m12}$	0.088	0.237	-0.041	0.217	0.077	0.345	-0.125	0.227	0.079	0.331	-0.113	0.225
Betas												
$\beta^{Country}$	0.946	0.141	0.895	1.047	1.012	0.332	0.801	1.195	1.002	0.310	0.825	1.143
$\beta^{Concentration}$	-0.004	0.022	-0.018	0.009	-0.008	0.040	-0.027	0.006	-0.007	0.038	-0.024	0.006
$\beta^{Sparisty}$	0.014	0.025	0.002	0.027	0.035	0.039	0.011	0.053	0.032	0.038	0.008	0.047
$\beta^{TransportationCosts}$	0.027	0.332	-0.174	0.269	0.014	0.327	-0.163	0.226	0.016	0.327	-0.167	0.231
β^{GSCPI}	0.003	0.020	-0.009	0.012	0.006	0.030	-0.011	0.023	0.006	0.029	-0.011	0.022
$\beta^{GeopoliticalRisk}$	-0.005	0.033	-0.021	0.012	0.010	0.045	-0.015	0.030	0.007	0.044	-0.016	0.027
Main Economy Variables												
$Consumption\ Growth$	0.028	0.025	0.018	0.036	0.015	0.028	0.011	0.023	0.028	0.026	0.022	0.037
$GDP\ Growth$	0.025	0.022	0.017	0.038	0.016	0.027	0.013	0.027	0.036	0.025	0.028	0.043

Table 3: US Industry Correlations of Choke Point Value from the Global Production Network with Centrality Measures from the Domestic US Network

This table presents an US industry correlation matrix of network centrality measures from a global and domestic production network. We also present the correlation of these centarlity measures with the industries' gross output as a measure of industry size. We compute Spearman correlations each year and then compute average values across all years.

	(1) Global CPV	(2) US $Eigen$	(3) US CPV	(4) $log(Output)$
Global Network				
(1) CPV	1.00			
Domestic US Network				
(2) $Eigenvector$	-0.33	1.00		
(3) CPV	-0.11	0.27	1.00	
Industry Size				
(4) $log(Output)$	0.06	0.43	0.53	1.00

Table 4: China Lockdowns and Plummeting Sales of Treated US Firms: Evidence in 2022

This table presents the results of OLS regressions of quarterly sales of US industries on the fraction of all of the economy-industry pair's shortest paths affected by the 2022 Covid Lockdown in China. The dependent variable is the log of US industry total sales in trillion USD. For each economy-industry pair in the United States, we compute the total number of treated paths as the the total number of shortest paths with either a source or a sink in that economy-industry pair that pass through any of the top 5 economy-industry choke points in China in year 2020. We assign a zero for all other economy-industry pairs. *Post* is an indicator variable equal to one for observations in 2022 and zero otherwise. $log(Exposure)$ is computed as log of the total number of treated paths divided by all the shortest paths with either a source or a sink in that economy-industry pair. $I_{Qnt1}^{Exposure}$ is an indicator variable taking the value of 1 if $log(Exposure)$ is in the top quintile and zero otherwise. We construct placebo treated paths based on the total number of shortest paths with either a source or a sink in that economy-industry pair that pass through any of the top 5 Chinese industries in terms of gross exports (GX) in 2020 or the top 5 Chinese industries in terms of *Eigenvector* centrality (EIG), additionally requiring that these Chinese industries are not part of the top 5 choke points used to compute $log(Exposure)$. $log(Placebo\ GX\ Exposure)$ ($log(Placebo\ EIG\ Exposure)$) is computed as log of the total number of placebo GX (EIG) treated paths divided by all the shortest paths with either a source or a sink in that economy-industry pair. $I_{Qnt1}^{Placebo\ GX\ Exposure}$ ($I_{Qnt1}^{Placebo\ EIG\ Exposure}$) is an indicator variable taking the value of 1 if $log(Placebo\ GX\ Exposure)$ ($log(Placebo\ EIG\ Exposure)$) is in the top quintile and zero otherwise. $log(GX^{China})$ is log of quarterly US industry gross sales to China in million USD. The sample spans the four quarters of 2021 and the four quarters of year 2022. All specifications include quarter fixed effects and industry fixed effects. t-statistics are given in parentheses, based on standard errors clustred on industry. Statistical significance at the 10%, 5%, and 1% level is indicated by *, **, and ***, respectively.

	(1)	(2)	(3)	(4)	(5)	(6)	(7)	(8)	(9)	(10)	(11)	(12)
$Post \times log(Exposure)$	−0.402**			−0.416**	−0.419**						−0.325*	
	(−2.068)			(−2.127)	(−2.130)						(−1.925)	
$Post \times log(Placebo\ GX\ Exposure)$		−0.013		−0.129								
		(−0.067)		(−0.709)								
$Post \times log(Placebo\ EIG\ Exposure)$			−0.006		−0.138							
			(−0.030)		(−0.760)							
$Post \times I_{Qnt1}^{Exposure}$						−0.143**			−0.138**	−0.135**		−0.111**
						(−2.354)			(−2.231)	(−2.143)		(−2.563)
$Post \times I_{Qnt1}^{Placebo\ GX\ Exposure}$							0.079		0.069			
							(0.768)		(0.704)			
$Post \times I_{Qnt1}^{Placebo\ EIG\ Exposure}$								0.119		0.109		
								(1.090)		(1.053)		
$log(GX^{China})$											−0.060	−0.059
											(−0.816)	(−0.853)
Time FE	YES	YES	YES	YES	YES	YES	YES	YES	YES	YES	YES	YES
Industry FE	YES	YES	YES	YES	YES	YES	YES	YES	YES	YES	YES	YES
Observations	344	344	344	344	344	344	344	344	344	344	160	160
R-squared	0.992	0.992	0.992	0.992	0.992	0.992	0.992	0.992	0.992	0.992	0.992	0.992

Table 5: Propagation of the Red Sea Shocks (Houthi Attacks) in the Global Stock Market

This table presents the results of OLS regressions of weekly economy-industry alphas on the fraction of all of the economy-industry pair's shortest paths affected by the Houthi's attacks. The dependent variable is weekly alpha, computed in two steps. In the first step over the period Oct 03, 2022 to Sep 29, 2023, for each economy-industry pair we regress its weekly excess returns on the weekly excess returns of the global market portfolio. In the second step over the four weeks prior and the four weeks after Dec 29, 2023, for each economy-industry pair we compute alphas as realized excess returns minus the product of the estimated beta and the realized weekly excess return of the market. For each economy-industry pair in Developed Europe and Developed and Emerging Asia, we compute the total number of treated paths as the the total number of shortest paths with either a source or a sink in that economy-industry pair that pass through any water transportation industry, additionally requiring that the shortest paths do not pass through any economy in North and South America. We assign a zero for all other economy-industry pairs. $log(Exposure)$ is computed as log of one plus the total number of treated paths divided by all the shortest paths with either a source or a sink in that economy-industry pair. $log(DirectLlink)$ is computed as log of the sum of all edges with a source (sink) the economy-industry pair and a sink (source) in treated Water Transport industries. $Post$ is an indicator variable equal to one for observations in 2024 and zero otherwise. The sample spans the last four weeks of 2023 and the first four weeks of 2024. β is the computed beta from the first stage of the weekly alpha estimation. All other variables are defined in Appendix B. All specifications include week fixed effects and depending on the specification, economy × sector fixed effects. t-statistics are given in parentheses, based on standard errors clustered on the economy-industry pair level. Statistical significance at the 10%, 5%, and 1% level is indicated by *, **, and ***, respectively.

	(1)	(2)	(3)	(4)	(5)
$log(Exposure)$	0.879	6.200**	6.676**	7.882*	
	(0.30)	(3.39)	(3.33)	(1.93)	
$Post \times log(Exposure)$		−10.683**	−10.495**	−10.573**	
		(−2.65)	(−2.61)	(−2.55)	
$log(Sum\ DirectLink)$					−1.446
					(−0.16)
$Post \times log(Sum\ DirectLink)$					1.764
					(0.38)
$log(Geo\ Distance)$			−0.543*		
			(−2.21)		
β			−0.122	−0.389	−0.397
			(−0.36)	(−1.77)	(−1.84)
$log(BookEquity)$			−0.053	−0.073	−0.084
			(−0.68)	(−1.22)	(−1.23)
$log(MarketEquity)$			0.077	0.064	0.069
			(1.10)	(0.98)	(1.03)
$Profitability$			0.592	−0.081	−0.031
			(1.19)	(−0.24)	(−0.09)
$Investment$			−0.155	−0.053	−0.068
			(−1.03)	(−0.34)	(−0.44)
$Dividends$			0.775	0.579**	0.509
			(1.35)	(2.37)	(1.84)
Ret^{m1}			3.268*	−0.064	−0.034
			(2.20)	(−0.08)	(−0.05)
$Ret^{m2:m12}$			−0.523	−1.273	−1.242
			(−0.86)	(−1.85)	(−1.84)
Time FE	Yes	Yes	Yes	Yes	Yes
Country × Sector FE	No	No	No	Yes	Yes
Observations	3,300	3,300	3,292	3,292	3,292
R-squared	0.064	0.070	0.090	0.166	0.159

Table 6: Choke Point Values and Stock Returns in the Global Stock Market: Portfolio Sorts

This table reports the performance of industry portfolios conditional on their Choke Point Value. At the end of each year between 1995 and 2020, we sort economy-industry pairs with sufficient financial data into five portfolios, based on their Choke Point Value. Next, we track the value-weighted monthly returns of the portfolios during the next 12 months, after which we rebalance. In Panel A, we report time-series averages of excess returns. In Panel B, we report alphas and factor loadings from a global 6-factor Fama-French model, including Mrk-rf, SMB, HML, MOM, CMA, and RMW as factors. In Panel C, we report alphas from alternative models for the spread portfolio in the portfolio sorts. WCAPM stands for a World CAPM model with time-varying betas. For each economy-industry pair and each month, we first estimate loadings on a value-weighted market portfolio consisting of all stocks in Compustat uisng the previous 36 months. Next, we compute the economy industry's alpha as its observed return in excess of the estimated market loading times this month's market excess return. We value-weight alphas across all economy-industry pairs in the portfolio and report time-series averages. WLCAPM stands for a World-Local CAPM, where we compute alphas analogously to the WCAPM model with an additional local factor, again using time-varying betas. Local factors are computed as the value-weighted returns of all stocks across a local region, orthogonalized on the market portfolio. We assign countries to regions following the classification in Table 1. We also present alphas using alternative standard asset global pricing models, based on Fama-French factors. CAPM includes Mrk-rf as a sole factor, FF3 adds SMB and HML, FF4 augments FF3 with MOM and FF5 augments FF3 with CMA and RMW. Last, we report alphas using local Fama-French factors, where we assign each economy-industry pair to its closest local Fama-French set of factors. Next, for each economy-industry pair and each month, we first estimate loadings on the local factors. Next, we compute the economy industry's alpha as its observed return in excess of the estimated market loading times this month's realized factor returns. We value-weight alphas across all economy-industry pairs in the portfolio and compute time-series averages. t-statistics are given in parentheses. Statistical significance at the 10%, 5%, and 1% level is indicated by *, **, and ***, respectively.

	Panel A: Excess Returns					
	1 (low)	2	3	4	5 (high)	5 – 1
Ret–rf	0.163	0.516	0.399	0.700***	0.673**	0.510***
	(0.55)	(1.59)	(1.25)	(2.92)	(2.13)	(3.03)
	Panel B: Alphas and Loadings from a Global 6-Factor FF Model					
	1 (low)	2	3	4	5 (high)	5 – 1
Alpha	−0.396***	−0.064	−0.090	0.126*	0.206**	0.602***
	(−2.97)	(−0.48)	(−0.90)	(1.65)	(2.51)	(3.87)
Mrkt–rf	0.901***	0.957***	1.001***	0.907***	1.001***	0.101**
	(25.63)	(26.94)	(38.09)	(45.04)	(46.46)	(2.46)
SMB	0.439***	0.322***	−0.069	−0.123***	−0.013	−0.452***
	(6.57)	(4.76)	(−1.38)	(−3.22)	(−0.31)	(−5.80)
HML	0.011	−0.088	0.005	0.014	−0.002	−0.013
	(0.14)	(−1.13)	(0.09)	(0.32)	(−0.04)	(−0.14)
MOM	−0.028	0.001	0.016	−0.027	−0.009	0.019
	(−0.83)	(0.04)	(0.62)	(−1.37)	(−0.44)	(0.48)
CMA	0.025	−0.077	−0.201**	0.044	−0.304***	−0.329**
	(0.23)	(−0.70)	(−2.47)	(0.70)	(−4.55)	(−2.59)
RMW	−0.003	0.013	−0.214***	0.127**	−0.262***	−0.258**
	(−0.04)	(0.13)	(−3.04)	(2.36)	(−4.52)	(−2.35)
	Panel C: Alpha Spreads using Alternative Models					
	WCAPM	WLCAPM	FF Global Factor Models			
			CAPM	FF3	FF4	FF5
Alpha Spread	0.487***	0.219**	0.382**	0.447***	0.452***	0.612***
	(2.90)	(2.03)	(2.47)	(3.06)	(3.02)	(3.98)
		FF Local Factor Models				
		CAPM	FF3	FF4	FF5	FF6
Alpha Spread		0.263**	0.348***	0.373***	0.432***	0.456***
		(2.57)	(3.52)	(3.69)	(4.34)	(4.33)

Table 7: Choke Point Values and Stock Returns in the Global Stock Market: Fama-Macbeth Regressions

This table reports the results of Fama-MacBeth regressions of economy-industry returns on their lagged Choke Point Value and lagged predictors of performance. The dependent variable is a value-weighted economy-industry monthly return, expressed in percentages. CPV^{PRCNTL} is the most recently available Choke Point Value, expressed as a percentile. Depending on the specification, we include financial control variables (β, $log(BookEquity)$, $log(MarketEquity)$, $Profitability$, $Investment$, $Dividends$, Ret^{m1}, and $Ret^{m2:m12}$), economy control variables ($log(POPULATION)$, $\Delta GDPHEAD$, ΔCPI, and $FX\ RET$), control variables based on World Input-Output Tables (WIOT, $log(Gross\ Output)$, $Value\ Added\ Share$), and controls related to betas ($\beta^{Country}$, β^{Transp}). All control variables are defined in Appendix B. t-statistics based on Newey-West standard errors with 12 lags are given in parentheses. Statistical significance at the 10%, 5%, and 1% level is indicated by *, **, and ***, respectively.

	(1)	(2)	(3)	(4)	(5)	(6)
CPV^{PRCNTL}	0.004***	0.003**	0.002**	0.002**	0.003***	0.003**
	(2.79)	(2.33)	(2.10)	(2.03)	(2.62)	(2.68)
β	−0.082	−0.074	−0.266	−0.193	−0.187	−0.177
	(−0.31)	(−0.28)	(−1.19)	(−0.92)	(−0.90)	(−0.70)
$log(BookEquity)$	0.031	0.039	0.082	0.056	0.046	0.029
	(0.35)	(0.42)	(1.14)	(1.06)	(0.85)	(0.68)
$log(MarketEquity)$	−0.038	−0.031	−0.075	−0.083	−0.068	−0.048
	(−0.39)	(−0.33)	(−1.07)	(−1.32)	(−1.02)	(−0.88)
$Profitability$		−0.005	0.021	0.059	0.062	0.074
		(−0.04)	(0.18)	(0.57)	(0.61)	(0.71)
$Investment$		−0.027	−0.053	−0.013	−0.032	−0.014
		(−0.51)	(−1.01)	(−0.27)	(−0.60)	(−0.35)
$Dividends$		0.329	0.152	0.110	0.069	0.039
		(0.72)	(0.39)	(0.32)	(0.21)	(0.13)
Ret^{m1}			1.766	1.790	1.604	1.202
			(1.24)	(1.42)	(1.28)	(0.99)
$Ret^{m2:m12}$			0.902	1.166**	1.112**	0.956*
			(1.40)	(2.36)	(2.17)	(1.84)
Economy Controls	No	No	No	Yes	Yes	Yes
WIOT Controls	No	No	No	No	Yes	Yes
Betas Controls	No	No	No	No	No	Yes
Observations	65,096	64,838	64,838	61,299	61,299	59,475
R-squared	0.143	0.169	0.246	0.362	0.376	0.420

Table 8: Predicting Consumption Growth with Choke Point Industry Returns

This table reports the results of quarterly regressions of aggregate consumption growth on the return of a spread portfolio long in high Choke Point Value (CPV) economy-industry pairs and short in low CPV economy-industry pairs. The dependent variable is cumulative growth in real (constant prices, seasonally-adjusted) consumption between quarters t to $t+4$. CPV H-L stands for the lagged cumulative 12 month return of the the spread portfolio long in high CPV economy-industry pairs and short in low CPV economy-industry pairs constructed in Panel A of Table 6. Mrkt-rf stands for the lagged cumulative 12 month return of the market portfolio (Mrkt-rf). The set of controls include the lagged cumulative 12 month return of the factors used in Panel A of Table 6 (SMB, HML, MOM, CMA, RMW), the cumulative four quarter growth in industrial production, lagged cumulative 12 month consumption growth, the term permium in the USA, and the change in the market yield on US treasury securities at 2-year constant maturity during the previous 12 months. In Panel A, we show results for the United States. In Panel B, we show results for the sample of developed countries (excluding the USA). In Panel C, we show results for all developed countries. In Panel D, we show show results for the whole sample. In Panels B, C, and D we aggregate country-level variables using lagged GDP in PPP before running the regressions. t-statistics are given in parentheses, based on Newey-West standard errors with 4 lags. Statistical significance at the 10%, 5%, and 1% level is indicated by *, **, and ***, respectively.

Panel A: USA

	(1)	(2)	(3)
CPV H–L	0.082***	0.078***	0.129**
	(3.55)	(3.10)	(2.45)
$Mrkt–rf$		0.010	0.020
		(0.69)	(0.89)
Controls	No	No	Yes
R-squared	0.144	0.148	0.314

Panel B: Developed excl USA

	(1)	(2)	(3)
CPV H–L	0.068**	0.060**	0.127***
	(2.55)	(2.52)	(2.79)
$Mrkt–rf$		0.016	−0.006
		(1.20)	(−0.25)
Controls	No	No	Yes
R-squared	0.081	0.092	0.356

Panel C: Developed incl USA

	(1)	(2)	(3)
CPV H–L	0.072***	0.066***	0.129***
	(3.05)	(2.86)	(2.96)
$Mrkt–rf$		0.013	0.000
		(1.21)	(0.01)
Controls	No	No	Yes
R-squared	0.108	0.116	0.356

Panel D: Whole Sample

	(1)	(2)	(3)
CPV H–L	0.053*	0.041	0.106**
	(1.97)	(1.60)	(2.46)
$Mrkt–rf$		0.025**	0.005
		(2.35)	(0.24)
Controls	No	No	Yes
R-squared	0.055	0.083	0.379

Table 9: Choke Point Values and Stock Returns in the Global Stock Market: Portfolio Analysis Using Double Sorts

This table reports the performance of double sorted economy-industry portfolios. At the end of each year, we sort economy-industry pairs with sufficient financial data into three portfolios, based on $Profitability$ (Panel A), betas with respect to the network factors of Herskovic (2018) $\beta^{Concentration}$ (Panel B) and $\beta^{Sparsity}$ (Panel C), *Eigenvector* centrality (Panel D), $MarketEquity$ (Panel E), beta with respect to the transportation cost factor of Barrot et al. (2019) $\beta^{TransportationCosts}$ (Panel F), beta with respect to the global supply chain pressure index of Benigno et al. (2022) β^{GSCPI} (Panel G), and beta with respect to the geopolitical index of Caldara and Iacoviello (2022) $\beta^{GeopoliticalRisk}$ (Panel H). In all Panels except for Panel G, we sort between years 1995 and 2020. In Panel G, we sort between years 2000 and 2020. See Appendix B for definitions of $\beta^{Concentration}$, $\beta^{Sparsity}$, $\beta^{TransportationCosts}$, β^{GSCPI}, and $\beta^{GeopoliticalRisk}$. We track the value-weighted monthly returns of the portfolios during the next 12 months, after which we rebalance. We report alphas from a 6 factor model, including Mrk-rf, SMB, HML, MOM, CMA, and RMW as factors. t-statistics are given in parentheses. Statistical significance at the 10%, 5%, and 1% level is indicated by *, **, and ***, respectively.

Panel A: Double Sorts on $Profitability$ and CPV

$Profitability$	CPV			
	1 (low)	2	3 (high)	H-L
1 (low)	−0.522***	−0.148	−0.101	0.421*
	(−2.97)	(−0.86)	(−0.50)	(1.84)
2	−0.263	0.079	0.202*	0.464**
	(−1.49)	(0.66)	(1.84)	(2.35)
3 (high)	0.080	0.162	0.102	0.022
	(0.71)	(1.50)	(1.10)	(0.15)
H - L	0.602***	0.310	0.203	
	(3.09)	(1.43)	(0.87)	

Panel B: Double Sorts on $\beta^{Concentration}$ and CPV

$\beta^{Concentration}$	CPV			
	1 (low)	2	3 (high)	H-L
1 (low)	−0.430**	−0.139	−0.346	0.085
	(−2.44)	(−0.75)	(−1.62)	(0.42)
2	−0.147	0.007	−0.116	0.032
	(−1.18)	(0.07)	(−1.43)	(0.23)
3 (high)	−0.260	0.197*	0.362***	0.622***
	(−1.33)	(1.88)	(3.61)	(2.76)
H - L	0.170	0.336	0.708***	
	(0.72)	(1.49)	(2.75)	

Panel C: Double Sorts on $\beta^{Sparisty}$ and CPV

$\beta^{Sparisty}$	CPV			
	1 (low)	2	3 (high)	H-L
1 (low)	−0.498***	−0.153	−0.016	0.482**
	(−2.91)	(−1.47)	(−0.19)	(2.53)
2	0.015	0.031	−0.038	−0.053
	(0.09)	(0.34)	(−0.30)	(−0.37)
3 (high)	−0.187	0.196	0.544***	0.731***
	(−1.09)	(1.30)	(3.80)	(3.64)
H - L	0.311	0.349*	0.560***	
	(1.55)	(1.93)	(3.06)	

Panel D: Double Sorts on *Eigenvector* centrality and CPV

Eigenvector	CPV			
	1 (low)	2	3 (high)	H-L
1 (low)	−0.448***	0.054	0.073	0.521***
	(−3.18)	(0.27)	(0.91)	(3.13)
2	−0.059	−0.147	−0.015	0.045
	(−0.44)	(−1.29)	(−0.18)	(0.32)
3 (high)	0.031	−0.149	0.530***	0.499**
	(0.15)	(−1.00)	(3.22)	(2.25)
H - L	0.479**	−0.202	0.457**	
	(2.05)	(−0.89)	(2.46)	

Panel E: Double Sorts on $MarketEquity$ and CPV

$MarketEquity$	CPV			
	1 (low)	2	3 (high)	H-L
1 (low)	0.003	0.001	0.151	0.147
	(0.984)	(0.994)	(0.415)	(0.407)
2	−0.244*	−0.068	−0.034	0.210
	(0.070)	(0.614)	(0.814)	(0.162)
3 (high)	−0.273**	0.072	0.150**	0.423***
	(0.030)	(0.299)	(0.041)	(0.004)
H - L	−0.276	0.071	−0.000	
	(0.126)	(0.685)	(0.998)	

Panel F: Double Sorts on $\beta^{TransportationCosts}$ and CPV

$\beta^{TransportationCosts}$	CPV			
	1 (low)	2	3 (high)	H-L
1 (low)	−0.170	0.035	0.419***	0.588***
	(−0.90)	(0.26)	(2.79)	(3.23)
2	−0.145	0.105	0.005	0.150
	(−0.94)	(0.93)	(0.05)	(0.84)
3 (high)	−0.339**	−0.240	−0.160	0.179
	(−2.00)	(−1.36)	(−1.28)	(0.96)
H - L	−0.170	−0.275	−0.579***	
	(−0.68)	(−1.15)	(−2.65)	

Panel G: Double Sorts on β^{GSCPI} and CPV

β^{GSCPI}	CPV			
	1 (low)	2	3 (high)	H-L
1 (low)	−0.121	−0.078	0.290**	0.411**
	(−0.73)	(−0.60)	(2.51)	(2.31)
2	0.094	0.077	0.097	0.003
	(0.63)	(0.66)	(1.07)	(0.02)
3 (high)	−0.402**	−0.094	−0.042	0.360*
	(−2.25)	(−0.49)	(−0.24)	(1.66)
H - L	−0.281	−0.016	−0.331	
	(−1.20)	(−0.07)	(−1.43)	

Panel H: Double Sorts on $\beta^{GeopoliticalRisk}$ and CPV

$\beta^{GeopoliticalRisk}$	CPV			
	1 (low)	2	3 (high)	H-L
1 (low)	−0.181	0.125	0.199*	0.380**
	(−1.16)	(1.10)	(1.70)	(2.02)
2	−0.199	0.242*	0.089	0.288*
	(−1.48)	(1.96)	(0.83)	(1.65)
3 (high)	−0.309	−0.162	−0.242	0.067
	(−1.59)	(−0.92)	(−1.49)	(0.31)
H - L	−0.128	−0.287	−0.441**	
	(−0.51)	(−1.26)	(−1.98)	

Table 10: Centrality Measures and Stock Returns

This table reports the results of Fama-MacBeth regression of economy-industry returns on lagged measures of network centrality and lagged predictors of performance. The dependent variable is value-weighted economy-industry return, expressed in percentages. All measures of network centrlality are defined in Appendix C and expressed as percentiles. In each specification, we include common predictors of performance (β, $log(BookEquity)$, $log(MarketEquity)$, $Profitability$, $Investment$, $Dividends$, Ret^{m1}, $Ret^{m2:m12}$), defined in Appendix B. t-statistics based on Newey-West standard errors are given in parentheses. Statistical significance at the 10%, 5%, and 1% level is indicated by *, **, and ***, respectively.

	(1)	(2)	(3)	(4)	(5)	(6)
CPV	0.004***	0.004***	0.004***	0.004***	0.002*	0.002**
	(3.08)	(3.11)	(3.12)	(2.84)	(1.75)	(2.14)
Eigenvector	−0.002					
	(−1.08)					
Katz-Bonacich		−0.002				
		(−1.15)				
Weighted Indegree			−0.002			
			(−1.25)			
In-Closeness				−0.003		
				(−1.33)		
Weighted Outdegree					0.002	
					(0.90)	
Out-Closeness						0.001
						(0.73)
Controls	Yes	Yes	Yes	Yes	Yes	Yes
Observations	64,838	64,838	64,838	63,278	64,838	64,838
R-squared	0.256	0.256	0.256	0.256	0.254	0.253

Table 11: Lagged Choke Point Values and Stock Returns

This table reports the performance of industry portfolios conditional on their lagged Choke Point Value. At the end of each year between 1995 and 2020, we sort economy-industry pairs with sufficient financial data into five portfolios, based on lagged Choke Point Value. Next, we track the value-weighted monthly returns of the portfolios during the next 12 months, after which we rebalance. We report excess returns and alphas from several standard asset pricing models, based on Fama-French models, separately for the low Portfolio 1, the high Portflio 5, and the spread portfolio between Portfolios 5 and 1. CAPM includes Mrk-rf as a sole factor, FF3 adds SMB and HML, FF4 augments FF3 with MOM and FF5 augments FF3 with CMA and RMW, and FF6 includes all factors together. t-statistics are given in parentheses. Statistical significance at the 10%, 5%, and 1% level is indicated by *, **, and ***, respectively.

Ret–rf	*Alphas*				
	CAPM	FF3	FF4	FF5	FF6
Portfolio 1 (low)					
0.231	−0.282**	−0.329**	−0.333**	−0.332**	−0.335**
(0.76)	(−2.01)	(−2.56)	(−2.53)	(−2.42)	(−2.41)
Portfolio 5 (high)					
0.648**	0.003	0.029	0.076	0.235***	0.251***
(2.03)	(0.03)	(0.34)	(0.86)	(2.74)	(2.90)
Portfolio 5 – 1					
0.417**	0.285*	0.358**	0.409**	0.567***	0.586***
(2.43)	(1.71)	(2.31)	(2.59)	(3.50)	(3.58)

Online Appendices

Appendix A Unpacking the Sources of Value-Added in Global Value Chains

We provide an example WIOT in Figure A.1. The Table contains a matrix $\mathbf{Z}$ of size $JS \times JS$ (for example, $77 * 45 \times 77 * 45$ as in our WIOT from OECD). Each entry Z_{ij}^{rs} contains the value of inputs from industry r in economy i (row arrays) that is used by industry s in economy j (column arrays). Values of the output of each economy-industry pair that are instead absorbed in final-use, such as household consumption, are reported to the right of $\mathbf{Z}$. $\mathbf{F_j}$ is defined as a vector of size $JS \times 1$ that stacks the values F_{ij}^{r} of output from industry r in economy i that is absorbed in the final use of economy j. We denote the the sum of these vectors over all destination economies by $\mathbf{F} = \sum_j \mathbf{F_j}$.

The starting point for the value added decomposition is a basic gross output accounting identity. Define $\mathbf{Y}$ as the $JS \times 1$ vector of gross output values Y_j^s. Let $\mathbf{A}$ then be the $JS \times JS$ matrix of direct requirement coefficients, $a_{ij}^{rs} = Z_{ij}^{rs}/Y_j^s$ (value of the input from industry r in economy i that is used in the production of 1 dollar unit of output for industry s in economy j). The gross output of an economy-industry can then be expressed as:

$$\mathbf{Y} = \mathbf{F} + \mathbf{AY} = \mathbf{F} + \mathbf{AF} + \mathbf{A^2F} + \dots \tag{A.1}$$

Gross output is the sum of value absorbed in final use as well as the one purchased for use as an input from all other economy-industry pairs. We obtain the infinite sum representation by iteratively substituting for $\mathbf{F}$. According to this representation, the set of direct requirements coefficients in $\mathbf{A}$ describes the production technology, both when the output is used in final consumption or as an intermediary output (also irrespective of the destination economy).

Equation A.1 can be rewritten as

$$\mathbf{Y} = (\mathbf{I} - \mathbf{A})^{-1}\mathbf{F} \tag{A.2}$$

where where $\mathbf{I}$ is a $JS \times JS$ identity matrix and $(\mathbf{I} - \mathbf{A})^{-1}$ stands for the Leontieff inverse matrix

(Leontief, 1986).

From the WIOT, we can compute the part of the gross output that is exported abroad, stacked in vector $\mathbf{GX}$ of size $JS \times 1$. For example, for each economy i we can compute an $S \times 1$ vector of gross exports, with the r-th entry equal to $\sum_{j \neq i} \sum_s Z_{ij}^{rs} + \sum_{j \neq i} F_{ij}^r$. In the value-added decomposition, $\mathbf{V}$ is the $JS \times 1$ vector that is the transpose of the row vector of value-added entries VA_j^s. Each value-added entry represents the output of the economy-industry pair in excess of all inputs used, that is, $VA_j^s = Y_j^s - \sum_{i,r} Z_{ij}^{rs}$. Following Hummels et al. (2001), we can decompose the sources of value-added embedded in the gross exports by (i) taking the diagonal matrix of gross exports $\mathbf{\hat{GX}}$, where the 'hat' notation denotes a diagonal matrix whose main diagonal entries are the entries of the corresponding column vector; (ii) using the Leontief inverse $(\mathbf{I} - \mathbf{A})^{-1}$ to back out the gross output needed to generate the diagonal gross export matrix; and then (iii) pre-multiplying this by a diagonal matrix of value-added shares in gross output, $\mathbf{\hat{V}\hat{Y}}^{-1}$:

$$\mathbf{\hat{V}\hat{Y}^{-1}}(\mathbf{I} - \mathbf{A})^{-1}\mathbf{\hat{GX}} \tag{A.3}$$

The above expression results in a matrix of size $JS \times JS$ that decomposes gross exports into domestic and foreign sources of value-added and is commonly referred to as Trade in Value Added (TiVA). For an overview of the literature using WIOT analysis, see Antràs and Chor (2022).

Figure A.1: Standard World Input-Output Table

This figure presents a visual representation of a World Input-Output Table.

			Input Use and Value Added							Final Use			Total Use
			Economy 1			⋯	Economy J			Economy 1	⋯	Economy J	
			Industry 1	⋯	Industry S	⋯	Industry 1	⋯	Industry S				
Output	Economy 1	Industry 1	Z_{11}^{11}	⋯	Z_{11}^{1S}	⋯	Z_{1J}^{11}	⋯	Z_{1J}^{1S}	F_{11}^{1}	⋯	F_{1J}^{1}	Y_1^1
		⋯	⋯	Z_{11}^{rs}	⋯	⋯	⋯	Z_{1J}^{rs}	⋯	⋯	⋯	⋯	⋯
		Industry S	Z_{11}^{S1}	⋯	Z_{11}^{SS}	⋯	Z_{1J}^{S1}	⋯	Z_{1J}^{SS}	F_{11}^{S}	⋯	F_{1J}^{S}	Y_1^S
	⋯	⋯	⋯	⋯	⋯	⋯	⋯	⋯	⋯	⋯	⋯	⋯	⋯
Supplied	Economy J	Industry 1	Z_{J1}^{11}	⋯	Z_{J1}^{1S}	⋯	Z_{JJ}^{11}	⋯	Z_{JJ}^{1S}	F_{J1}^{1}	⋯	F_{JJ}^{1}	Y_J^1
		⋯	⋯	Z_{J1}^{rs}	⋯	⋯	⋯	Z_{JJ}^{rs}	⋯	⋯	⋯	⋯	⋯
		Industry S	Z_{J1}^{S1}	⋯	Z_{J1}^{SS}	⋯	Z_{JJ}^{S1}	⋯	Z_{JJ}^{SS}	F_{J1}^{S}	⋯	F_{JJ}^{S}	Y_J^S
Value Added			VA_1^1	⋯	VA_1^S	⋯	VA_J^1	⋯	VA_J^S				
Gross Output			Y_1^1	⋯	Y_1^S	⋯	Y_J^1	⋯	Y_J^S				

Appendix B Data Sources and Cleaning Procedures

We collect accounting and stock level data from COMPUSTAT Global and CRSP, following the data-cleaning and constructing procedures of Jensen et al. (2023). In order to match companies to OECD's TiVA industries, we use the reported NAICS industry code, which can be directly mapped to TiVA industries. For companies without a NAICS code, we use the following approach. We first construct a map between GICS and NAICS, using companies with both industry identifications available. We assign a GICS code to a NAICS code based on matching frequency. The NAICS with the largest number of matches to a given GICS is assigned as the NAICS code that corresponds to the given GICS code. Next, we convert all companies with an available GICS code to a NAICS code, which we then map to a TiVA industry. We collect information on stock returns, market equity, book equity, profitability (defined as operating profits scaled book equity), investment (defined as the annual growth rate of assets) and dividends (scaled by book equity). To account for short term reversal and momentum, we include lagged return and the cumulative return in the eleven months preceding the lagged return. Since we construct economy-industry level variables, we weight returns and characteristics using lagged market value. To include an economy-industry portfolio in our asset pricing tests, we require at least 20 stocks with valid return and market equity at the end of the previous year. Data on monthly U.S. exports are obtained from USA Trade Online, published by the US Census Bureau. We measure geographical distance in the Houthi experiment as the log of thousands of kilometers between the country's capital and the Bab el-Mandeb strait. We collect data on population, GDP per capita, inflation, and industrial production form the World Bank. Exchange rates are from COMPUSTAT Global. The source for the data on the term premium on a 10 Year Zero Coupon Bond and the change in the market yield on US treasury securities at 2-year constant maturity during the previous 12 months is the Federal Reserve Bank of St. Louis. We estimate economy-industry and economy betas using a CAPM model based on the past 60 months of data and the global market portfolio as a risk factor. We require at least 24 monthly observations to compute either beta.

We estimate betas with respect to the network *Concentration* and *Sparsity* factors of Herskovic (2018) ($\beta^{Concentration}$ and $\beta^{Sparsity}$). Each year y, we compute *Concentration* as the concentration of log output shares, weighted by their output share and *Sparsity* as the concentration of log input shares, averaged across nodes and weighted by their output shares.

Next, we follow Herskovic (2018) and run the following model:

$$R_{s,j,y} = \alpha_{s,j} + \beta_{s,j}^{Concentration} \Delta Concentration_y + \beta_{s,j}^{Sparsity} \Delta Sparsity_y + \delta \times \mathbf{X}_y + \xi_{s,j,y} \quad \text{(B.1)}$$

where $\Delta Concentration_y$ and $\Delta Sparsity_y$ are innovations in *Concentration* and *Sparsity* and $\mathbf{X}_y$ is a vector of control variables, including lagged levels of *Concentration* and *Sparsity* and changes in residual TFP, computed as the residual from regressing TFP growth on factor innovations. We compute a World TFP by aggregating economy-level TFP from the Penn World Table 11.0 (see Feenstra et al. (2015) and `www.ggdc.net/pwt`) using lagged GDP in PPP as the weight, sourced from the World Bank. We run the model using yearly data across the full sample and use the estimated $\beta^{Concentration}$ and $\beta^{Sparsity}$ each year for our portfolio sorts. We rescale the estimated betas (divided by 100) for readability. In alternative specifications, we either replace the World TFP with economy-specific TFP or add the economy-specific TFP as an additional control. Our results remain qualitatively similar using either of the alternative specifications.

For each industry s in economy j with sufficient financial data, we estimate betas with respect to the transportation costs factor of Barrot et al. (2019) ($\beta^{TransportationCosts}$), the global supply chain pressure index of Benigno et al. (2022) (β^{GSCPI}), and the geopolitical index of Caldara and Iacoviello (2022) ($\beta^{GeopoliticalRisk}$). To do this, we run a market model augmented with an additional factor F:

$$R_{s,j,t} = \alpha_{s,j} + \gamma_{s,j} \times (Mrkt\text{–}rf)_t + \beta_{s,j} \times F_t + \epsilon_{s,j,t}, \quad \text{(B.2)}$$

where F is either $TransportationCosts$, $GSCPI$, or $GeopoliticalRisk$. To compute $TransportationCosts$, we follow Barrot et al. (2019) and use their replication code and files. We download the data for $GSCPI$, and $GeopoliticalRisk$ from the websites of the respective authors. We estimate the betas each year using monthly data during the last five years, requiring at least 24 valid monthly observations. We rescale $\beta^{GeopoliticalRisk}$ (multiplied by 100) for readability.

Appendix C Glossary of Network Terminology

C.1 Key TiVA Variables

$\boldsymbol{GX_j^s}$ Dollar value of gross exports of industry s in economy j

$\boldsymbol{VA_{i,j}^{r,s}}$ Dollar value added of the gross exports of industry s in economy j that stems from imported intermediate inputs from industry r in economy i

$\boldsymbol{FVA_{i,j}^{r,s}}$ Foreign value added by industry r in economy i to industry s in economy j, computed as $VA_{i,j}^{r,s}$ divided by GX_j^s. Note that any domestic links are set to zero, i.e. $FVA_{i,j}^{r,s} = 0$ if $i = j$.

C.2 Network Definitions and Variables

$\boldsymbol{G(V,E)}$ The directed graph representing trade in value-added among 77 economies and 45 industries, defined by the set of nodes $\boldsymbol{V}$ and the set of edges $\boldsymbol{E}$.

$\boldsymbol{V}$ The set of nodes (economy-industry pairs), comprising 3465 pairs (77 economies $\times$ 45 industries) denoted as $n(s,j)$ or v.

$\boldsymbol{E}$ The set of directed edges $e_{i,j}^{r,s}$ connecting two nodes $n(r,i)$ and $n(s,j)$, equal to the value added by industry r in economy i to industry s in economy j, i.e. $FVA_{i,j}^{r,s}$. Note that since $FVA_{i,j}^{r,s} = 0$ if $i = j$, all edges linking industries from the same economy are set to 0.

$\boldsymbol{P}$ A path in the graph $\boldsymbol{G}$ representing a collection of nodes $n(r,i)$ and directed edges $e_{i,j}^{r,s}$ that link them, forming a route from a source node to a target node.

$\boldsymbol{A}$ The adjacency matrix representing the connections between nodes in the network. The entry $A_{n(r,i),n(s,j)}$ in the matrix is $FVA_{i,j}^{r,s}$ if there exists a directed edge from $n(r,i)$ to node $n(s,j)$, and 0 otherwise.

$\boldsymbol{Length(P)}$ The length of a path is the number of nodes part of the path.

$\boldsymbol{DirectPath_{n(r,i)\to n(s,j)}}$ The direct path from node $n(r,i)$ to node $n(s,j)$ in the graph $\boldsymbol{G(V,E)}$, con-

sisting of the source node $n(r,i)$, the target node $n(s,j)$, and the edge connecting them $e_{i,j}^{r,s}$. It represents the direct value flows between the two nodes.

$\boldsymbol{ShortestPath_{n(r,i)\rightarrow n(s,j)}}$

The shortest path from node $n(r,i)$ to node $n(s,j)$ in the graph $\boldsymbol{G(V,E)}$, given by:

$$ShortestPath_{n(r,i)\rightarrow n(s,j)} = \arg\min_{P} \sum_{e\in P} c(e)$$

where P represents a path in $\boldsymbol{G}$, and $c(e)$ is the cost of an edge e along the path P equal to e^{-1}. This path minimizes the total accumulated *cost* between industry r in economy i and industry s in economy j. Because the costs are defined as the inverse of the edges, the shortest path represents the path with the strongest supply chain flows. See Opsahl et al. (2010) for an overview of the literature that uses weights as inverse of the edges and the application of the algorithm of Dijkstra (1959) for finding minimum cost paths in networks.

$\boldsymbol{Upstreamness_{n(s,j)}}$

Following Antràs et al. (2012) the upstreamness of a node is defined as the weighted average number of production stages the node is from final demand:

$$Upstreamness_{n(s,j)} = \boldsymbol{Y}^{-1} \cdot (1 \cdot \boldsymbol{I} + 2 \cdot \boldsymbol{A} + +3 \cdot \boldsymbol{A}^2 + \cdots) \cdot \boldsymbol{F}$$

C.3 Network Centrality Measures

Below the definition of the centrality measures used in this paper, computed at the end of each calendar year t. We present a correlation matrix of the centrality measures in Table C.1.

$\boldsymbol{CPV(v)}$ The Choke Point Value of node v is the betweenness centrality of node v, computed as the total number of shortest passing through the node, scaled by the total number of shortest paths in the network:

$$\sum_{j\neq k\neq v,t} \frac{\sigma_{jk,t}(v)}{\delta_t}$$

where j and k are two distinct production nodes other than v, $\sigma_{jk,t}(v)$ is the

number of the shortest paths from j to k passing through v, and δ_t is the total number of shortest paths in the network ($\sum_{j \neq k,t} \sigma_{jk,t}$).

***Eigenvector*(v)**

The eigenvector centrality of node v, computed iteratively based on the connections of neighboring nodes and their own centralities:

$$\frac{1}{\lambda} \sum_{t \neq v} A_{v,t} \cdot EIGEN(t)$$

***Katz-Bonacich*(v)**

The Katz-Bonacich centrality of node v, computed based on the number of paths of varying lengths connecting v to other nodes, with a parameter α controlling the influence of distant nodes:

$$\alpha \sum_{t} A_{v,t} + \alpha^2 \sum_{n \neq v} A_{v,n} \cdot A_{n,t} + \alpha^3 \sum_{n \neq v} A_{v,n} \cdot A_{n,m} \cdot A_{m,t} + \ldots$$

***Weighted Indegree*(v)**

The weighted indegree centrality of node v, computed as the sum of the weights of incoming edges:

$$\sum_{n} A_{n,v} \cdot e_{n,v}$$

***In-Closeness*(v)**

The in-closeness centrality of node v, computed as the reciprocal of the average shortest path cost (d) ending in v from all other nodes:

$$\frac{1}{\frac{1}{n-1} \sum_{n \neq v} d(n, v)}$$

***Weighted Outdegree*(v)**

The weighted outdegree centrality of node v, computed as the sum of the weights of outgoing edges:

$$\sum_{t} A_{v,t} \cdot e_{v,t}$$

***Out-Closeness*(v)**

The out-closeness centrality of node v, computed as the reciprocal of the average shortest path cost (d) from v to all other nodes:

$$\frac{1}{\frac{1}{n-1}\sum_{t \neq v} d(v,t)}$$

Table C.1: Correlation of Network Centrality Measures in the Global Production Nework

This table presents a correlation matrix of network centrality measures. We compute Spearman correlations each year and then compute average values across all years.

	(1)	(2)	(3)	(4)	(5)	(6)	(7)
Betweenness:							
(1) *CPV*	1.00						
Foreign Dependence:							
(2) *Eigenvector*	0.41	1.00					
(3) *Katz-Bonacich*	0.41	1.00	1.00				
(4) *Weighted Indegree*	0.41	0.96	0.98	1.00			
(5) *In-Closeness*	0.10	0.26	0.24	0.17	1.00		
Foreign Influence:							
(6) *Weighted Outdegree*	0.58	0.04	0.04	0.04	0.07	1.00	
(7) *Out-Closeness*	0.62	0.11	0.11	0.09	0.18	0.92	1.00

Appendix D Additional Findings

D.1 The Production Network and Choke Points in 2019

In Sections 1 and 4, we provide graphs depicting the global production network in 2020, the end of our sample. However, as Covid-19 affected global value chains during that year, our graphs may reflect information that is specific to the shock. Therefore, we provide an overview of the distribution of choke points in 2019, prior to the Covid-19 pandemic. Both Figure D.1 and Figure D.2 indicate that the topology of choke points was similar in 2019 to the one we present in the main body of the paper. Thus, the visual representation of the topology of the global production network in the main body of the paper does not appear to reflect the Covid-19 pandemic.

D.2 Top Water Transport industries affected by the Houthi Attacks

Table D.1 provides key descriptive statistics for the top 5 Water Transport industries used in the identification strategy in Section 4.2.1.

D.3 Predictability of Consumption Growth over 12 Quarters

In Section 5.2 and Table 8, we show that the return of the zero cost portfolio long in high CPV economy-industry pairs and short in low CPV economy-industry pairs predicts subsequent four (continuously compounded) quarter consumption growth across the USA, the rest of the developed world, as well as over the whole sample of countries. In addition, the graphical depiction of the predictability of consumption growth in Figure 16 suggests that impact of CPV on consumption growth is persistent beyond the first four quarters, as the graph shows no reversals in the estimated impact of the zero cost portfolio on long-term consumption growth. In Table D.2, we examine more formally the longer term impact of CPV on consumption growth by studying consumption growth on year-by-year basis over a period of 12 quarters. In specifications (1) and (2) , we show the same results as in Table 8: a decrease in the returns of high CPV economy-industry pairs, relative to their peripheral counterparts, leads to a decrease in subsequent four quarter consumption. In specifications (3)-(6), we look at predictability

of consumption growth over the subsequent two years. We find that the estimated coefficient on the return of the spread portfolio of high CPV economy-industry pairs relative to their peripheral counterparts is not statistically significant in any specification. Hence, the decrease in consumption associated with a decrease in high CPV economy-industry pairs is persistent beyond the first quarters with no signs of reversals.

D.4 Predictability of GDP Growth

Next, we show that the predictive relationship between CPV and consumption growth is not confined to consumption dynamics but reflects broader macroeconomic fluctuations. Specifically, we replace the dependent variable four (continuously compounded) quarter consumption growth in Table 8 with four (continuously compounded) quarter GDP growth. Results are reported in Table D.3. We find similar predictability in the USA and the developed markets: a decrease in the returns of high CPV economy-industry pairs, relative to their peripheral counterparts, leads to a decrease in subsequent four quarter GDP.

D.5 Country and Industry CPV as Drivers of Return Predictability

To assess whether the predictive power of CPV captures broader features of economies or industries, we extend the Fama–MacBeth regressions by including economy-level and industry-level aggregates of CPV. Specifically, $Economy\ CPV^{PRCNTL}$ is defined as the percentile-ranked average CPV across all industries within an economy. Similarly, $Industry\ CPV^{PRCNTL}$ is the percentile-ranked average CPV across all countries within a given industry. These variables allow us to test whether the CPV premium can be attributed to country-specific and/or industry-specific features. Results are reported in Table D.4. We find that the return premium associated with CPV is not attributable to an economy being systematically more central in global production networks, or to an industry being globally important, but instead reflects variation at the economy–industry level.

D.6 Double Sorts on Output and CPV

In Section 6.1, we show that the predictability of economy-industry returns using CPV cannot be explained by size. That test is based on the total market capitalization of the economy-industry pair as a measure for size. For robustness, we use an alternative proxy for size – the economy-industry pair's total output. We double sort economy-industry pairs in buckets based on output and CPV. We present abnormal returns of the portfolios in Table D.5. Again, we find that CPV explains subsequent returns over and above the size of the economy-industry pair, consistent with the findings in Panel C of Table 9.

D.7 Alternative Cost for Computing Shortest Paths

As a robustness check, we construct an alternative measure of CPV that employs the following cost per edge:

$$c(e) = -log(e) \tag{D.1}$$

The next steps of computing shortest paths and CPV follow the same methodology as described earlier. By taking logs, we dampen the influence of exceptionally large trade flows, which may otherwise disproportionately drive shortest paths. This allows the alternative computation of CPV to reflect economically meaningful connections beyond a small set of dominant links. Again, each year we sort economy-industy pairs based on this altrnative CPV and track their subsequent performance. Results are presented in Table D.6 and consistent with our main findings.

Figure D.1: Geographic Distribution of Choke Point Index in 2019

This figure depicts economy Choke Point Value (CPV) for 2019, computed as the number of shortest paths passing via a economy, expressed as a percentage of all shortest paths. Higher intensity of blue represents higher economy CPV. Countries with no data are depicted in light gray.

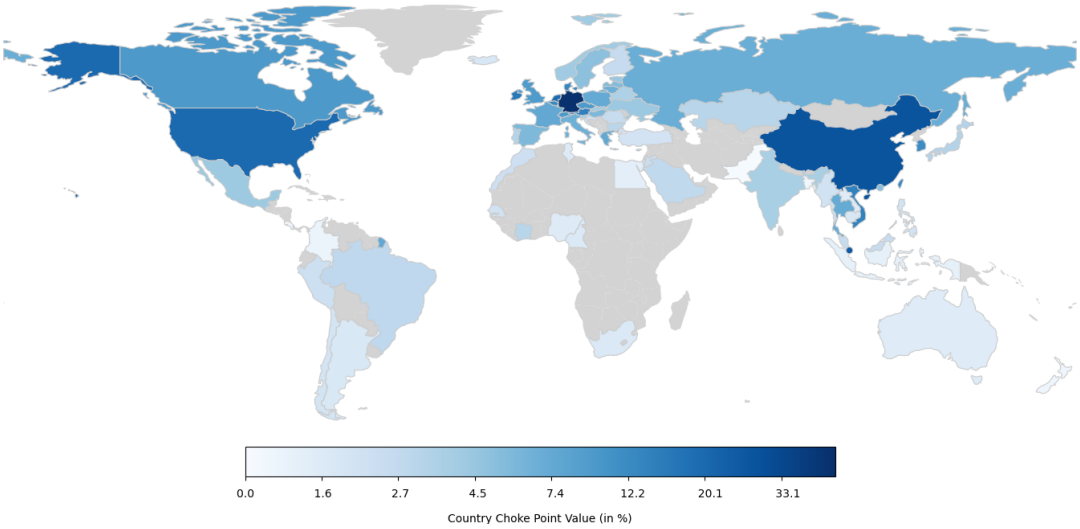
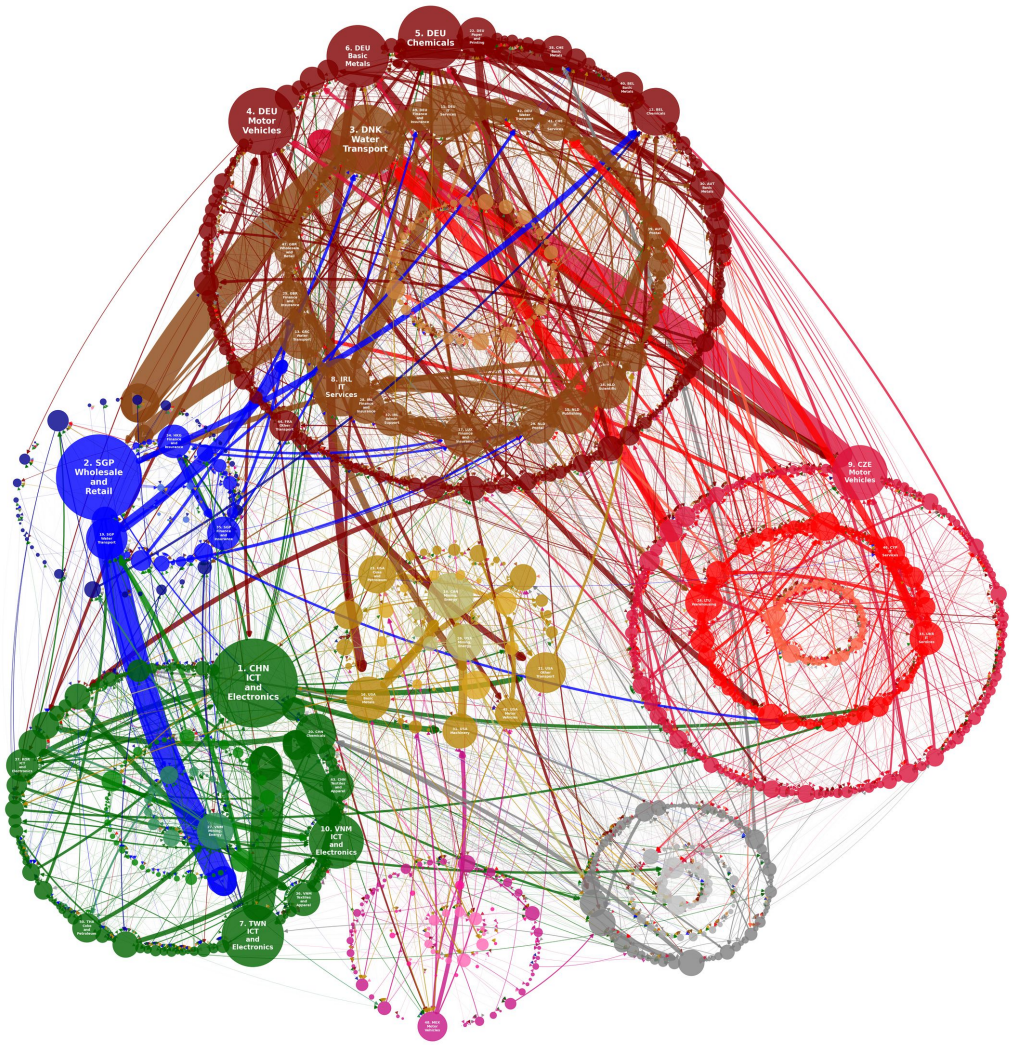


Figure D.2: The Global Network of Choke Points in 2019

This figure presents a visual representation of the global network of choke points in 2019, where each node is an economy-industry pair. The thickness of the arrow from node A to node B represents the total number of shortest paths passing from node A to node B. The size of the node represents the total number of shortest paths passing via the node, i.e. the node's Choke Points Value. We group nodes into seven groups, based on the geography and economic development, following the classification in Table 1. Within each group of nodes, we place all manufacturing industries in the outer circle, all business services industries in the middle cirlce, and all other industries in the inner circle.



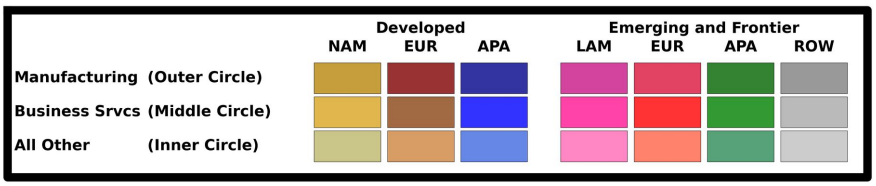


Table D.1: Top 5 Affected Water Transport Industries Around the Houthi Attacks

This table presents key statistics for the five Water Transport industries, most affected by the Houthi attacks. We report CPV rank, total shortest paths passing via the node used to compute the CPV, the number of treated paths (computed as the total number of shortest paths between Asia and Developed Europe that pass through the water transportation industry, additionally requiring that the shortest path does not pass through North or South America), also expressed as a percentage of the total shortest paths passing via. All data is based on the 2020 global production network.

	DNK	GRC	SGP	CYP	NOR
CPV Rank	3	12	29	57	82
Total Shortest Paths Passing Via	1,800,144	615,224	295,417	184,332	130,010
Treated Shortest Paths	215,781	86,049	44,242	34,417	30,927
Percentage Affected Shortest Paths	12%	14%	15%	19%	24%

Table D.2: Predictability of Consumption Growth on a Year-by-Year Basis

This table reports the results of quarterly regressions of aggregate consumption growth on the return of a spread portfolio long in high Choke Point Value (CPV) economy-industry pairs and short in low CPV economy-industry pairs. The dependent variable is cumulative growth in real (constant prices, seasonally-adjusted) consumption between quarters t to $t+4$ (specifications (1)-(2)), quarters $t+4$ to $t+8$ (specifications (3)-(4)), and quarters $t+8$ to $t+12$ (specifications (5)-(6)). CPV H-L stands for the lagged cumulative 12 month return of the the spread portfolio long in high CPV economy-industry pairs and short in low CPV economy-industry pairs constructed in Panel A of Table 6. In specifications (2), (4) and (6), we additionally include lagged cumulative 12 month return of the market portfolio (Mrkt-rf), the lagged cumulative 12 month return of the factors used in Panel A of Table 6 (SMB, HML, MOM, CMA, RMW), the cumulative four quarter growth in industrial production, lagged cumulative 12 month consumption growth, the term permium in the USA, and the change in the market yield on US treasury securities at 2-year constant maturity during the previous 12 months. In Panel A, we show results for the United States. In Panel B, we show results for the sample of developed countries (excluding the USA). In Panel C, we show results for all developed countries. In Panel D, we show show results for the whole sample. In Panels B, C, and D we aggregate country-level variables using lagged GDP in PPP before running the regressions. t-statistics are given in parentheses, based on Newey-West standard errors with 4 lags. Statistical significance at the 10%, 5%, and 1% level is indicated by *, **, and ***, respectively.

Panel A: USA

	(1)	(2)	(3)	(4)	(5)	(6)
	$\Delta C^{t:t+4}$		$\Delta C^{t+4:t+8}$		$\Delta C^{t+8:t+12}$	
CPV H-L	0.082***	0.129**	0.031	0.011	0.026	0.013
	(3.55)	(2.45)	(1.25)	(0.24)	(1.45)	(0.67)
Mrkt-rf		−0.341		0.180		0.310
		(−0.38)		(0.36)		(0.62)
Controls	No	Yes	No	Yes	No	Yes
R-squared	0.144	0.314	0.021	0.128	0.015	0.143

Panel B: Developed excl USA

	(1)	(2)	(3)	(4)	(5)	(6)
	$\Delta C^{t:t+4}$		$\Delta C^{t+4:t+8}$		$\Delta C^{t+8:t+12}$	
CPV H-L	0.068**	0.127***	0.028*	0.006	0.015	−0.036
	(2.55)	(2.79)	(1.76)	(0.21)	(0.88)	(−0.81)
Mrkt-rf		0.015		0.391		1.321
		(0.02)		(0.60)		(0.89)
Controls	No	Yes	No	Yes	No	Yes
R-squared	0.081	0.356	0.014	0.138	0.004	0.105

Panel C: Developed incl USA

	(1)	(2)	(3)	(4)	(5)	(6)
	$\Delta C^{t:t+4}$		$\Delta C^{t+4:t+8}$		$\Delta C^{t+8:t+12}$	
CPV H-L	0.072***	0.129***	0.028	0.012	0.019	−0.013
	(3.05)	(2.96)	(1.53)	(0.33)	(1.15)	(−0.36)
Mrkt-rf		−0.224		0.139		0.842
		(−0.27)		(0.23)		(0.70)
Controls	No	Yes	No	Yes	No	Yes
R-squared	0.108	0.356	0.017	0.110	0.008	0.105

Panel D: Whole Sample

	(1)	(2)	(3)	(4)	(5)	(6)
	$\Delta C^{t:t+4}$		$\Delta C^{t+4:t+8}$		$\Delta C^{t+8:t+12}$	
CPV H-L	0.053*	0.106**	0.010	0.009	−0.005	−0.032
	(1.97)	(2.46)	(0.57)	(0.23)	(−0.26)	(−1.21)
Mrkt-rf		−0.486		−0.020		1.018
		(−0.59)		(−0.03)		(1.22)
Controls	No	Yes	No	Yes	No	Yes
R-squared	0.055	0.379	0.002	0.090	0.000	0.088

Table D.3: Predictability of GDP Growth

This table reports the results of quarterly regressions of aggregate GDP growth on the return of a spread portfolio long in high Choke Point Value (CPV) economy-industry pairs and short in low CPV economy-industry pairs. The dependent variable is cumulative growth in real (constant prices, seasonally-adjusted) GDP between quarters t to $t+4$. CPV H-L stands for the lagged cumulative 12 month return of the the spread portfolio long in high CPV economy-industry pairs and short in low CPV economy-industry pairs constructed in Panel A of Table 6. Mrkt-rf stands for the lagged cumulative 12 month return of the market portfolio (Mrkt-rf). The set of controls include the lagged cumulative 12 month return of the factors used in Panel A of Table 6 (SMB, HML, MOM, CMA, RMW), the cumulative four quarter growth in industrial production, lagged cumulative 12 month consumption growth, the term permium in the USA, and the change in the market yield on US treasury securities at 2-year constant maturity during the previous 12 months. In Panel A, we show results for the United States. In Panel B, we show results for the sample of developed countries (excluding the USA). In Panel C, we show results for all developed countries. In Panel D, we show show results for the whole sample. In Panels B, C, and D we aggregate country-level variables using lagged GDP in PPP before running the regressions. t-statistics are given in parentheses, based on Newey-West standard errors with 4 lags. Statistical significance at the 10%, 5%, and 1% level is indicated by *, **, and ***, respectively.

Panel A: USA			
	(1)	(2)	(3)
CPV H-L	0.059***	0.051**	0.104**
	(2.96)	(2.29)	(2.31)
Mrkt-rf		0.017	0.007
		(1.23)	(0.28)
Controls	No	No	Yes
R-squared	0.097	0.115	0.270

Panel B: Developed excl USA			
	(1)	(2)	(3)
CPV H-L	0.051*	0.037	0.098**
	(1.95)	(1.50)	(2.51)
Mrkt-rf		0.028**	−0.010
		(2.27)	(−0.43)
Controls	No	No	Yes
R-squared	0.049	0.084	0.400

Panel C: Developed incl USA			
	(1)	(2)	(3)
CPV H-L	0.053**	0.042*	0.104***
	(2.50)	(1.97)	(2.68)
Mrkt-rf		0.024*	−0.003
		(1.97)	(−0.13)
Controls	No	No	Yes
R-squared	0.065	0.095	0.364

Panel D: Whole Sample			
	(1)	(2)	(3)
CPV H-L	0.010	−0.005	0.052
	(0.38)	(−0.18)	(1.43)
Mrkt-rf		0.031**	0.006
		(2.29)	(0.30)
Controls	No	No	Yes
R-squared	0.002	0.048	0.404

Table D.4: Choke Point Values and Stock Returns: Regression Analysis including Country and Industry averages of CPV

This table reports the results of Fama-MacBeth regressions of economy-industry returns on their lagged Choke Point Value (CPV), lagged country and industry averages of CPV, and lagged predictors of performance. The dependent variable is a value-weighted economy-industry return, expressed in percentages. CPV^{PRCNTL} is the most recently available Choke Point Value, expressed as a percentile. *Economy* CPV^{PRCNTL} is the economy average of the most recently available Choke Point Value, expressed as a percentile. *Industry* CPV^{PRCNTL} is the industry average of the most recently available Choke Point Value, expressed as a percentile. Depending on the specification, we include financial control variables (β, $log(BookEquity)$, $log(MarketEquity)$, $Profitability$, $Investment$, $Dividends$, Ret^{m1}, and $Ret^{m2:m12}$), economy control variables ($log(POPULATION)$, $\Delta GDPHEAD$, ΔCPI, and $FX\ RET$), control variables based on World Input-Output Tables (WIOT, $log(Gross\ Output)$, $Value\ Added\ Share$), and controls related to betas ($\beta^{Country}$, $\beta^{Concentration}$, $\beta^{Sparsity}$, β^{Transp}). All control variables are defined in Appendix B. t-statistics based on Newey-West standard errors are given in parentheses. Statistical significance at the 10%, 5%, and 1% level is indicated by *, **, and ***, respectively.

	(1)	(2)	(3)	(4)	(5)	(6)
CPV^{PRCNTL}	0.002**	0.002**	0.002**	0.002*	0.003**	0.003**
	(2.104)	(2.313)	(2.287)	(1.909)	(2.183)	(2.242)
Economy CPV^{PRCNTL}	0.000	0.003	0.002			
	(0.133)	(1.227)	(0.943)			
Industry CPV^{PRCNTL}				−0.000	−0.000	−0.001
				(−0.160)	(−0.037)	(−0.499)
Financial Controls	Yes	Yes	Yes	Yes	Yes	Yes
Economy Controls	No	Yes	Yes	No	Yes	Yes
WIOT Controls	No	Yes	Yes	No	Yes	Yes
Betas Controls	No	No	Yes	No	No	Yes
Observations	64,838	61,299	59,475	64,838	61,299	59,475
R-squared	0.263	0.389	0.431	0.251	0.382	0.426

Table D.5: Choke Point Values, Gross Output, and Stock Returns: Portfolio Analysis Using Double Sorts

This table reports the performance of industry portfolios double sorted on their gross output and their Choke Point Value. At the end of each year between 1995 and 2020, we sort economy-industry pairs with sufficient financial data into three portfolios, based on their gross output. Next, we double sort each portfolio into three portfolios, based on their Choke Point Value (CPV). Next, we track the value-weighted monthly returns of the portfolios during the next 12 months, after which we rebalance. We report alphas from a 6 factor model, including Mrk-rf, SMB, HML, MOM, CMA, and RMW as factors. t-statistics are given in parentheses. Statistical significance at the 10%, 5%, and 1% level is indicated by *, **, and ***, respectively.

OUTPUT	*CPV*			
	1 (low)	2	3 (high)	3 – 1
1 (low)	−0.134	−0.173	−0.263	−0.129
	(−0.69)	(−1.07)	(−1.36)	(−0.62)
2	−0.174	0.046	−0.108	0.066
	(−1.18)	(0.46)	(−0.90)	(0.38)
3 (high)	−0.276*	0.132	0.209**	0.485***
	(−1.74)	(1.60)	(2.53)	(2.77)
H - L	−0.141	0.306	0.472**	
	(−0.60)	(1.61)	(2.12)	

Table D.6: Choke Point Values Using an Alternative Cost and Stock Returns

This table reports the performance of industry portfolios conditional on alternative Choke Point Value, computed using the alternative edge cost $c(e) = -log(e)$. At the end of each year between 1995 and 2020, we sort economy-industry pairs with sufficient financial data into five portfolios, based on the alternative Choke Point Value. Next, we track the value-weighted monthly returns of the portfolios during the next 12 months, after which we rebalance. We report excess returns and alphas from several standard asset pricing models, based on Fama-French models, separately for the low Portfolio 1, the high Portflio 5, and the spread portfolio between Portfolios 5 and 1. CAPM includes Mrk-rf as a sole factor, FF3 adds SMB and HML, FF4 augments FF3 with MOM and FF5 augments FF3 with CMA and RMW, and FF6 includes all factors together. t-statistics are given in parentheses. Statistical significance at the 10%, 5%, and 1% level is indicated by *, **, and ***, respectively.

Ret–rf	*Alphas*				
	CAPM	FF3	FF4	FF5	FF6
Portfolio 1 (low)					
0.077	−0.469***	−0.504***	−0.472***	−0.515***	−0.490***
(0.26)	(−3.43)	(−3.96)	(−3.62)	(−3.78)	(−3.57)
Portfolio 5 (high)					
0.684**	0.073	0.074	0.101	0.187***	0.196***
(2.42)	(1.06)	(1.07)	(1.44)	(2.62)	(2.72)
Portfolio 5 – 1					
0.607***	0.542***	0.578***	0.573***	0.702***	0.687***
(3.46)	(3.44)	(3.92)	(3.78)	(4.50)	(4.35)